

MICROBIAL TREATMENT STRATEGIES: AN INTEGRATIVE APPROACH

A Dissertation

Presented to

The Graduate Faculty of The University of Akron

In Partial Fulfillment

of the Requirements for the Degree

Doctor of Philosophy

Justin S. Brantner

August, 2015

MICROBIAL TREATMENT STRATEGIES: AN INTEGRATIVE APPROACH

Justin S. Brantner

Dissertation

Approved:

Accepted:

Advisor
Dr. John M. Senko

Department Chair
Dr. Monte E. Turner

Committee Member
Dr. Donald W. Ott

Dean of the College
Dr. Chand K. Midha

Committee Member
Dr. Wiley J. Youngs

Interim Dean of the Graduate
School
Dr. Rex D. Ramsier

Committee Member
Dr. Robert Joel Duff

Committee Member
Dr. Rolando Juan Jose Ramirez

ABSTRACT

Understanding microbial treatment strategies represents a unique challenge for integrative biologists. From one viewpoint, the metabolic diversity of naturally occurring bacteria could be utilized to develop passive treatment strategies that target specific systems impacted by environmental contamination. On the other hand, from a medical perspective many bacteria are capable of establishing residence within host environments often resulting in difficult to treat infections. The purpose of this research was to explore two specific scenarios, acid mine drainage (AMD) and cystic fibrosis (CF), as a means to further develop potentially useful microbial treatment strategies.

In order to develop effective passive treatment options for water pollution caused by AMD, it becomes necessary to first evaluate how natural soil bacteria respond to sustained AMD intrusion. Data presented shows how the population of soil microorganisms from an AMD site exhibiting “sheet flow” characteristics shifts from a highly diverse community towards a less metabolically robust community composed of higher relative percentages of organisms capable of metabolic iron(II) oxidation. Data is also shown for depth dependent organization of microbial communities through a “mature” iron mound that has formed as a

result of continuous iron(II) oxidation and subsequent precipitation of various iron(III)-(hydr)oxides.

From a medical perspective, more clinically relevant microbial treatment methodologies are necessary to combat infections such as those commonly caused by *Pseudomonas aeruginosa* in the lungs of CF patients. Utilizing conditions that better approximate the chemical composition and bacterial population of the CF lung environment, various antimicrobial compounds (including two novel silver carbene complexes) were examined for efficacy against planktonic and biofilm phenotypes of multiple strains of *P. aeruginosa*. Data shows that mucin (a key component of the CF lung environment) concentration greatly impacts the efficacy of multiple classes of antimicrobial compounds. Further, it was found that silver carbene complexes were more effective at treating the biofilm phenotype of *P. aeruginosa* strains compared to other currently utilized antibiotics in conditions that approximate the CF lung environment.

Ultimately, results from both scenarios represent useful data that environmental and medical scientists respectively can use in attempts to begin developing more integrative approaches to effective microbial treatment strategies.

DEDICATION

This dissertation is proudly dedicated to my advisor and mentor Dr. Amy Milsted. Without her advice, encouragement, and mentoring, none of this would have been possible. Thank you so much for everything Dr. M!

ACKNOWLEDGEMENTS

Without question, this section more than any other is the most important portion of this dissertation. For those reading this dissertation, and more specifically to those who know me well enough, this document represents more than just the final requirement for a degree. It represents the final chapter in a long journey spent here at The University of Akron. There are so many individuals that have played instrumental roles in allowing me to reach this stage of my life. So, bear with me as I take you through the list of so many influential people and their contributions that have allowed me to arrive at this destination.

First and foremost, I want to acknowledge and profusely thank my parents (Donald and Colleen Brantner) for their unending love and support throughout this journey. No words will ever be able to capture how truly thankful I am for having the two of you in my life. Together, your guidance, wisdom, and most importantly love are what have shaped me into the man I am today. I will always be indebted to the two of you. Thank you for all of your love and encouragement throughout the years. Know always that the two of you mean the world to me. I would next like to thank my brother (Jeremy Brantner), sister (Elizabeth Brantner), and their son (Ramsey Brantner) for always being there for me. No matter how dark certain days were (and there were many), I could always count

on the three of you for laughter, love, and encouragement. This has, and will always mean, so very much to me. Sorry Jeremy, still no positron collider, but you never know what the future holds. I would also like to thank my very best of friends Arkann Al-Khalilee. If there is one person I have met that embodies the true nature of friendship, it is without question Arkann. Her encouragement, kindness, and support along this journey have meant so very much to me. Arkann, you truly are a remarkable human being. I am eternally humbled and grateful to have such an incredible best friend. Thank you, now and always, for everything Arkann.

Anyone who has had the extraordinary pleasure of knowing Chris Kolacewski-Ferris knows full well that words will never begin to capture how remarkable of a human being she is. Over the last ten years, I have worked for Chris as a tutor, a learning assistant, and as a graduate assistant. In that time, I have come to hold an unbelievable amount of respect for her. She has played such a critical role in allowing me to pursue my dreams. I will never be able to repay her for everything she has done for me. From the bottom of my heart, thank you Chris for remaining a guiding light during these many years. I have and will always cherish our friendship.

There are a number of faculty, students, and friends that must be thanked for their support at various times while I have been at The University of Akron. I would like to thank pretty much every member of the Biology Department (past and present) at The University of Akron. They have all played some hand in

assisting me down the path of becoming a successful biologist. I would like to thank the following individuals for encouraging and assisting me in various aspects of this dissertation: Bruce Sieracki, Marlana Gouin, Hope Badawy, Charles and Laura Monroe, Michael Reed, Nathan Kraynack, Mirades (Mira) Brown, Curtis Clemons, Gerald Young, Teresa Cutright, Edward Evans, James (Kyle) Miller, Jeremy Prokop, Patrick Wagers, Ashley Gordon, Sarah Klein, Catherine Kurian, Shane Hotchkiss, and Bayann Al-Khalilee. I truly appreciate all of the long talks, encouragement, and help you have provided me along the way to make this dissertation possible.

I would also like to acknowledge various sources of funding and specific individuals that allowed aspects of the research contained in this dissertation to be completed. For the acid mine drainage components of this dissertation, funding was provided by The Ohio Water Resources Research Center and National Science Foundation EAR Geobiology and Low Temperature Geochemistry award (0851847). In addition, I would like to thank both John Wilson (owner of the Mushroom Farm) and Cheryl Socotch (Ohio Department of Natural Resources) for their helpfulness in allowing me to complete work at the acid mine drainage field site mentioned herein. For the cystic fibrosis components in this dissertation, funding was provided by a grant from the National Institutes of Health (Institute of General Medical Sciences 1RO1 (GM086895)) and a Foundation Research Fund grant from Akron Children's Hospital. I want to also thank Dr. Søren Molin for providing our lab with a

Pseudomonas aeruginosa strain (PAO1/*gfp*) and Dr. Jeff Leid for providing our lab with the *P. aeruginosa* strains PDO300 and 7119.

I want to also individually thank the members of my committee. I would first like to thank Dr. Donald Ott. His concomitant sincerity and friendship define Dr. Ott's character. As my Master's thesis advisor and now as a committee member on my doctoral dissertation, Dr. Ott has unquestionably been an integral individual in shaping me into the scientist I am today. At the end of the day, I will still always admit with pride that I'm "one of Ott's boys." I would also like to thank Dr. Wiley Youngs for his insightful suggestions and for making it an absolute joy to work with chemists. Without Dr. Youngs and his years of working with silver, parts of this dissertation would not have been possible. I would also like to thank Dr. Robert Joel Duff for all of our conversations and his unending support ever since I was an undergraduate. I have always looked up to and admired Dr. Duff for his teaching and research abilities as well as his genuine attitude for helping others. It is my hope that I will be able to collaborate with him on various projects in the future. I also can not thank Dr. J.J. Ramirez enough for agreeing to be on my committee. I know how much he loved reading my integrative physiology and renal physiology essays, so I figured he would equally love to read a dissertation from me. Seriously, thank you Dr. J for being both an amazing instructor and also for being on my dissertation committee.

I want to also express my sincerest gratitude to Dr. John Senko for multiple reasons. First, I want to deeply thank him for agreeing to take over as

my acting advisor due to unforeseen circumstances. I seriously can not thank you enough for agreeing to do this for me. In addition, I would like to send my sincerest appreciation to Dr. Senko for his help with various aspects of the research presented in this dissertation. I would still be staring at mounds of sequence data if it wasn't for his guidance and assistance parcing through everything. I knew absolutely nothing about microbial ecology or acid mine drainage prior to the start of this dissertation. It is solely because of him that I have developed a continued interest in both fields. He has always had my back and best interest at heart, and for that I am eternally grateful.

I would also like to acknowledge Dr. Monte Turner. Dr. Turner is one of the most remarkable teachers and scientists I have ever known. His views on philosophy and pretty much every conversation I have ever had with him are intriguing, thought provoking, and on a typical day, hilarious. Thank you Dr. Turner for everything you have done for me all these years. I hope you enjoy and live up your retirement; you absolutely have earned and deserve it.

Finally I have come to the end of the acknowledgements section of this dissertation, and I would like to finish it off by thanking one of the most extraordinary individuals I have met during my time at The University of Akron: Dr. Amy Milsted. Dr. Milsted embodies absolutely everything I could hope to become as a scientist, teacher, and human being. Her dedication for helping students is a rare gift, one I can only hope to adopt. As a researcher and mentor, I have ALWAYS known her to put her students' interests and goals first. She has

always taken time to guide me and point me in the right direction along this challenging journey. You truly are a remarkable woman and scientist Dr. Milsted. Know always that you have been such an influential person in my life. While working in your lab these last five years, the most important and significant finding/conclusion I have made is how much of an honor and privilege it has been to work with you. I'll always be appreciative and humbled to tell my future students that I was advised by such a remarkable human being. Thank you so very much Dr. Milsted for everything.

TABLE OF CONTENTS

	Page
LIST OF TABLES.....	xvii
LIST OF FIGURES.....	xviii
CHAPTER	
I. INTRODUCTION.....	1
Integrative Approaches to Microbial Treatment Strategies.....	1
What is Acid Mine Drainage (AMD)?.....	2
AMD Treatment Options.....	3
Sheet Flow Systems as a Possible Passive AMD Treatment Option.....	5
Cystic Fibrosis Defined.....	7
General Microbiology of the CF Lung Environment.....	8
Antibiotics and the Resurgence of Silver Based Antimicrobials.....	11
Outlined Projects.....	13
II. EVALUATION OF MICROBIAL COMMUNITIES IN RESPONSE TO ACIDIC COAL MINE DRAINAGE.....	16
Introduction.....	16
Materials and Methods.....	20
Mushroom Farm Material Collections.....	20

‘Pristine’ Soil/AMD Incubations to Evaluate Fe(II) Oxidation Rates of ‘Pristine’ Soil Exposed to AMD.....	21
Soil/Iron Mound Sediment/AMD Microcosms to Evaluate Microbial Community Response to AMD Intrusion.....	22
Analytical Techniques (Dissolved Fe(II) and pH Measurements)....	24
Iron(II) Oxidizing Bacteria (FeOB) Ennumerations.....	25
Culture Independent Nucleic Acid-Based Microbial Community Analysis.....	25
Results and Discussion.....	29
Fe(II) Oxidizing Rates and Associated pH Changes in ‘Pristine’ Soil Exposed to AMD.....	29
Microbiological Activities of Long-Term Microcosm Incubations Consisting of Combinations of Soil/Iron Mound Sediment/AMD....	30
Nucleic Acid Based Analysis of MF ‘Pristine’ Soil, Iron Mound Sediment, and AMD.....	34
Shifts in Microbial Communities Associated with Soil and Iron Mound Sediment in Response to Long-Term AMD Intrusion in Microcosm Environments.....	36
Source of Microorganisms Responsible for Microbially Mediated Fe(II) Oxidation at the Mushroom Farm and Future Environmental Implications.....	44
Depth Dependent Analysis of Microbial Communities in Mature Iron Mound Sediment.....	46
Conclusions.....	54
Figures/Tables.....	57

III. THE INFLUENCE OF MUCIN AND SYNTHETIC CYSTIC FIBROSIS MEDIUM ON THE <i>IN VITRO</i> BIOACTIVITY OF SILVER CARBENE COMPLEXES AND SELECT ANTIMICROBIALS.....	77
Introduction.....	77
Materials and Methods.....	82
<i>Pseudomonas aeruginosa</i> Strains and Cystic Fibrosis Medium...	82
Bacterial Growth Curves.....	84
Treatment of Planktonic <i>P. aeruginosa</i> Strains with Various Antimicrobial Compounds Using Conditions that Approximate the CF Lung Environment.....	85
Statistical Analysis.....	87
Results.....	88
Growth Curves for Multiple <i>P. aeruginosa</i> strains Grown Using CF Relevant Media Conditions.....	88
Killing Curves to Establish Minimum Inhibitory Concentrations (MICs) and Minimum Bactericidal Concentrations (MBCs).....	90
Effect of <i>P. aeruginosa</i> strain type on MIC/MBC Values.....	92
Effect of CF Relevant Growth Medium on MIC/MBC Values.....	93
Effect of Antibiotic on MIC/MBC Values.....	94
Effects of CF Relevant Growth Medium (Controlling for Antibiotic) on MIC/MBC Values.....	96
Discussion/Conclusions.....	98
Figures/Tables.....	106

IV. BIOACTIVITY OF NOVEL SILVER CARBENE COMPLEXES AND SELECT ANTIMICROBIAL AGAINST <i>PSEUDOMONAS AERUGINOSA</i> BIOFILMS GROWN USING CF RELEVANT CONDITIONS.....	122
Introduction.....	122
Materials and Methods.....	127
Static <i>P. aeruginosa</i> Biofilm Growth Curves Using CF Relevant Conditions.....	127
Treatment of <i>P. aeruginosa</i> Biofilms with Various Antimicrobial Compounds.....	128
Results.....	129
Growth of Static Biofilms of Multiple <i>P. aeruginosa</i> strains Using CF Relevant Growth Media.....	129
Effects of Silver Carbene Complexes and Other Antimicrobials Against Static Biofilms of <i>P. aeruginosa</i> Grown in CF Medium Without Mucin.....	132
Effects of Silver Carbene Complexes and Other Antimicrobials Against Static Biofilms of <i>P. aeruginosa</i> Grown in CF Medium With Mucin.....	133
Discussion/Conclusions.....	136
Figures/Tables.....	143
V. SUMMARY/CONCLUSIONS.....	146
Integrative Microbial Treatment Strategies.....	146
The Case for Passive AMD Remediation Using Microbial Populations.....	146
The Case for Treating CF Related Infections.....	149
The Future for Microbial Treatment Strategies.....	151

REFERENCES.....	153
APPENDIX.....	180

LIST OF TABLES

Table		Page
2.1	Total number of partial 16S rRNA gene sequences acquired from each sample and designated Sequence Read Archive (SRA) accession numbers.....	59
2.2	Sequence Read Archive (SRA) accession numbers and associated number of 16S rRNA gene sequences, Operational Taxonomic Units based on 97% sequence similarity (OTU _{0.03}), and Chao1 and Shannon species diversity indices generated from each indicated mature iron mound core depth interval.....	60
2.3	GenBank accession numbers for cultured organisms and environmental samples of 16S rRNA gene sequences to which Figure 2.7 OTU _{0.03} are most closely related.....	67
2.4	Nearest 16S rRNA gene sequences from environmental surveys and cultured microorganisms resulting from BLASTn searches of OTU _{0.03} representing ≥0.5% of sequences found in libraries derived for each 1 cm depth interval of MF iron mound sediment shown in Figure 2.12.....	73
3.1	MIC values (µg/mL) for each strain of <i>P. aeruginosa</i> (PAO1, PAO1/ <i>gfp</i> , PDO300, and 7119) tested grown using three different growth media (100% SCFM with no mucin, 90% SCFM + 0.1% mucin (final wt/vol), or 90% SCFM + 1% mucin (final wt/vol)) and treated with Tobramycin, Ciprofloxacin, Meropenem, SCC-1, or SCC-22.....	120
3.2	MBC values (µg/mL) for each strains of <i>P. aeruginosa</i> (PAO1, PAO1/ <i>gfp</i> , PDO300, and 7119) tested grown using three different growth media (100% SCFM with no mucin, 90% SCFM + 0.1% mucin (final wt/vol), or 90% SCFM + 1% mucin (final wt/vol)) and treated with Tobramycin, Ciprofloxacin, Meropenem, SCC-1, or SCC-22.....	121

LIST OF FIGURES

Figure	Page
2.1	The Mushroom Farm, an acid mine drainage (AMD) impacted site exhibiting ‘sheet flow’ characteristics located in Mahoning County, OH.....57
2.2	Various material collection sites at the Mushroom Farm.....58
2.3	(●) Fe(II) concentrations and (○) pH values for semicontinuous incubations consisting of ‘pristine’ soil and AMD (A), ‘pristine’ soil and filter-sterilized AMD (B), heat-deactivated soil and AMD (C), and heat deactivated soil and filter-sterilized AMD (D).....61
2.4	Fe(II) concentrations, pH values, Fe(II)-oxidizing bacteria (FeOB) counts, and Shannon species diversity index for long-term microcosm incubations to evaluate microbial activity in response to AMD intrusion.....62
2.5	Ninety seven percent (97%) sequence similarity standard rarefaction curves of 16S rRNA gene sequence libraries obtained from AMD, iron mound sediment, ‘pristine’ soil, as well as for each long-term microcosm incubation type (iron mound sediment and AMD, ‘pristine’ soil and AMD, and ‘pristine’ soil supplemented with iron mound sediment and AMD) at incubation days 0, 6, 12, 18, and 24.....63
2.6	Relative phylum level (and class-level for the Proteobacteria) abundances of 16S rRNA gene OTU _{0.03} from gene sequence libraries of ‘pristine’ soil, iron mound sediment, AMD (all shown to the left of all three microcosm incubation types for clarity), and for each long term AMD microcosm incubation type (iron mound sediment, ‘pristine’ soil, and ‘pristine’ soil seeded with iron mound sediment) at incubation days 0, 6, 12, 18, and 24.....64

2.7	Relative abundances of select OTU _{0.03} that belong to Euryarchaeota, Betaproteobacteria, Gammaproteobacteria, or Firmicutes in long-term AMD microcosm incubations that consisted of ‘pristine’ soil (solid blue lines), iron mound sediment (solid red lines), or ‘pristine’ soil supplemented with iron mound sediment (solid pink lines).....	65
2.8	Principal coordinate analysis (PCoA) of ‘pristine’ soil (blue cross), iron mound sediment (red cross), or AMD (green cross) microbial communities and long term microcosm incubations consisting of ‘pristine’ soil (blue shapes), ‘pristine’ soil supplemented with iron mound sediment (pink shapes), and iron mound sediment (red shapes) after 0 (●), 6 (■), 12 (◆), 18 (▲), and 24 (▼) days of incubation using the weighted UniFrac metric (151, 152).....	68
2.9	Shared OTU _{0.03} over the course of 24 day long term AMD microcosm incubation experiments between ‘pristine’ soil (A), iron mound sediment (B), or AMD (C) and incubations consisting of either ‘pristine’ soil (blue lines), ‘pristine’ soil seeded with iron mound sediment (pink lines), and iron mound sediment (red lines).....	69
2.10	UPGMA trees constructed using the weighted and unweighted UniFrac metrics to illustrate microbial community clustering associated with each 1 cm depth interval through a core sample of iron mound material taken from the MF.....	70
2.11	Phylum-level (and class-level in the case of the Proteobacteria) taxonomic resolutions for relative abundances of 16S rRNA gene sequences in libraries generated from sequences recovered from 1 cm depth intervals of iron mound core collected from the MF.....	71
2.12	Heatmap projection illustrating relative abundances of OTU _{0.03} that make up ≥0.5% of total OTU _{0.03} recovered from various depths (1 cm intervals) of MF iron mound sediment, and associated Ribosomal Database Project (RDP) taxonomic identities.....	72
3.1	Bacterial growth curves for <i>P. aeruginosa</i> strains PAO1 (A), PAO1/ <i>gfp</i> (B), PDO300 (C), and 7119 (D) grown in either 100% SCFM with no mucin (red ■), 90% SCFM + 0.1% mucin (final wt/vol) (green ▲), 90% SCFM + 1% Mucin (final wt/vol) (purple ●), or a control using 100% SCFM diluted to 90% SCFM using sterile DI water (blue ◆).....	106

3.2	Bacterial killing curves for <i>P. aeruginosa</i> strains PAO1 (A), PAO1/ <i>gfp</i> (B), PDO300 (C), and 7119 (D) grown in 100% SCFM (red ■), 90% SCFM + 0.1% mucin (final wt/vol) (blue ●), or 90% SCFM + 1% mucin (final wt/vol) (green ▲) and subsequently treated with various concentrations of Tobramycin for 24 hours.....	107
3.3	Bacterial killing curves for <i>P. aeruginosa</i> strains PAO1 (A), PAO1/ <i>gfp</i> (B), PDO300 (C), and 7119 (D) grown in 100% SCFM (red ■), 90% SCFM + 0.1% mucin (final wt/vol) (blue ●), or 90% SCFM + 1% mucin (final wt/vol) (green ▲) and subsequently treated with various concentrations of Ciprofloxacin for 24 hours.....	108
3.4	Bacterial killing curves for <i>P. aeruginosa</i> strains PAO1 (A), PAO1/ <i>gfp</i> (B), PDO300 (C), and 7119 (D) grown in 100% SCFM (red ■), 90% SCFM + 0.1% mucin (final wt/vol) (blue ●), or 90% SCFM + 1% mucin (final wt/vol) (green ▲) and subsequently treated with various concentrations of Meropenem for 24 hours.....	109
3.5	Bacterial killing curves for <i>P. aeruginosa</i> strains PAO1 (A), PAO1/ <i>gfp</i> (B), PDO300 (C), and 7119 (D) grown in 100% SCFM (red ■), 90% SCFM + 0.1% mucin (final wt/vol) (blue ●), or 90% SCFM + 1% mucin (final wt/vol) (green ▲) and subsequently treated with various concentrations of SCC-1 for 24 hours.....	110
3.6	Bacterial killing curves for <i>P. aeruginosa</i> strains PAO1 (A), PAO1/ <i>gfp</i> (B), PDO300 (C), and 7119 (D) grown in 100% SCFM (red ■), 90% SCFM + 0.1% mucin (final wt/vol) (blue ●), or 90% SCFM + 1% mucin (final wt/vol) (green ▲) and subsequently treated with various concentrations of SCC-22 for 24 hours.....	111
3.7	Box-and-whisker-plots of median (solid line within each box plot) and mean (shaded circles) comparing MIC ($\mu\text{g/mL}$) values for <i>P. aeruginosa</i> strains 7119 (blue), PAO1 (red), PAO1/ <i>gfp</i> (green), and PDO300.....	112
3.8	Box-and-whisker-plots of median (solid line within each box plot) and mean (shaded circles) comparing MBC ($\mu\text{g/mL}$) values for <i>P. aeruginosa</i> strains 7119 (blue), PAO1 (red), PAO1/ <i>gfp</i> (green), and PDO300.....	113

- 3.9 Box-and-whisker-plots of median (solid line within each box plot) and mean (shaded circles) MIC values ($\mu\text{g/mL}$) for all four *P. aeruginosa* strains (PAO1, PAO1/*gfp*, PDO300, and 7119) treated with Tobramycin, Ciprofloxacin, Meropenem, SCC-1 and SCC-22 grown in either 100% SCFM (purple), 90% SCFM + 0.1% mucin (final wt/vol) (red), or 90% SCFM + 1% mucin (final wt/vol) (green).....114
- 3.10 Box-and-whisker-plots of median (solid line within each box plot) and mean (shaded circles) MBC values ($\mu\text{g/mL}$) for all four *P. aeruginosa* strains (PAO1, PAO1/*gfp*, PDO300, and 7119) treated with Tobramycin, Ciprofloxacin, Meropenem, SCC-1 and SCC-22 grown in either 100% SCFM (purple), 90% SCFM + 0.1% mucin (final wt/vol) (red), or 90% SCFM + 1% mucin (final wt/vol) (green).....115
- 3.11 Box-and-whisker-plots of median (solid line within each box plot) and mean (shaded circles) MIC values ($\mu\text{g/mL}$) for all four *P. aeruginosa* strains (PAO1, PAO1/*gfp*, PDO300, and 7119) grown in 100% SCFM, 90% SCFM + 0.1% mucin (final wt/vol), and 90% SCFM + 1% mucin (final wt/vol) and treated with either Ciprofloxacin (blue), Meropenem (red), SCC-1 (green), SCC-22 (brown), or Tobramycin (purple).....116
- 3.12 Box-and-whisker-plots of median (solid line within each box plot) and mean (shaded circles) MBC values ($\mu\text{g/mL}$) for all four *P. aeruginosa* strains (PAO1, PAO1/*gfp*, PDO300, and 7119) grown in 100% SCFM, 90% SCFM + 0.1% mucin (final wt/vol), and 90% SCFM + 1% mucin (final wt/vol) and treated with either Ciprofloxacin (blue), Meropenem (red), SCC-1 (green), SCC-22 (brown), or Tobramycin (purple).....117
- 3.13 Box-and-whisker-plots of median (solid line within each box plot) and mean (shaded circles) MIC values ($\mu\text{g/mL}$) for all four *P. aeruginosa* strains (PAO1, PAO1/*gfp*, PDO300, and 7119) by growth medium (100% SCFM (blue), 90% SCFM + 0.1% mucin (final wt/vol) (red), or 90% SCFM + 1% mucin (final wt/vol) (green) and antibiotic.....118
- 3.14 Box-and-whisker-plots of median (solid line within each box plot) and mean (shaded circles) MBC values ($\mu\text{g/mL}$) for all four *P. aeruginosa* strains (PAO1, PAO1/*gfp*, PDO300, and 7119) by growth medium (100% SCFM (blue), 90% SCFM + 0.1% mucin (final wt/vol) (red), or 90% SCFM + 1% mucin (final wt/vol) (green) and antibiotic.....119

4.1	Growth curves of <i>P. aeruginosa</i> strains PAO1 (A), PDO300 (B), and 7119 (C) grown in 100% SCFM with no mucin (blue ●) and 90% SCFM supplemented with 1% mucin (final wt/vol) (red ■).....	143
4.2	Killing curves of <i>P. aeruginosa</i> strains PAO1 (A), PDO300 (B), and 7119 (C) grown as static biofilms in 100% SCFM without mucin for 24 hours, and subsequently treated with Tobramycin (red ■), Ciprofloxacin (green ▲), Meropenem (purple X), SCC-1 (blue ◆), or SCC-22 (orange ●) at various concentrations for 24 hours.....	144
4.3	Killing curves of <i>P. aeruginosa</i> strains PAO1 (A), PDO300 (B), and 7119 (C) grown as static biofilms in 90% SCFM supplemented with 1% mucin (final wt/vol) for 24 hours, and subsequently treated with Tobramycin (red ■), Ciprofloxacin (green ▲), Meropenem (purple X), SCC-1 (blue ◆), or SCC-22 (orange ●) at various concentrations for 24 hours.....	145

CHAPTER I

INTRODUCTION

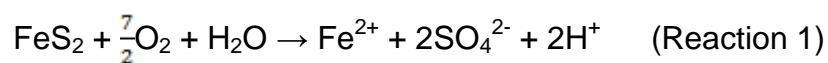
Integrative Approaches to Microbial Treatment Strategies

Bacteria represent the most ubiquitous group of organisms on the planet, capable of surviving and often thriving under various environmental conditions. From harsh geochemical environments to nutrient rich niches inside host organisms, bacteria have been able to capitalize on a wide array of habitats. Due to this innate ability of bacteria to thrive and persist under various environmental stresses, the concept of microbial treatment strategies can be viewed from two different perspectives. One treatment scenario involves capitalizing on the natural metabolic processes that certain bacteria possess in an attempt to effectively remediate environmental contamination. In this sense, the bacteria are essentially being used as a potential “treating” agent to metabolically remove/convert certain chemical species found associated with contaminated environments. On the other hand, pathogenic bacteria that gain access to a nutrient rich environment inside a host organism can often lead to chronic infection, which in many cases leads to mortality. To combat such difficult chronic infections, innovative chemotherapeutic methods are necessary. In this instance, treatment refers to using different agents that can combat the unwanted growth

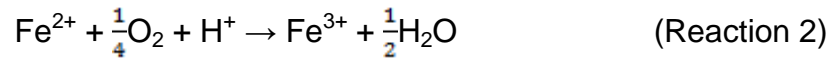
of bacteria responsible for the infection. Specifically, this dissertation focuses on two main areas of current research to better elucidate the above mentioned microbial 'treatment' scenarios: acidic coal mine drainage contamination and persistent infections that occur in patients affected by cystic fibrosis. Regardless of which view of "treatment" is being upheld, it becomes apparent that integrative approaches are necessary in order to develop more successful microbial treatment strategies. By working across the disciplines of microbiology, chemistry, geology, and medicine, the projects outlined will provide necessary data that can be used in the development of effective microbial treatment strategies. To begin looking at such treatment strategies however, some background is necessary to set the framework for the two different microbial systems/approaches that are extensively discussed throughout this dissertation.

What is Acid Mine Drainage?

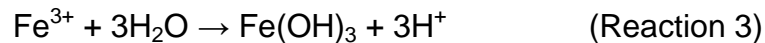
Acid mine drainage (AMD) is the result of a hydro(bio)geochemical process initiated when iron sulfide rich mineral phases (most notably pyrite (FeS_2)) unearthed during the mining process come into contact with oxygenated surface waters (12, 19, 114, 115, 172, 207, 218). The rapid oxidation and dissolution of the iron sulfide minerals leads to low-pH surface waters that contain abundant ferrous iron and sulfate species as illustrated by reaction 1 (19, 218):



The iron(II) becomes further oxidized in circumneutral pH waters yielding high abundances of iron(III) as seen in reaction 2 (19, 123, 218):



In the presence of water, the ferric iron generated by reaction 2 undergoes rapid hydrolysis, forming further acidified waters as well as iron(III)-(hydr)oxides depicted in reaction 3 (19, 123, 218):



The end result of the above reactions is highly acidified water that contains (among other elements) abundant dissolved and precipitated iron species that can often have devastating effects on associated terrestrial and aquatic ecosystems. In fact, AMD represents one of the leading surface water contamination issues currently in the United States. Recent estimates suggest that between 8,000-16,000 km of streams in the western US, and approximately 10,000 km of stream systems in the eastern US (specifically the coal mining sectors of northern Appalachia) have been exposed to AMD (104, 202). With such negative impacts on wetland ecosystems, AMD cleanup efforts have widened, employing multiple techniques in an attempt to remedy a growing environmental concern.

AMD Treatment Options

Treatment strategies for AMD sites are often divided into two general categories; “active” and “passive.” Active treatment strategies involve chemical

additions (typically pH neutralizing compounds) to AMD waters which subsequently aids in precipitation of various metals out of solution (114, 252). Often, the resulting precipitates are then removed from the site via human intervention (116). However, the high costs, labor involvement, and general infeasible nature of active treatment strategies are often extensive. Thus, the second general category of AMD treatment strategies (i.e., passive treatment options) has received more recent attention primarily due to reduced human intervention/maintenance. Various passive treatment strategies have been explored including (but not limited to) limestone based systems (47, 114, 116, 252), anaerobic based systems that rely on sulfate reducing bacteria (SRB) (37, 114), and wetland based systems (114, 116, 226, 232). However, even these forms of passive treatment each consist of notable limitations. For example, the limestone material used as a neutralizer of pH in AMD waters can often become 'armored' by iron(III) hydroxides, reducing the buffering effects of the limestone and, in some cases, requiring frequent removal and replacement of the limestone (46, 47, 114, 252). The pitfall of anaerobic based systems is that even once iron(II) is co-precipitated out with sulfide via sulfate reducing bacteria (SRB), oxygen infiltration into the sediment by any means can result in re-dissolution of the FeS phases back into free sulfate and iron(II), thereby generating more acidified waters containing abundant dissolved ferrous iron (114, 116). Wetland based systems can often underperform due to depleted oxygen availability, which ultimately hinders iron(II) oxidation and subsequent ferric iron

sequestration (226). Wetland based systems also have limitations due in part to overall size of wetland landscape, climatic region influence on wetland performance, and total organic carbon availability (116). Further, evidence has been provided that metals sequestered as metal oxides in sediments of wetland based systems can potentially undergo re-dissolution, thereby re-releasing the various metal species (namely iron and manganese) back into surrounding waters (225, 226, 232). In addition, metals that bioaccumulate in native vegetation in wetland treatment systems risk being re-released back into the surrounding waters upon death and decomposition of the vegetative material (116). Clearly as evidenced by some of the pitfalls of current active and passive treatment methods, more novel passive treatment options must be explored in order to effectively treat AMD pollution.

Sheet Flow Systems as a Possible Passive AMD Treatment Option

One passive treatment design for AMD systems that has garnered recent attention is that of a 'sheet flow' system. 'Sheet flow' systems are described as natural systems in which shallow AMD (often 0.5-1 cm deep) flows down the gradient of a thick iron(III)-hydroxide crust (26, 27, 56, 91, 199-201). The shallow depths and reduced flow rate increases residence time of the AMD waters over the iron(III)-hydroxide mound. This causes enhanced exposure of AMD to oxidative forces (i.e., free and dissolved oxygen) which could aid in maximizing abiotic oxidation of iron(II) (56, 199). As the water continues to acidify based on

the reactions listed previously however, the abiotic oxidation of iron(II) quickly becomes hindered due to kinetic constraints (12, 19, 123, 207, 218). However, these constraints are circumvented via native microorganisms, which have been shown to enhance the oxidation of iron(II) via lithotrophic metabolic pathways even as pH values continue to decline (12, 21, 27, 41, 56, 95, 114, 123, 172, 199, 200, 207, 218). Thus, an increased residence time of AMD over a large, aerated surface of iron hydroxide crust, in conjunction with enhanced metabolic activities of acidophilic microorganisms found in the iron mound material at 'sheet flow' sites, provides an optimal situation for the removal of dissolved ferrous iron (in the form of iron(III) hydroxides) abiotically and biotically early on in the AMD flow path (56, 199, 200). As such, since removal of dissolved iron is one of the hallmark goals of AMD treatment (56, 123, 200), 'sheet flow' systems seem to represent an ideally efficient passive AMD treatment model.

However, despite the encouraging data generated thus far on AMD 'sheet flow' systems as potential models for passive treatment (56, 91, 199-201), a basic understanding of the microbial communities and subsequent activities associated with 'sheet flow' systems is still lacking. In fact, data is limited to suggest how such microbial communities developed from formerly 'pristine' soil (soil not impacted by AMD). Therefore, as an understanding of microbial systems is critical to the development of successful passive treatment strategies (55, 56, 91, 95, 114, 200), the following outlined research projects were tailored towards developing a more basic understanding of the microbial community dynamics

associated with 'sheet flow' conditions at a specific AMD impacted site (i.e., the Mushroom Farm, Mahoning County, OH). Further, the work proposed here will provide useful data regarding how native soil microbial communities respond and adapt to AMD intrusion, and whether or not these responses/adaptations can be accelerated. Lastly, a broadened knowledge base of microbial community dynamics in a specific AMD type system (i.e., 'sheet flow') will provide relevant information to be used long term for the potential development of more efficient passive AMD treatment strategies.

While certain microorganisms can have a physiological role in passive remediation efforts, it is also abundantly clear that from a medical perspective certain bacteria can pose a very serious health threat. In this light, it becomes necessary to collaborate in the attempt to develop integrative treatment strategies to eliminate the source of infection. This next section explains the nature of one specific disease (cystic fibrosis) that can often lead to bacterial infections responsible for high morbidity and mortality rates. This section also goes into detail about current treatment methodologies, and the necessity for more basic research on potential novel microbial treatment strategies to eliminate cystic fibrosis associated infections.

Cystic Fibrosis Defined

Cystic fibrosis (CF) is characterized as an autosomal recessive disease that affects approximately 30,000 individuals in the United States (74). The cause

of CF is attributed to mutations that arise in the cystic fibrosis transmembrane conductance regulator (CFTR) gene located on chromosome 7 (10, 22, 85, 122, 157, 186, 189). While a number of mutations have been identified in the CFTR gene that give rise to CF (22, 77, 85, 157, 179), the most common mutation, which accounts for approximately 70% of all CF patients, is a three base pair deletion in the CFTR gene ultimately resulting in a deletion of a phenylalanine at the 508 position ($\Delta F508$) in the CFTR polypeptide (10, 22, 85, 122, 157, 179, 186, 189). As the CFTR polypeptide functions normally as an apical ion transporter in epithelial cells, mutations in the CFTR gene can cause imbalances in the transport of various ions across the cell membrane including Na^+ , Cl^- , and HCO_3^- (22, 51, 85, 157, 186). In the respiratory tract of CF patients specifically, these ionic imbalances brought on by CFTR mutations result in abnormally viscous, dehydrated mucus that impedes the mucociliary clearance mechanism of lung epithelial cells (35, 51, 77, 85, 157, 163). Due to these impedances, the respiratory tract of patients afflicted with CF is prone to chronic infection by various pathogens, which can often lead to high incidence of morbidity and mortality among CF patients.

General Microbiology of the CF Lung Environment

The lungs of both non-CF and CF patients harbor a naturally nutrient rich, hospitable environment, affording microorganism an ideal niche for survival. Not surprisingly, mucus possesses various nutrients/macromolecules such as various

salts, lipids, glycoproteins (i.e., mucins), actin, other various proteins, and water (163, 176, 190, 192, 212, 234). In the case of a healthy, non-CF lung, the mucociliary clearance mechanism often lead to trapping and immediate expulsion of microorganisms trapped in the mucus layer from the lungs prior to onset of any substantial health complications. In the case of the CF lung environment however, the defective CFTR gene causes a buildup of thickened mucus plaques that weigh down the apical cilia of the epithelial cells, thereby impeding the removal of both mucus and trapped microorganisms from the lung environment (22, 163). As such, the CF lung is highly susceptible to infection by various microorganisms (249). Young CF patients experience early colonization of the lung predominantly by *Staphylococcus aureus* strains, with *Pseudomonas aeruginosa*, *Burkholderia cepacia*, and *Haemophilus influenzae* strains also noticeably present (77, 85, 157, 160, 245, 249). However, as the CF patient ages, there is a dynamic microbial community shift, whereby the opportunistic pathogen *P. aeruginosa* becomes the dominant colonizer of the CF lung environment (77, 85). As *P. aeruginosa* continues to establish itself as the dominant pathogen in the lungs of CF patients, population densities have been cited to range from $10^8 - 10^{10}$ CFU/mL (175, 176, 208). Complicating matters beyond the high population density is the fact that *P. aeruginosa* strains commonly express the biofilm phenotype in the CF lung environment (15, 106, 157, 208, 248). The biofilm phenotype is defined as a switch from planktonic counterparts to a highly organized community of microorganisms encased in a

self-produced polymeric substance composed primarily of water, various ions, polysaccharides, proteins, and nucleic acids (3, 42, 60, 76, 216, 222). This shift to the biofilm phenotype is due (in part) to a process known as quorum sensing (QS), whereby upon reaching high population densities of planktonic bacterial counterparts, certain signal molecules are produced that activate various genes that are responsible for biofilm formation (16, 18, 52, 97, 111, 138, 238). In Gram negative bacteria, such as *P. aeruginosa*, small signaling molecules known as N-acyl homoserine lactones are synthesized, and upon reaching high concentrations due to high bacterial populations densities, can activate proteins responsible for the transcription of various genes (111, 138, 238). For *P. aeruginosa* specifically, the *las* and *rhl* signal/receptor systems produce the N-acyl homoserine lactone QS molecules 3-oxo-C12-HSL and C4-HSL respectively, while the PQS (*Pseudomonas* quinolone signal) pathway produces a 4-quinolone compound (2-heptyl-3-hydroxy-4-quinolone) (16, 18, 238). These various QS systems in *P. aeruginosa* have been linked to the formation of biofilms (18). It is well established that biofilm structures formed specifically in the CF lung environment display a greater tolerance, and in many cases resistance, to antimicrobial compounds compared to planktonic counterparts (3, 15, 16, 38, 62, 63, 78, 102, 133, 168, 214, 215). The CF lung environment is nutritionally and physically prone to heavy colonization by *P. aeruginosa*, and the fact that *P. aeruginosa* strains are commonly found to form multi-drug resistant biofilms, it is

not surprising that *P. aeruginosa* represents the target organism for development of novel microbial treatment strategies for patients afflicted with CF.

Antibiotics and the Resurgence of Silver Based Antimicrobials

One of the greatest challenges in developing a successful clinically relevant microbial treatment strategy is the development and understanding of how certain antimicrobial compounds interact within a given environment. As already detailed, the infected CF lung environment is remarkably complex, filled with both multi-drug resistant bacterial strains and viscous mucus that impedes the clearance mechanisms of the lungs. For *P. aeruginosa* strains specifically, it has been well documented that strains of *P. aeruginosa* not only show resistance to multiple antibiotics (79, 103, 157, 181, 184, 185, 203, 230), but many of these strains are often protected from the effects of antibiotics based on the physiochemical conditions of the CF lung environment (110, 133, 142, 158, 164). Very few studies however have actually examined the effects that CF relevant conditions have on the bioactivity of clinically relevant antimicrobial compounds (30, 110, 141, 142, 164). Despite current use of several clinically relevant antimicrobial compounds to treat *P. aeruginosa* infections in the cystic fibrosis lung (77, 157), the rise of antimicrobial resistance as well as the complex nature of the CF lung environment has prompted researchers to explore alternative treatments to deal with such challenging infections. Specifically, silver based antimicrobials have garnered recent interest as possible candidates for treating

CF associated infections for multiple reasons. Silver has a long standing history as an effective antimicrobial agent against multiple types of infectious Gram positive and Gram negative pathogens (125, 126, 134, 193). One definitive benefit of silver (aside from its ability to work against multiple species of bacteria) is that although the exact mechanism for silver is not completely established in bacteria, a large body of evidence suggests that the silver(I) ion (Ag^+) has multimodal action. These modes of action include protein inactivation due to binding with amino acid residues containing sulfhydryl groups (i.e., cysteine residues) (73, 143, 193), disruption of cell wall synthesis (240), interference with cellular respiration (23, 107), hindrances in nucleic acid activity due to nitrogen base binding (193), and potential secondary effects on DNA replication (73). In addition to the multimodal action of silver as an antimicrobial, there is also very low incidence reported for silver related resistance among bacterial isolates (206). In addition, resurgence of silver as an antimicrobial has been shown to effectively eradicate *P. aeruginosa* biofilms even at low concentrations (17). However, despite the potent activity that silver(I) has as an antimicrobial agent, reactivity of silver(I) with various halides in solution often results in co-precipitation thereby greatly affecting the antimicrobial effects of silver(I) (206). Consequently, ligands capable of effective binding and release of the silver(I) ion are necessary. One class of compounds with significant promise consists of the N-heterocyclic silver carbene complexes (SCCs) (105, 120). SCCs afford extra binding stability to the metal center of the silver(I) cation allowing the silver cation

to be slowly released over time (120). Two SCC compounds, SCC-1 (silver acetate bound to methylated caffeine), and SCC-22 (hydroxylated 4,5 dichloroimidazole bonded with silver acetate), have shown great promise as water soluble/stable, broad-spectrum antimicrobials (31, 119, 139, 166, 177). Yet, despite SCC complexes representing possible candidates to treat CF related infections caused by pathogens such as *P. aeruginosa*, very little data has been generated with respect to how effective SCC complexes are when used to treat *P. aeruginosa* strains grown in conditions mimicking the CF lung environment (166). It has also been demonstrated that *in vitro* medium selection in general can have noticeable effects on antimicrobial effectiveness against *P. aeruginosa* strains, and that mucin (when added to synthetic cystic fibrosis medium (SCFM) (175)) can hinder the antimicrobial effectiveness of an SCC complex (166). As reports of antibiotic resistant strains of various pathogens continue to rise in patients afflicted with cystic fibrosis, it is clear that more effective antimicrobial treatment strategies are necessary. Specifically, as it relates to cystic fibrosis, more basic research into understanding the efficacy, efficiency, and interactions that antimicrobial compounds have in environments mimicking the CF lung are necessary.

Outlined Projects

As discussed, microbial treatment strategies can be viewed from two radically different perspectives. From an environmental perspective, the

metabolic processes that various microorganisms possess could aid in the remediation of severely contaminated natural environments. Looking at microorganisms from a biomedical perspective, the common aim is to effectively design, deliver, and hopefully eradicate microorganisms responsible for contributing to high incidence of morbidity and mortality in patients afflicted with various diseases. Regardless of the perspective, the dynamic field of microbiology has prompted researchers to take a more integrative approach to solving complex issues that involve microorganisms. As such, this dissertation contains multiple collaborative projects across various disciplines that address this growing need of more integrative biology when examining microbial treatment avenues. In chapter two, projects pertaining to both microbial community structure and involvement in an AMD contamination site are addressed. From the perspective of microbial treatment strategies, chapter two examines the utilization of microorganisms as a potential means of passively treating environmental contamination brought on by coal mine derived acidic mine drainage, and is done so by employing an integrative geomicrobiological approach. In chapters three and four, microbial treatment strategies are addressed from a medicinal perspective, specifically aimed at understanding antimicrobial effects in conditions that approximate the early cystic fibrosis lung environment. In both of these chapters, novel SCC antimicrobial compounds (as well as currently clinically relevant antimicrobials) are used as agents to treat various strains of *P. aeruginosa* grown under various conditions that attempt to

better approximate the early CF lung environment. Further, chapters three and four aim to apply a more integrative approach (from a biological, medical, and chemical perspective) in order to obtain clinically relevant data that can be used to design more effective treatment options for patients afflicted with CF. By utilizing various integrative techniques, approaches, and problem solving, the research contained in the next three chapters addresses various microbiological issues in an attempt to broaden basic research in microbial treatment strategies.

CHAPTER II
EVALUATION OF MICROBIAL COMMUNITIES IN RESPONSE TO ACIDIC
COAL MINE DRAINAGE

Introduction

Acidic coal mine drainage, which is the result of iron-rich deposits unearthed during the coal mining process coming into contact with oxygenated waters, represents a serious environmental concern currently in the United States (12, 19, 114, 115, 172, 207, 218). The upheaval of such iron-rich mineral phases during can often leave surface waters highly acidified, often possessing high concentrations of sulfates and various other metals (most notably iron) (19, 44, 45, 218). This combination of low pH and high levels of metal pollution culminates into a growing environmental concern regarding widespread contamination and devastation of aquatic based ecosystems. Various treatment strategies have been suggested and attempted, however, each is known to possess various pitfalls (47, 114, 116, 225, 226, 232, 252). Novel treatment options are being explored in order to circumvent some of the pitfalls of such AMD clean-up strategies. One such attractive method is the use of knowledge from natural hydro(bio)geochemical systems that have developed with no human intervention in response to AMD intrusion. Such a system has been described as

a 'sheet flow' system, whereby the natural landscape is known to enhance aeration of AMD waters and thus aid in naturally occurring acidophilic, Fe(II) oxidizing bacterial communities in the oxidative precipitation of dissolved iron (II) (26, 27, 56, 91, 199-201). This method of dissolved Fe(II) removal can lead to thick, iron hydroxide formations collectively termed iron mounds, that terrace the landscape (26, 29, 56, 91, 200). While these 'sheet flow' systems are thought to possess ideal characteristics of a potentially successful passive treatment option for AMD remediation, very little is known regarding how such systems develop. More specifically, very little is available regarding the microbiological nature of such systems, despite the significant roles that such communities are known to play in the formation of these 'sheet flow' systems (56, 200). Therefore, in order to even consider 'sheet flow' systems as a potential AMD treatment method, more basic information regarding the microbiological (and associated geochemical) nature of these systems is essential.

To this end, an AMD site that exhibits these 'sheet flow' characteristics has been identified in Mahoning County, OH (40°56'9.20"N, 80°40'6.35"W). The 'Mushroom Farm' (MF) has experienced AMD emergence for approximately 18 years. Although the actual entrance of the abandoned coal mine remains unclear, the basement of the abandoned residence serves as an AMD 'pool,' with AMD flowing out from the basement window down a slight gradient in the front yard (Figure 2.1A) (27, 49). The AMD flows as a 0.5-1 cm deep sheet along the incline of a 6-10 cm iron(III)-hydroxide crust encompassing a total land area of

approximately 45 m² (26, 49, 91) (Figure 2.1B). The depth of the iron crust, coupled with the approximated number of years of AMD emergence, suggests an annual growth rate for the iron crust of about 0.4-0.7 cm/yr. Following the AMD flow path for approximately 30 m from the emergence point of the basement window, it has been previously shown that pH decreases (from approximately 4.5 to 3.0), dissolved oxygen increases (from about 1.0 mg/l to 9.0 mg/l), and nearly complete oxidative precipitation (mediated by microorganisms) of 12 mM iron(II) is achieved (91). Using this knowledge gained from preliminary field work at the MF site, a two-dimensional mathematical model of the 'sheet flow' regime was constructed (91). It was found that the principle factors responsible for the iron(III)-hydroxide crust formation were pH, dissolved oxygen, concentrations of both ferric and ferrous iron, rates of chemical reactions, and fluid flow dynamics associated with the gradient of the iron mound. In addition, the model predicted that an increase in iron(II)-oxidizing bacteria can also influence the rate at which the iron(III)-hydroxide mound forms.

Based on the characteristics thus far described at the Mushroom Farm, this site represents an ideal location to better explore the microbiology associated with 'sheet flow' AMD systems. More specifically, research conducted at the Mushroom Farm aimed to accomplish three research goals:

- Identify the source for microorganisms responsible for the microbially mediated iron(II) oxidation at the Mushroom Farm, and

characterize initial Fe(II) oxidation kinetics associated with such organisms.

- Conduct long term microcosm incubations to characterize the microbial activities of native soil microorganisms in response to AMD intrusion, and investigate whether these responses can be enhanced.
- Characterize the vertical microbial community structure at an AMD impacted site consistent with 'sheet flow' characteristics.

From these research aims, various hypotheses/predictions were generated. It was hypothesized that the microorganisms from both the AMD water and 'pristine' soil are required to effectively mediate the iron(II) oxidation reactions seen at the Mushroom Farm. In addition, it was hypothesized that rates of microbially mediated iron(II) oxidation will increase as the soil microbial community shifts from primarily organotrophic to lithotrophic organisms in response to continuous AMD intrusion. Further, 'pristine' soil microbial communities would shift from relatively high diversity communities of mostly organotrophic organisms to communities of low species diversity dominated by organisms capable of lithotrophic processes, and that as the soil microorganism community shifts, it would begin to resemble the microbial community structure exhibited by 'mature' iron mound sediment. It was also predicted that the augmentation of formerly 'pristine' soil with 'mature' iron mound sediment (and associated microorganisms) will accelerate the development of microbial

communities capable of iron(II) oxidation. Lastly, it was hypothesized that microbial diversity is depth dependent, such that species diversity would likely be restricted to mostly aerobic organisms capable of lithotrophic processes in the iron mound phase, while a higher diversity of species capable of anaerobic metabolism exists at the iron hydroxide/soil interface and in the underlying soil layer.

Materials and Methods

Mushroom Farm Material Collections

Various materials were collected from the Mushroom Farm (MF), an AMD-impacted site located in North Lima, OH (26, 27, 49, 91). A site situated on the property that had no evidence of AMD intrusion was identified, and 'pristine' soil (soil that was not exposed to AMD contamination) was collected (Figure 2.1A). This was achieved by first excavating and discarding the top 3 cm of overlying debris and vegetation, followed by collection of the underlying soil into sterile containers. Iron mound sediment found along the AMD flow path was collected by removing the top 2 cm of iron mound deposit and placing it into sterile containers (Figure 2.2B). Acid mine drainage was collected into sterile bottles from a collecting pool located upstream of the AMD flow path (Figure 2.2C). In addition, core samples were taken from approximately the same location as the iron mound sediment (Figure 2.2B). This was achieved by driving a sterile 2.5 cm diameter polypropylene liner into the iron mound sediment to a depth of 10 cm

(beginning from the iron mound/AMD interface downward), and pulling up the resulting core. The cores were then sealed with sterile caps. All materials were transported from the Mushroom Farm to The University of Akron on either ice (materials for soil/sediment incubations) or dry ice (samples for microbial DNA based analyses). 'Pristine' soil, iron mound sediment, and cores collected in the field and intended for nucleic acid based microbial analysis were stored in a -80°C freezer until further processing. In addition, one liter of Mushroom Farm AMD was filtered through a Supor-200 0.2 µm membrane filter (Pall Corporation, Port Washington, NY), following which the 0.2 µm membrane was also placed into a -80°C freezer. Iron sediment, AMD, and 'pristine' soil to be used for incubations were stored in a 4°C refrigerator for no more than one week prior to usage.

'Pristine' Soil/AMD Incubations to Evaluate Fe(II) Oxidation Rates of 'Pristine' Soil Exposed to AMD

A total of 4 unique microcosm environments (in duplicate) were designed in order to establish the Fe(II) oxidation activities of 'pristine' soil when exposed to AMD intrusion. These microcosms consisted initially of 4 g of MF 'pristine' soil and 50 mL of MF AMD added to sterile 125 mL Erlenmeyer flasks covered with aluminum foil in the following combinations: non-sterile 'pristine' soil and non-sterile AMD, non-sterile 'pristine' soil and filter-sterilized MF AMD, sterile 'pristine' soil (heat deactivated by autoclave) and non-sterile MF AMD, and sterile 'pristine'

soil (heat deactivated) and filter-sterilized MF AMD. Periodic sampling was conducted to monitor dissolved Fe(II) and pH (see analytical techniques below). In order to simulate AMD intrusion, these microcosms were run in a semi-continuous fashion (188), whereby once approximately 95% or greater of the dissolved Fe(II) was removed from solution, 25 mL of the fluid layer from each microcosm environment was removed and replaced with 25 mL of filter-sterilized Synthetic Acid Mine Drainage (SAMD) (Senko, 2008). One liter of SAMD consisted of 0.5 mM $\text{Al}_2(\text{SO}_4)_3$, 5 mM CaSO_4 , 4 mM MgSO_4 , 0.4 mM MnSO_4 , 1 mM Na_2SO_4 , and 0.1 mM $(\text{NH}_4)_2\text{Fe}(\text{SO}_4)_2$, and was pH adjusted to 3.5 using 1 M H_2SO_4 (200). While SAMD is usually prepared with FeSO_4 as well (Senko, 2008), this was prepared and added to each microcosms separately (1 mL of filter sterilized 500 mM FeSO_4) after the 25 mL of SAMD was added. A total of 3 replacements was achieved in each of the microcosm environments described above (except for the sterile 'pristine' soil and filter-sterilized MF AMD microcosm).

Soil/Iron Sediment/AMD Microcosms to Evaluate Microbial Community Response to AMD Intrusion

Long-term microcosm environments to evaluate microbial community response to sustained AMD intrusion were established and maintained for 24 days. These microcosms consisted of adding either 5 g 'pristine' soil, 5 g MF iron mound sediment, or a combination of 4 g 'pristine' soil amended with 1 g MF iron

mound sediment to sterile 125 mL Erlenmeyer flasks capped with aluminum foil. Next, fresh, non-sterile MF site AMD (50 mL) was added to each incubation type. A total of three experimental incubations were conducted for each microcosm type, while controls (1% v/v formaldehyde deactivated) were run in duplicate for each of the microcosm types. Periodic sampling was conducted to measure dissolved Fe(II) and pH (see analytical techniques below). As with the previous microcosms, these incubations were run in a semi-continuous fashion (188) based on Fe(II) oxidation rates. Every two days (which corresponded to approximately 95% or greater removal of dissolved Fe(II) from solution), approximately 50% of the total fluid volume from each incubation was removed and replaced with filter sterilized MF site AMD. Every sixth day, 50% of the fluid volume from each microcosm incubation was removed and replaced with fresh, non-sterile AMD from the Mushroom Farm. On days 0, 6, 12, 18, and 24, sediment slurry samples were taken (approximately 0.5 mL per microcosm at each time point) for enumerations of Fe(II) oxidizing bacteria (FeOB), and samples were also taken from each microcosm for nucleic acid based analysis of microbial communities (approximately 5 mL from each microcosm at each indicated time point). These samples were stored at -80°C until further processing.

Analytical Techniques (Dissolved Fe(II) and pH Measurements)

During periodic intervals of the microcosm environments described above, samples were obtained for pH and dissolved Fe(II) analysis. Samples taken for pH measurements (0.8 mL each) were measured using an Orion 370 PerpHect pH meter (ThermoFisher Scientific, Waltham, MA). For dissolved Fe(II) analysis, samples were analyzed colorimetrically with Ferrozine assay described previously (149, 150, 217). Briefly, 0.2 mL of solution was taken from each incubation periodically, centrifuged (to remove unwanted soil/iron sediment), and then 0.05 mL of the resulting supernatant was preserved by acidification with 0.45 mL of 0.5 M HCl. From each of these, 0.02 mL was removed and added to a cuvette that contained 1 mL of ferrozine solution (1 g Ferrozine reagent (217) per 1 L of 50 mM HEPES buffer) (149, 150). Absorbance was measured using a Helios Zeta UV-vis spectrophotometer (ThermoFisher Scientific, Waltham, MA) preset to measure at a wavelength of 562 nm (217). Upon obtaining absorbance values, dissolved Fe(II) concentrations were calculated (accounting for HCl dilutions) by comparing to known Fe(II) standards (0 mM, 0.025 mM, 0.1 mM, 0.25 mM, 0.5 mM, and 1 mM). First-order kinetic rate constants were determined for Fe(II) oxidation rates in each microcosm environment after each replacement with either SAMD (200), filter-sterilized MF AMD, or non-sterile MF AMD. This was achieved by plotting Fe(II) concentrations versus time and using least-squares linear regression analysis with the following equation (200):

$$\ln[Fe(II)_t] = -kt + \ln [Fe(II)_{initial}]$$

Iron(II) Oxidizing Bacteria (FeOB) Enumerations

Sediment slurry samples taken on days 0, 6, 12, 18, and 24 of long term soil/iron sediment/AMD incubations were used for culture dependent enumerations of Fe(II) oxidizing bacteria (FeOB). Samples taken were serially diluted in a prepared solution which consisted of 1.25 g/L $(\text{NH}_4)_2\text{SO}_4$ and 0.5 g/L MgSO_4 , pH adjusted to 4.0 with 1 M H_2SO_4 . Serial dilutions were spread (triplicate plates for each sample from each microcosm replicate) onto FeTSB medium plates (113, 118) which use Fe(II) as an electron donor. These FeTSB plates consisted of (per 1 liter): 1.25 g of $(\text{NH}_4)_2\text{SO}_4$, 0.5 g of MgSO_4 , 0.25 g of tryptic soy broth without glucose, 5 mL of a 200x stock vitamin solution and 5 mL of a 200x trace metal solution prepared as previously described (224, 241), 25 mM FeSO_4 , and 10 g of agarose as a solidifying agent. After spreading the serially diluted samples onto FeTSB plates, the plates were stored at room temperature with adequate moisture to prevent rapid drying out of the plates for approximately 3 weeks. Plates were closely monitored and colony forming units (CFUs) were enumerated based on the appearance of FeOB, which were distinguishable as very small red/orange colonies.

Culture Independent Nucleic Acid-Based Microbial Community Analysis

Field materials collected at the Mushroom Farm (i.e., 'pristine' soil, iron mound sediment, and one-third of the 0.2 μm filter membrane with 1L of immobilized AMD), sediment slurry samples from days 0, 6, 12, 18, and 24 of

microcosm incubations, and the depth core were all first removed from the -80°C freezer. The polypropylene core tube was sliced open using a small rotating saw. Due to the frozen nature of the core, the outer portion of the core in the two halves of the polypropylene tube adhered to the walls following sectioning, exposing only the middle of the core. Using a sterile spatula, 1 cm intervals of the interior of the core (to a depth length of 10 cm) were removed and placed into sterile 50 mL conical tubes. Prior to DNA extractions, core depths, MF iron mound sediment, and sediment slurry samples from the various time points listed above were first treated with 0.3 M ammonium oxalate washes (buffered to pH 3 with oxalic acid) to remove as much Fe(III) deposits as possible, as Fe(III) phases are known to interfere with DNA extraction protocols (172, 200). Fe(III) removal was noted based on lack of orange color to pelleted sediment and absence of neon green supernatant following centrifugation, and was achieved after approximately one to three 24-hour wash periods (at room temperature, in foil rapped tubes, with slight agitation (100 rpm shaking)). Following 0.3 M ammonium oxalate washes, samples were rinsed three times with sterile deionized water and prepared for DNA extraction processing.

DNA extraction for all materials listed above was performed using the MoBio Power Biofilm DNA isolation kit (MoBio Laboratories, Inc., Carlesbad, CA) according to manufacturer's protocols. Extracted DNA was then shipped to Molecular Research Laboratories, LP (Shallowwater, TX) for partial 16S rRNA gene sequencing by means of bacterial tag-encoded FLX amplicon

pyrosequencing (bTEFAP) (61). Briefly, universal primer pairs (515F and 806R) designed from the 16S rRNA gene sequence from *Escherichia coli* (34) were used in a 30 cycle, single-step PCR run utilizing the HotStarTaq Plus Master Mix Kit (Qiagen, Valencia, CA) with the following cycle parameters: an initial denaturation step of 94°C for 3 minutes, followed by 28 cycles at 94° C (30 seconds), 53°C (40 seconds), and 72° C (1 minute). A final elongation step occurred at 72°C for five minutes. All PCR amplified gene products were purified and mixed in equal concentrations using Agencourt Ampure beads (Agencourt Bioscience Corporation, MA, USA). Finally, sequencing was performed on PCR amplicons using Roche 454 FLX titanium instruments and reagents (Roche Diagnostics Corp., Indianapolis, IN).

Sequences obtained were screened and processed by first removing all primers and barcodes, followed by discarding sequences that contained fewer than 200 base pairs, ambiguous base calls, greater than 6 base pair homopolymers, and/or chimeras (89). Sequence libraries were generated and submitted to the Sequence Read Archive (SRA) using the accession numbers and code designations shown in Tables 2.1 & 2.2. After initial screening, further sequence analysis and processing for all 16S rRNA gene sequence libraries obtained was performed utilizing the Qualitative Insights Into Microbial Ecology (QIIME) software (33) using default parameters in the MacQIIME (<http://www.wernerlab.org/software/macqiime>) environment. While still in the MacQIIME environment, QIIME scripts (66) were used to assign operational

taxonomic units (OTUs) based on 97% sequence similarity ($OTU_{0.03}$), upon which taxonomic assignment was performed using the RDP-II classifier function (236).

For MF site materials and microcosm incubations, standard rarefaction curves (97% sequence similarity) and Shannon diversity indices were generated in the QIIME environment based on rarefied sequence libraries (6240 sequences). A single phylogenetic tree was generated in FastTree 2 (182) by taking OTU sequences and aligning them against the Greengenes core set (57) using the Python Nearest Alignment Space Termination (PyNAST) algorithm (32). The weighted UniFrac metric (151, 152) was used to generate distance matrices based on Jack-knife sampling techniques and iterative rarefaction of 6573 sequences (MF site materials and microcosm incubations) based on $OTU_{0.03}$ tables obtained from each sample. Principle coordinate analysis (PCoA) was then used based on the weighted UniFrac distance matrix (151, 152) in order to discern any noticeable temporal shifts in microbial community structure for the long term microcosm environments. Using the Basic Local Alignment Search Tool (BLASTn), abundant $OTU_{0.03}$ phyla in sequence libraries were compared to similar sequences contained in the National Biotechnology Information (NCBI) database (7).

For core depth interval samples, screened 16S rRNA gene sequence libraries were uploaded into the Ribosomal Database Project-II (RDP-II) Pyrosequencing Pipeline (40), Shannon and Chao1 species diversity indices were determined, and standard rarefaction curves based on 97% similarity

sequence similarities were generated. In addition, sequences were aligned in the QIIME environment using the PyNAST algorithm (32) against the Greengenes core set (57) to construct a single phylogenetic tree based on OTU_{0.03} obtained from each depth interval. Using each depth interval's OTU_{0.03} table, iterative rarefaction of 7844 sequences by means of jack-knifing sample selection was performed. Based on the results, weighted and unweighted UniFrac metrics were used to generate distance matrices (152). In addition, distance matrices generated were used to evaluate potential microbial community clustering at varied depth intervals using unweighted pair group method with arithmetic mean (UPGMA) trees (152).

Results/Discussion

Fe(II) Oxidation Rates and Associated pH Changes in 'Pristine' Soil Exposed to AMD

In order to evaluate the microbial influence on Fe(II) oxidation rates when 'pristine' soil from the MF is exposed to AMD intrusion, microcosm incubations were established and operated under 'semi-continuous' flow conditions (188), whereby approximately 50% of the fluid layer was replaced with SAMD (200) after $\geq 95\%$ dissolved Fe(II) oxidation occurred. Fe(II) oxidation rates continued to increase with a concomitant pH decrease in microcosm incubations (Figure 2.3). Incubations that consisted of non-sterile 'pristine' soil exposed to non-sterile AMD had the greatest initial rate of Fe(II) oxidation (Figure 2.3A), where Fe(II)

oxidation was lowest in incubations containing heat-deactivated 'pristine' soil and filter-sterilized AMD (Figure 2.3D). Initial rates of Fe(II) oxidation were relatively low in microcosm environments that contained non-sterile 'pristine' soil and filter-sterilized AMD (Figure 2.3B) and heat-deactivated 'pristine' soil and non-sterile AMD (Figure 2.3C), however rates continued to increase upon continuous exposure to AMD following SAMD (200) fluid replacements. Further, all incubations containing either non-sterile 'pristine' soil and/or non-sterile AMD (Figure 2.3A-C) had a steady increase in Fe(II) oxidation rates as opposed to the microcosm environment containing sterile 'pristine' soil and filter-sterilized AMD (Figure 2.3D). A continuous decrease in pH coupled with a simultaneous increase in Fe(II) oxidation rates in microcosms that initially consisted of some non-sterile component ('pristine' soil or AMD), suggests that enhanced oxidative precipitation of dissolved Fe(II) at the Mushroom Farm is influenced by certain Fe(II) oxidizing microorganisms that inhabit both MF site soil that has never been previously exposed to AMD, as well as metabolically similar microorganisms found in MF AMD.

Microbiological Activities of Long-Term Microcosm Incubations Consisting of Combinations of Soil/Iron Mound Sediment/AMD

In order to better understand the development of 'pristine' soil microbial activities in response to continued AMD exposure, long-term (24 day) microcosm environments were established and maintained under 'semi-continuous' flow

conditions (188). Specifically, microbial activities of 'pristine' soil were compared to parallel microbial activities in mature iron mound sediment when both were exposed to AMD. The microbial activities in microcosm incubations that contained solely mature iron mound material and AMD were viewed as the potential trajectory that a parallel 'pristine' soil microbial community may reach upon continued exposure to AMD. In addition, in order to examine if iron mound sediment could augment 'pristine' soil microbial activities (i.e., by increasing the level of Fe(II) oxidizing bacteria communities and associated metabolic activities), microcosms were established that contained 'pristine' soil supplemented with mature iron mound sediment and exposed to AMD.

Microcosm incubations consisting of iron mound sediment/AMD showed oxidation of dissolved Fe(II) with a simultaneous decrease in pH (Figure 2.4A,D), suggesting dissolution of Fe(II) into Fe(III)-(hydro)oxides (see Reactions 2 and 3 in Chapter I). A continued increase in first-order rate constants for dissolved Fe(II) oxidation for iron mound material/AMD incubations was observed for the first five fluid exchanges, but eventually stabilized at a rate of approximately 0.17 day (d)⁻¹ (Figure 2.4G). Culturable FeOB remained relatively consistent at approximately 10⁴ CFU/mL (Figure 2.4G) in incubations containing iron mound material/AMD, suggesting that FeOB communities are relatively robust in iron mound sediment and AMD collected from the MF. In microcosms that consisted initially of 'pristine' soil/AMD, Fe(II) oxidation also occurred with a concomitant decrease in pH (Figure 2.4 B,E). However, this decrease in pH was noticeably

smaller than that seen in microcosm incubations containing iron mound sediment/AMD (Figure 2.4D, E). First order rate constants for dissolved Fe(II) oxidation in 'pristine' soil/AMD increased until about the sixth fluid replacement, eventually plateauing at approximately 0.17 d^{-1} around day twelve of incubation (Figure 2.4H). As rates of Fe(II) oxidation continued to increase throughout incubation, FeOB in 'pristine' soil/AMD environments also increased reaching approximately 10^3 CFU/mL following 24 days of sustained AMD exposure (Figure 2.4H). In incubations that consisted of 'pristine' soil supplemented with iron mound sediment (and exposed to AMD), dissolved Fe(II) oxidation continued as pH values continued to decrease (Figure 2.4C,F). First order rate constants for dissolved Fe(II) oxidation for 'pristine' soil seeded with iron mound sediment continued to increase throughout incubation, and appeared to be leveling off around approximately day 22 of incubation (approximately 0.25 d^{-1}) (Figure 2.4I). In addition, as dissolved Fe(II) oxidation rates continued to increase in 'pristine' soil seeded with iron mound sediment incubations, culturable FeOB also continued to increase eventually reaching approximately 10^4 CFU/mL by day 24 of incubation (Figure 2.4I). In the microcosm environments that contained 'pristine' soil, Fe(II) oxidation rates appeared to increase more rapidly than microcosm incubations containing only iron mound sediment (Figure 2.4A-C). However, the formaldehyde-deactivated controls in both microcosm types that consisted of 'pristine' soil also saw continuous rates of Fe(II) oxidation, suggesting that in soil containing microcosms, Fe(II) oxidation is most likely

mediated by abiotic processes and adsorption of Fe(II) to solid iron phases, specifically within the first 10 days of incubation (Figure 2.4A-C).

Noticeably between the three AMD microcosm environments established (iron mound material only, 'pristine' soil only, and 'pristine' soil supplemented with iron mound), the two microcosms that contained 'pristine' soil exhibited similar trends in dissolved Fe(II) oxidation and associated concomitant pH decrease (Figure 2.4B,C,E,F). However despite this similarity, overall rates of Fe(II) oxidation were markedly greater in the microcosms that contained 'pristine' soil supplemented with iron mound sediment (Figure 4H,I). Further, the 'pristine' soil supplemented with iron mound sediment microcosms saw a more rapid (and robust) increase in culturable FeOB than microcosms consisting of only 'pristine' soil (Figure 2.4H,I). In fact, levels of FeOB in incubations that contained 'pristine' soil seeded with iron mound sediment reached abundances similar to those found in microcosms that contained only iron mound sediment (Figure 2.4G,I). Overall, these data suggest that microbial communities are present in MF 'pristine' soil that are capable of efficient Fe(II) oxidative activities. Furthermore, these Fe(II) oxidizing microbial communities (and associated metabolic activities) can be enhanced by the addition of mature iron mound sediment that contains a robust community of FeOB that can further aid in the precipitation of dissolved Fe(II) from AMD waters.

Nucleic Acid Based Analysis of MF 'Pristine' Soil, Iron Mound Sediment, and AMD

Next generation sequencing (454 pyrosequencing) of partial 16S rRNA gene sequences was performed on starting materials for long term microcosm experiments which included 'pristine' soil (soil that had not previously been exposed to AMD intrusion), iron mound sediment, and AMD from the Mushroom Farm. Numbers of 16S rRNA gene sequences as well as Sequence Read Archive (SRA) accession numbers for sequence libraries are provided in Table 2.1 for 'pristine' soil, iron mound sediment, and AMD. Shannon diversity indices were lower for iron mound sediment and AMD compared to Shannon diversity indices for 'pristine' soil (Figure 2.4J,K,L). In addition, standard rarefaction curves based on 97% sequence similarity of 16S rRNA gene sequences showed greater number of OTU_{0.03} per number of sequence reads for 'pristine' soil compared to iron mound sediment or AMD (Figure 2.5). The results from these two species diversity indicators (Shannon indices and standard rarefaction curves) suggest that microbial species diversity is lower in MF iron mound sediment and AMD than the diversity found in 'pristine' MF soil that had not previously been exposed to AMD. Low levels of microbial species diversity are in fact common among AMD-impacted systems (12, 94). Examining microcosm 'starting' materials for relative abundances and phylotype distribution, 16S rRNA gene sequences recovered from MF 'pristine' soil consisted of a wider variety of phylotypes based on OTU_{0.03} gene sequence libraries compared to relative abundances (and

phylotypes) of either iron mound sediment or AMD (Figure 2.6). The most prominent phyla represented (based on relative abundances) for 'pristine' soil were the Proteobacteria, Planctomycetes, Chloroflexi, Acidobacteria, and Actinobacteria. These phyla have been shown to represent the dominant phyla in other similar soil surveys, however the relative abundances in the present study of MF soil microorganisms were more uniform when compared to the relative abundances of the same phylotypes from other similar soil studies (68, 137, 204). Within iron mound sediment 16S rRNA gene sequences specifically, it was observed that the dominant phyla represented by these sequences was the Gammaproteobacteria (63% relative abundance) (Figure 2.6). Sequences recovered from AMD showed that the two dominant phyla to which 16S rRNA gene sequences belonged were the Betaproteobacteria and the Euryarchaeota (collectively comprising 67% relative abundance) (Figure 2.6). More specifically, one OTU_{0.03} from within the Euryarchaeota constituted 66% of the Euryarchaeota sequences recovered from MF AMD (Figure 2.7A). Using the RDP-II classifier tool, this specific OTU_{0.03} was assigned to the Parvarchaea and has been identified from other AMD-impacted sites (13). In addition, two OTU_{0.03} comprised 59% of the Betaproteobacteria sequences recovered from MF AMD. These two OTU_{0.03} were identified as *Leptothrix ochracea* (75) and *Sideroxydans lithotrophicus* (239), both of which are neutrophilic iron oxidizing bacteria (Figure 2.7B,C).

Shifts in Microbial Communities Associated with Soil and Iron Mound Sediment in Response to Long-Term AMD Intrusion in Microcosm Environments

Using 454 pyrosequencing of 16S rRNA gene segments (average read lengths of approximately 290 bp), microbial communities were analyzed in each long term microcosm every six days to determine any shifts that may have occurred in microbial community structure in response to sustained AMD intrusion. More specifically, microbial community profiles were examined in soil/iron mound sediment microcosms to better understand if shifts in microbial communities were associated with the noticeable increase in Fe(II) oxidation rates in microcosm environments with increasing exposure to AMD. Based on Shannon indices, microbial diversity within microcosm environments containing only iron mound sediment remained relatively low (Figure 2. 4J). In microcosms that contained either only 'pristine' soil or 'pristine' soil supplemented with iron mound sediment, initial microbial diversity based on Shannon indices was relatively high (matching diversity levels observed in strictly 'pristine' soil), but decreased over time as these environments were further exposed to AMD intrusion (Figure 2.4K,L). Examining standard rarefaction curves for microcosm incubations, similar trends were noticed. Microcosms containing only iron mound sediment had consistently low numbers of OTU_{0.03} throughout the twenty four day exposure to AMD (Figure 2.5). Microcosms containing only 'pristine' soil or 'pristine' soil augmented with iron mound material had initially high numbers of OTU_{0.03} but decreased over the twenty four day incubation period (Figure 2.5).

These diversity metrics together (Shannon indices and standard rarefaction curves) suggests that the harsh environmental conditions of AMD intrusion into natural microbial communities found in 'pristine' soil causes a dynamic population shift toward a smaller fraction of AMD tolerant microorganisms capable of surviving in such abrasive conditions.

Further investigation into microbial community shifts was carried out by Principal Coordinate Analysis (PCoA) using the UniFrac metric. Microbial diversity associated with Initial starting materials (i.e., 'pristine' soil, iron mound sediment, and AMD) was compared to each microcosm environment ('pristine' soil only, iron mound sediment only, and 'pristine' soil seeded with iron mound sediment) with increasing time of AMD exposure. Principal coordinate analysis showed very little deviation in microbial community structure in long term incubations containing only iron mound sediment exposed to AMD. In fact, regardless of incubation time with AMD (over the course of 24 days), those microcosms consisting only of iron mound sediment had diversity levels that clustered relatively close to microbial diversity levels of iron mound sediment that was collected from the Mushroom Farm (Figure 2.8). As seen with both Shannon indices and standard rarefaction curves, microbial diversity associated with microcosms containing only 'pristine' soil only or 'pristine' soil supplemented with iron mound sediment initially had diversity similar to that found in 'pristine' soil from the Mushroom Farm that had not previously been exposed to AMD intrusion (Figure 2.8). However, with increased time of AMD incubation, microbial

community diversity in 'pristine' soil containing microcosms appeared to follow a trajectory along PCo1 toward iron mound sediment and iron mound sediment incubations. More specifically, this trajectory (based on PCo1) appeared to be enhanced in 'pristine' soil containing microcosms that were supplemented with iron mound sediment (Figure 2.8). Comparing the number of shared OTU_{0.03} between long term incubation starting materials against each long term microcosm incubation environment, it was observed that shared number of OTU_{0.03} between 'pristine' soil and microcosms containing iron mound sediment exposed to AMD remained very low during the entire twenty four day incubation period (Figure 2.9A). Initially, number of shared OTU_{0.03} between 'pristine' soil and microcosm environments containing 'pristine' soil only or 'pristine' soil seeded with iron mound material was relatively high, however continued to decrease with sustained exposure of AMD to each microcosm (Figure 2.9A). Shared OTU_{0.03} between iron mound sediment and iron mound sediment only incubations deviated only slightly early during sustained AMD exposure, however remained fairly stable beginning around day twelve (Figure 2.9B). Interestingly however, number of shared OTU_{0.03} between iron mound sediment and 'pristine' soil containing incubations continued to increase with sustained exposure to AMD (Figure 2.9B). Noticeably, the increased number of shared OTU_{0.03} between iron mound sediment and incubation type occurred more rapidly in incubations that contained 'pristine' soil that was supplemented with iron mound sediment. Shared number of OTU_{0.03} between AMD and all three microcosm environments

remained relatively similar (beginning at approximately day six) throughout the twenty four day incubation period (Figure 2.9C). These results together suggest that continued exposure of 'pristine' soil to AMD causes the native soil microbiome to shift towards a microbial communities that more closely resembles those found in mature iron mound sediment. Further, it appears as though this community shift can be enhanced when 'pristine' soil is seeded with iron mound material (i.e., a fraction of an already well established iron mound sediment microbial community).

Comparison of taxonomic diversity using 16S rRNA gene sequences recovered from each microcosm environment every six days throughout the twenty four day incubation period was performed to evaluate phylotype diversity and microbial community shifts in response to sustained AMD intrusion. Incubations that contained only iron mound sediment demonstrated very little change in microbial community structure despite continued exposure to AMD (Figure 2.6). In sequence libraries generated for microcosms that contained only iron mound sediment, the Gammaproteobacteria represented the dominant phylum represented. More specifically, 90% of the Gammaproteobacteria assigned phlotypes belonged to *Metallibacterium* sp. X11 (Figure 2.7D). *Metallibacterium* sp. X11, and the other closely related acidophilic strains *M. scheffleri*, A4F5, WJ2, and YE-D1-10-CH represent a group of organisms that are all capable of aerobic Fe(II) oxidation as well as Fe(III) reduction (Figure 2.7D) (54, 242). This ability of iron mound sediment microorganisms to resist any

large scale shifts brought on by the addition of AMD-associated microbial communities suggests that microorganisms found in mature iron mound material are well adapted to sustained AMD intrusion, and that AMD microbial communities have little effect on the microbiome of these already established iron mound microbial communities. This is further suggested by the fact that two neutrophilic organisms capable of metabolic Fe(II) oxidation (*L. ochracea* and *S. lithotrophicus*) initially detectable in the starting AMD material continued to decrease in iron mound sediment incubations over the twenty four day microcosm incubation period (75, 239) (Figure 2.7B,C).

In incubations that consisted of 'pristine' soil mixed with AMD, continued exposure to the 'pristine' soil with AMD revealed increases in certain taxonomic groups based on recovered 16S rRNA gene sequences, including phylotypes attributable to the Gammaproteobacteria, Betaproteobacteria, and most notably the Firmicutes (Figure 2.6). Inclusive to the Gammaproteobacteria, these microcosm incubations with only 'pristine' soil and AMD consisted of OTU_{0.03} attributable to *Metallibacterium* spp. X11 (54) that increased overtime, though not to the same extent as seen in the iron mound sediment incubations with sustained AMD exposure (Figure 2.7D). Interestingly however, Gammaproteobacteria recovered from the 'pristine' soil and AMD incubations did consist of a large relative abundance of OTU_{0.03} of a closely related acidophilic iron oxidizing bacterium A4F5 (242) that continued to increase with sustained AMD exposure (Figure 2.7E). Within the Betaproteobacteria, an OTU_{0.03}

belonging to the acidophilic iron oxidizing bacterium *Ferrovum myxofaciens* (117) was recovered and showed continued increase in relative abundance with sustained AMD exposure to 'pristine' soil incubations (Figure 2.7F). This increase in relative abundance for the OTU_{0.03} attributable to *F. myxofaciens* (117) was noticeably similar to the increase of the same OTU_{0.03} found in iron mound sediment and AMD incubations (Figure 2.7F). Another OTU_{0.03} representing the Betaproteobacteria that continued to increase in relative abundance with AMD exposure time in 'pristine' soil only microcosm incubations was that of the acidophilic FeOB C4C6 (242) (Figure 2.7G). Despite having increased in relative abundance in 'pristine' soil only incubations, this OTU_{0.03} attributable to FeOB C4C6 (242) did not comprise a significant fraction of the relative abundance of the Betaproteobacteria recovered from iron mound sediment only incubations (Figure 2.7G). Lastly, within the Betaproteobacteria, OTU_{0.03} attributed to *Herbispirillum* sp. T59 (108) and *H. huttiense* (59) represented an initially small relative abundance within 'pristine' soil incubations exposed to AMD, but began to increase in relative abundance with sustained AMD exposure (specifically beginning around day 18 of incubation with AMD) (Figure 2.7H). These OTU_{0.03} attributable to *Herbispirillum* spp. (59, 108) were found to contribute a somewhat larger initial fraction of the Betaproteobacteria within incubations consisting of iron mound sediment and iron mound seeded 'pristine' soil incubations, and though an initial increase in relative abundance was observed, a decrease in relative abundance was observed beginning around day 18 of AMD exposure

(Figure 2.7H). In fact, relative abundance for these OTU_{0.03} attributable to *Herbispirillum* spp. (59, 108) all appeared to reach approximately similar relative abundances in all three microcosm environmental types by day 24 of continued incubation with AMD. However, the contributions of such organisms with respect to Fe(II) metabolism in acidic settings still remains unclear primarily because these *Herbispirillum* spp. are predominantly found in circumneutral pH environments (59, 108). Lastly, the OTU_{0.03} comprising the significant portion of the Firmicutes phylotypes recovered from 'pristine' soil microcosms exposed to AMD were attributable to *Bacillus* spp. (1, 109, 140, 161) (Figure 2.7I). While representing the dominant phylotype within the Firmicutes sequences recovered, the total relative abundances of these *Bacillus* spp. did not appear to change much despite 'pristine' soil being continuously exposed to AMD over 24 days. In fact, the relative abundance of OTU_{0.03} attributable to *Bacillus* spp. recovered from 'pristine' soil only incubations and associated lack of change in relative abundance was very similar to that of similar OTU_{0.03} recovered from iron mound only incubations that were continuously subjected to AMD (Figure 2.7I). This lack of change in relative abundance within the Firmicutes is most likely due to the spore forming nature of *Bacillus* spp., such that the spores are able to remain dormant in such harsh geochemical conditions (i.e., relative abundances would remain similar throughout despite continuous exposure to AMD).

Evaluation of taxonomic diversity based on 16S rRNA gene sequences recovered from incubations consisting of 'pristine' soil supplemented with iron

mound sediment and exposed to AMD revealed similar taxonomic patterns to that of 'pristine' soil only microcosm environments. The primary relatively abundant phyla that showed continued increase in relative abundance with sustained AMD exposure in iron mound seeded 'pristine' soil incubations were the Gammaproteobacteria, Firmicutes, and Betaproteobacteria (Figure 2.6). As seen in the 'pristine' soil only microcosm environments, the dominant phylotypes represented from the Gammaproteobacteria and Betaproteobacteria in iron mound seeded 'pristine' soil incubations consisted of acidophilic, iron oxidizing bacteria, while phylotypes attributable to the Firmicutes were most closely related to *Bacillus* spp. (Figure 2.7). Despite 'pristine' soil supplemented with iron mound sediment incubations showing similar patterns of relative abundance increase to those found in 'pristine' soil only incubations, the relative abundance of Gammaproteobacteria in 'pristine' soil supplemented with iron mound sediment increased observably quicker (and to a greater proportion) than observed in 'pristine' soil only incubations (Figure 2.6). This noticeable rapidity in increased relative abundance in iron oxidizing Gammaproteobacteria is likely due to the inherently high proportion of Gammaproteobacterial communities found in iron mound sediment (Figure 2.6). Thus, these results suggest that augmentation of 'pristine' soil with a fraction of well established iron oxidizing microbial communities found in iron mound sediment can enhance the development of already existent natural populations of iron oxidizing bacteria found in 'pristine' soil, thereby ultimately leading to an overall increase Fe(II) oxidation rates.

Source of Microorganisms Responsible for Microbially Mediated Fe(II) Oxidation at the Mushroom Farm and Future Environmental Implications

Initial results of Fe(II) oxidation rates and associated pH changes from short term microcosm experiments consisting of non-sterile 'pristine' soil with non-sterile AMD, non-sterile 'pristine' soil with filter-sterilized AMD, heat-deactivated soil with non-sterile AMD, and heat-deactivated soil with filter-sterilized AMD suggested that the most rapid rates of Fe(II) oxidation were associated in environments that consisted of metabolically active microorganisms from both 'pristine' soil and AMD (Figure 2.3). Nucleic acid based analyses concurred with this observation such that recovered 16S rRNA gene sequences of phylotypes belonging to the Gammaproteobacteria and Betaproteobacteria from long term microcosms consisting of 'pristine' soil exposed to AMD for 24 days were also detected in mature iron mound sediment incubations. These relatively abundant phylotypes continued to increase with increased exposure time to AMD conditions (Figure 2.7D-G). It is very possible that such phylotypes, which were acidophilic in nature and capable of Fe(II) oxidation, may belong to what has been collectively described as components of the "rare biosphere" found in many different types of soil (68, 82, 210). Unique to note is that with continued AMD exposure time, OTU_{0.03} that were detectable in 'pristine' soil containing long-term microcosm incubations decreased with respect to OTU_{0.03} recovered from MF site 'pristine' soil. However as this decrease in shared similarity with 'pristine' soil phylotypes occurred (Figure 9A), OTU_{0.03} that were detected in MF mature iron mound sediment noticeably increased in 'pristine' soil

containing microcosm environments as these microcosms were exposed long-term to AMD conditions (Figure 2.9B). Despite an initial shared increase in OTU_{0.03} found in AMD to microcosm incubations containing 'pristine' soil, after day six, there was a continued decrease in shared number of OTU_{0.03} (Figure 2.9C). One of the more interesting findings was that a high relative abundance of Euryarchaeota was observable in 16S rRNA sequences recovered from MF AMD, however such phylotypes did not appear as significant proportions to the microbial diversity in any of the three microcosm environments, nor did the relative abundances for the Euryarchaeota change with any appreciation in any of the microcosm incubations despite increased exposure time to AMD (Figure 2.6). With regards to native 'pristine' soil microorganisms, two initially detectable neutrophilic, iron oxidizing phylotypes belonging to the Betaproteobacteria, *L. ochracea* and *S. lithotrophicus* (75, 239) were relatively abundant in 'pristine' soil containing incubations and increased up until day 6, then continued to decrease with increased AMD exposure time (Figure 2.7A,B). With the 'natural' pH of Mushroom Farm AMD flow being approximately 4.5 (91), coupled with the fact that surrounding 'pristine' soil pH is circumneutral, it is not surprising that the Betaproteobacteria *L. ochracea* and *S. lithotrophicus* were initially detectable and even showed a slight increase upon initial AMD exposure. However, as the pH of the microcosm environments began to decrease, such neutrophilic iron oxidizing communities began to die off, gradually being replaced by communities more tolerant to the harsh, acidified conditions of AMD. This was observed in all

microcosms containing 'pristine' soil. In such systems, as pH continues to decrease as a result of oxidative precipitation of dissolved Fe(II) (Figure 2.3, 2.4A-F), microorganisms capable of metabolic Fe(II) oxidation that favor harsher acidified conditions such as *Metallibacterium* and *Ferrovum* spp. began to increase in relative abundance upon sustained AMD exposure (Figure 2.7D-G).

Depth Dependent Analysis of Microbial Communities in Mature Iron Mound Sediment

Using a 10 cm core obtained through mature iron mound sediment obtained from the MF, 454 pyrosequencing was utilized to examine potential depth dependent gradients that may exist in microbial community structure. Recovered 16S rRNA gene sequences from each 1 cm interval beginning at the liquid/solid interface (i.e., AMD/solid iron mound sediment material) were approximately 264 bp in read length, with total recovered sequences ranging from between 7,844 to 18,385 (Table 2.3). Shannon and Chao1 non-parametric species diversity indices indicated very minimal species diversity throughout the 10 cm core sample of iron mound sediment (Table 2.3). This low communal species level diversity throughout the iron mound sediment is in stark difference to the greater levels of species diversity seen in soil collected from the Mushroom Farm that had not previously been exposed to AMD flow (Figure 2.4, 2.5, Table 2.3). Utilizing the weighted and non-weighted UniFrac metric (152), UPGMA trees were generated as a means to observe potentially microbial community

clustering in association with each 1 cm depth interval (Figure 2.10). UPGMA trees illustrated that depth dependent clustering does exist amongst microbial communities at various depths in the iron mound sediment. While the communities associated with the 1-2 cm depth interval were not observed to cluster with either 0-1 cm or 2-4 cm, there was an observable clustering of communities beginning at an approximate 4 cm depth and below. This demarcation in microbial community clustering for communities below the 4 cm depth mark is most likely attributable to an oxygen availability factor, such that microbial community profiles would appear similar based on total available oxygen for aerobically driven metabolism.

Based on 16S rRNA gene sequence libraries from each 1 cm depth through the 10 cm core of mature iron mound sediment, the Gammaproteobacteria represented the dominant relatively abundant phyla throughout the entire core (Figure 2.11). Beginning at a depth of approximately 2 cm all the way through approximately 9 cm, the relative abundance of the Gammaproteobacteria increased with depth (with a slight drop off at the 9-10 cm interval) (Figure 2.11). In addition to the Gammaproteobacteria, phylotypes attributable to Unclassified Bacteria, Chloroflexi, and Euryarchaeota also increased in relative abundances with increasing depth through the iron mound (Figure 2.11). Despite the Betaproteobacteria and to a lesser extent the Cyanobacteria representing a larger proportion of recovered 16S rRNA gene sequences from 0-4 cm, these phyla continued to decrease in relative

abundance with increasing depth (Figure 2.11). While other phylotypes ascribed to Actinobacteria, Acidobacteria, WPS-2, Firmicutes, and AD3 comprised between 1-5% each of total recovered 16S rRNA gene sequences, there were no detectable gradients of relative abundance distribution throughout the core depth (Figure 2.11).

Analyzing sequence libraries for each depth interval, it was found that $\geq 0.5\%$ of sequences in each library were represented by between 19-26 OTU_{0.03}, of which these OTU_{0.03} collectively represented 72-78% of the total sequences recovered for each depth interval library (Figure 2.12). More specifically, nine of the above mentioned OTU_{0.03} were found at levels $\geq 0.5\%$ throughout the entire core depth, and included phylotypes inclusive to the Gammaproteobacteria, Betaproteobacteria, Chloroflexi, Acidobacteria, AD3, and Unclassified Bacteria. Using the BLASTn feature in GenBank (7), these nine representative OTU_{0.03} were compared to nearest environmental 16S rRNA and nearest cultured 16S rRNA gene sequences in the GenBank database (Figure 2.12, Table 2.4) in order to better ascertain taxonomic identity. Approximately 96-100% sequence identity was matched between these nine OTU_{0.03} and sequences found in other AMD-type environments (Figure 2.12, Table 2.4).

Of the abundant OTU_{0.03} that were attributed to the Gammaproteobacteria, the RDP-II classifier tool identified the majority of them to belong to the order Xanthomonadales, which have been previously shown to be prominent in other AMD systems that contained iron mound formations (200). In addition, of the

OTU_{0.03} represented in the Gammaproteobacteria, the most abundantly represented phylotype found in high abundance regardless of core depth interval was matched (98-99% sequence similarity) to *Metallibacterium* sp. X11 and *M. schefferi* (Figure 2.12, Table 2.4). Both of these strains fall into a metabolically diverse group that also includes strains A4F5, WJ2, and YE3-D1-10-CH, which are acidophilic heterotrophs that are capable of both anaerobic Fe(III) respiration as well as lithotrophic respiration using either Fe(II) or reduced sulfur species as electron donors (43, 54, 154, 242, 251). The abundance of various iron species found throughout the iron mound sediment at the Mushroom Farm could explain the fact that these two strains (*Metallibacterium* sp. X11 and *M. schefferi*), which share similarity with organisms capable of metabolically utilizing both Fe(II) and Fe(III), are found at such high levels regardless of depth interval through the iron mound material. Despite Gammaproteobacteria phylotypes being prominent throughout the iron mound core, the well-known acidophilic iron oxidizer *Acidothiobacillus* was not found in high relative abundances throughout the core (Figure 2.12, Table 2.4). However, *Acidothiobacillus* phylotypes were found to comprise between 1.3-2.2% relative abundances in depth intervals below 4 cm (Figure 2.12, Table 2.4). Since *Acidothiobacillus* spp. are known facultative anaerobes (99), this could explain the high relative abundance of such species in depths of the iron mound where oxygen availability becomes depleted, and other anaerobic metabolic pathways may be favored.

Despite the fact that Cyanobacteria are not typically prominent in AMD-impacted systems (90), there was a substantial relative abundance of phylotypes representative of the Cyanobacteria within the top 3 cm of the core taken from the Mushroom Farm. These representative Cyanobacteria phylotypes were actually chloroplast 16S rRNA gene sequences from microeukaryotes capable of phototrophic metabolism (Figure 2.12, Table 2.4). Certain phototrophic microeukaryotes have been noted to be found in AMD environments (70, 191, 199), most notably *Euglena mutabilis* (2, 24, 25) which was the dominant organism represented from the phototrophic microeukaryote sequences recovered in the top 3 cm of iron mound sediment from the MF (Figure 2.12, Table 2.4). Relative abundances of phototrophic microeukaryotes were noticeably higher in the oxygen rich layers of the MF iron mound sediment, and tapered off as dissolved oxygen levels began to decrease (26), indicating the very likely possibility that these phototrophic microeukaryotes are responsible (in part) for the higher dissolved oxygen concentrations found in the upper layers of iron mound sediment. Specifically, relative abundances of phototrophic microeukaryotes began to fall (and stay low) beginning around the 2 cm depth interval, despite still being detectable to some degree even at lower depths in the iron mound core. It still remains unclear why such phototrophic microeukaryotes were found at lower depths of the iron mound sediment core. If light is still able to penetrate the iron mound sediment (the dynamics of such interactions is still unknown), then these phototrophic microeukaryotes at lower depths may still be

able to remain metabolically active. The more likely explanation is that as the iron mound has proceeded in a vertical growth, phototrophic microeukaryotes may have been trapped at lower depths, and essentially become entombed in the iron phases of the iron mound. As such, phototrophic microeukaryote DNA was still recoverable, but these organisms may not have been metabolically active (as would be suggested by the lowered dissolved oxygen content found at the lower depths of the iron mound) (26).

Using the RDP-II classifier tool, the most abundant OTU_{0.03} from the Betaproteobacteria were initially identified as neutrophilic, iron oxidizing *Gallionella* spp. (69) (Figure 2.12, Table 2.4). Yet BLASTn results for the same relatively abundant OTU_{0.03} identified these Betaproteobacteria as iron oxidizing “*Ferrovum*” spp. and *Leptothrix ocracea* (Figure 2.12, Table 2.4) (75, 98, 100, 228). The “*Ferrovum*” spp. identified from the iron mound sediment at the MF are known iron oxidizers that inhabit acidophilic environments (98, 100, 228). Such “*Ferrovum*” species have also been previously identified as abundantly prevalent phylotypes in other AMD-impacted systems similar in conditions as those found at the MF (29, 94).

Throughout the iron mound sediment core, phylotypes of both Chloroflexi and unclassified Bacteria were found throughout despite core interval, however were found in higher relative abundances at lower depths in the iron mound (Figure 2.12). Chloroflexi phylotypes have been identified in other AMD sites that exhibit similar iron mound formation characteristics (155, 200). The high relative

abundance of Chloroflexi at lower depths in the MF iron mound sediment core suggests that such Chloroflexi phylotypes may be capable of anaerobic metabolism. Further, the unclassified Bacteria sequences recovered from the iron mound sediment were 97-99% similar to sequences of other unclassified Bacteria recovered from AMD environments (Figure 2.12, Table 2.4). More specifically, noticeable percentages of OTU_{0.03} were attributable to unclassified Bacteria at lower depths in the iron mound sediment. As these lower depths in the iron mound sediment consist of more anoxic zones, it is possible that substantial communities of unclassified Bacteria capable of anaerobic metabolism are able to thrive at lower depths. These communities of 'unknown' bacteria represent a stark difference compared to the relatively well characterized microbial communities found in the more surface layers of iron mound sediments (8, 29, 200).

Two other phyla, the Euryarchaeota and Nitrospirae, were also found to increase in relative abundance with increasing depth in the iron mound core (specifically beginning below the 4 cm demarcation) (Figure 2.10). Phyloypes belonging to the Euryarchaeota were taxonomically identified more specifically as belonging to the class Thermoplasmata (Figure 2.12). Although Thermoplasmata contains *Ferroplasma* spp., which are obligate aerobes known to thrive in very low pH environments and are able to autotrophically oxidize Fe(II) (67, 87), the RDP-II classifier tool identified the dominant Euryarchaeota phylotypes recovered as similar to microorganisms that live in methanogenic sediments

(Figure 2.12, Table 2.4). This assignment suggests that at the lower, anoxic depths in the iron mound sediment, there could possibly be organisms participating in methanogenesis. Dominant phylotypes belonging to the Nitrospirae were identified taxonomically as belonging to the genus *Leptospirillum* (Figure 2.12). While *Leptospirillum* spp. are capable of Fe(II) oxidation and are found in low pH environments (95, 229), it is somewhat surprising that such species were found in a higher relative abundance at lower depths in the iron mound as the *Leptospirillum* spp. recovered are exclusively obligate aerobes (80). Presently, it still remains unclear as to why such obligate aerobes belonging to both Thermoplasmata and *Leptospirillum* are found in higher abundance at the lower anoxic depths in the iron mound sediment.

Although OTU_{0.03} attributed to the phyla WPS-2, AD3, Acidobacteria, and Firmicutes comprised between 1-5% of the total OTU_{0.03} relative abundance in sequences recovered from the iron mound core, there were no appreciable changes in relative abundances of these phyla regardless of depth in the iron mound (Figure 2.12). With respect to WPS-2 phylotypes, though further taxonomic clarity to the species level was not achievable, these phylotypes were shown to be similar to other phylotypes identified from sequences recovered from other AMD-impacted environments (Figure 2.12, Table 2.4). The phylotype belonging to AD3 was most closely related (99% sequences similarity) to the acidophilic Fe(II) oxidizing strain A10G4 (242). From the Acidobacteria, the most abundant phylotype was shown to be 97% similar to the acidophilic

organotrophic strain CH1, which was recovered from an AMD-impacted site (58). Lastly, Firmicutes associated phylotypes appeared to show heterogeneity in dispersal throughout the iron mound sediment (Figure 2.12, Table 2.4). The upper 4 cm of the iron mound was dominated by phylotypes ascribed to the acidophilic iron oxidizing and iron reducing strain iFeo-D4-31-CH that had previously been recovered from an AMD-impacted lake environment (154). One Firmicutes-phylotype that were found at relatively consistent levels regardless of depth in the iron mound sediment was most closely related to the thermoacidophilic bacterium *Alicyclobacillus acidoterrestris* C-ZJB-12-17 (250). One last OTU_{0.03} of significance belonging to the Firmicutes that was only detectable between the 8-10 cm depth interval, was shown to be most closely related to *Desulfosporosinus* sp. GBSRB4.2, a sulfate and Fe(III)-reducing strain that was recovered from a different iron mound forming AMD-system (201).

Conclusions

The data generated herein provide ample support for how naturally occurring communities of microorganisms in formerly 'pristine' soil respond to sustained AMD exposure. As formerly 'pristine' soil is exposed to AMD waters rich with dissolved Fe(II), naturally occurring communities of microorganisms respond in such a way that they shift from relatively abundant organotrophic communities towards communities dominated by acidophilic, Fe(II) oxidizing communities. This shift in community structure can be enhanced by

supplementing formerly 'pristine' soil with mature iron mound that already contains well developed communities of microorganisms capable of lithotrophic processes. Ultimately, microbial community structure, upon sustained exposure to AMD, consists of highly efficient Fe(II) oxidative populations, thereby leading to an efficient microbially mediated Fe(II) oxidizing system such as those found at other iron mound sites (29, 56, 136, 200). Further, this data demonstrates that as iron mound structures form under 'sheet flow' conditions, there are specific transitions that occur in microbial community structure as the iron mound 'matures.' Specifically for the Mushroom Farm, demarcation and clustering of microbial communities appears to occur for sequences recovered above and below the 4 cm depth interval in the iron mound sediment. As evidenced by sequence analysis, the upper layers of the iron mound were dominated by a microeukaryotic organism capable of photoautotrophy (i.e., *Euglena mutabilis*). Despite the most abundant phylotype throughout the iron mound including acidophilic Fe(II) oxidizing/Fe(III) reducing bacteria, the lower depths (beginning below 3 cm) of the 'mature' iron mound sediment consisted of phylotypes that were most closely related to organisms capable of metabolically thriving in anoxic environments. This suggests that as the iron mound evolved and succeeding layers were deposited, more anaerobic conditions developed in the lower strata, which in turn promoted the development of more robust microbial communities consisting of microorganisms capable of different types of anaerobic metabolism. Therefore, not surprisingly, the microbial community profile through the 10 cm

iron mound sediment core was correlated to the oxygen availability within the iron mound (26). As time progresses and the iron mound continues to grow due to appositional growth, it is very likely that oxygen availability will continue to influence microbial metabolism, thereby directly impacting the microbial community development at discrete depth intervals.

Ultimately, future promise exists with such iron mound systems in their capabilities of significant Fe(II) removal from dissolved AMD discharge without human intervention. Indeed, the hallmark of better understanding the dynamics associated with microbial communities associated with AMD impacted sites is to develop non-invasive, passive treatment options in order to generate a sustained model for AMD clean-up (29, 56, 136, 200). The data collected not only demonstrate the microbial dynamics associated with AMD intrusion, but also provide an avenue of exploration such that microbial communities taken from mature iron mound sites can be 'seeded' in an attempt to ameliorate the process of oxidative precipitation of dissolved Fe(II) from AMD flow. Therefore, data generated from these experiments can be used as a means to not only investigate other iron mound associated AMD sites, but also can serve as a way to develop more efficient (and affordable) techniques aimed at cleaning up contamination ascribed to acidic coal mine drainage.

Figures/Tables



Figure 2.1: The Mushroom Farm, an acid mine drainage (AMD) impacted site exhibiting 'sheet flow' characteristics located in Mahoning County, OH. A) AMD flows from a collecting 'pool' found on the side of the house on the property down a slight gradient of iron hydroxide crust. B) Thick iron hydroxide terraces (iron mounds) form as a result of iron (III) mineral phase deposition along the AMD flow path.



Figure 2.2: Various material collection sites at the Mushroom Farm. A) 'Pristine' soil collection location found on the property in an area that had not previously been exposed to AMD. B) Mature iron mound sediment collection site found along the AMD flow path. C) Emergent AMD collection site. [Panels A and C were reprinted (adapted) with permission from **Brantner, J.S. & Senko, J.M.** 2014. Response of soil-associated microbial communities to intrusion of coal mine-derived acid mine drainage. *Environmental Science and Technology* **48**:8556-8563. Copyright © 2014, American Chemical Society.] (27)

Sample	Number of Sequences	SRA accession #
Soil	6,573	SRR1207208
AMD	11,485	SRR1207206
Iron Mound	13,441	SRR1207207
Iron Mound incubation t=0 d	11,789	SRR1207209
Iron Mound incubation t=6 d	48,554	SRR1207210
Iron Mound incubation t=12 d	27,855	SRR1207211
Iron Mound incubation t=18 d	21,492	SRR1207212
Iron Mound incubation t=24 d	13,126	SRR1207213
Soil incubation t=0 d	10,877	SRR1207214
Soil incubation t=6 d	13,526	SRR1207215
Soil incubation t=12 d	12,590	SRR1207216
Soil incubation t=18 d	16,749	SRR1207217
Soil incubation t=24 d	9,206	SRR1207218
Soil + Iron Mound incubation t=0 d	9,031	SRR1207219
Soil + Iron Mound incubation t=6 d	13,084	SRR1207220
Soil + Iron Mound incubation t=12 d	9,667	SRR1207221
Soil + Iron Mound incubation t=18 d	9,779	SRR1207222
Soil + Iron Mound incubation t=24 d	14,843	SRR1207223

Table 2.1: Total number of partial 16S rRNA gene sequences acquired from each sample and designated Sequence Read Archive (SRA) accession numbers. Average sequence read length obtained from all sequence libraries was 290 bp. [Reprinted (adapted) with permission from **Brantner, J.S. & Senko, J.M.** 2014. Response of soil-associated microbial communities to intrusion of coal mine-derived acid mine drainage. *Environmental Science and Technology*, **48**(15), 8556-8563. Copyright © 2014, American Chemical Society.] (27)

Sample	Number of Sequences	Number of OTU _{0.03}	Chao1 Index	Shannon Index	SRA accession #
0-1 cm Depth Interval	18,385	668	994	4.44	SRR1206276
1-2 cm Depth Interval	14,350	457	737	4.02	SRR1206277
2-3 cm Depth Interval	10,718	522	824	4.35	SRR1206278
3-4 cm Depth Interval	8,654	523	653	4.09	SRR1206279
4-5 cm Depth Interval	8,529	423	491	3.99	SRR1206280
5-6 cm Depth Interval	15,694	673	968	4.49	SRR1206281
6-7 cm Depth Interval	13,553	652	866	4.53	SRR1206282
7-8 cm Depth Interval	8,204	498	637	3.98	SRR1206283
8-9 cm Depth Interval	7,844	366	418	3.91	SRR1206284
9-10 cm Depth Interval	17,645	637	936	4.33	SRR1206285

Table 2.2: Sequence Read Archive (SRA) accession numbers and associated number of 16S rRNA gene sequences, total number of Operational Taxonomic Units based on 97% sequence similarity (OTU_{0.03}), and Chao1 and Shannon species diversity indices generated from each indicated mature iron mound core depth interval. [Copyright © 2014 Brantner, Haake, Burwick, Menge, Hotchkiss and Senko] (26)

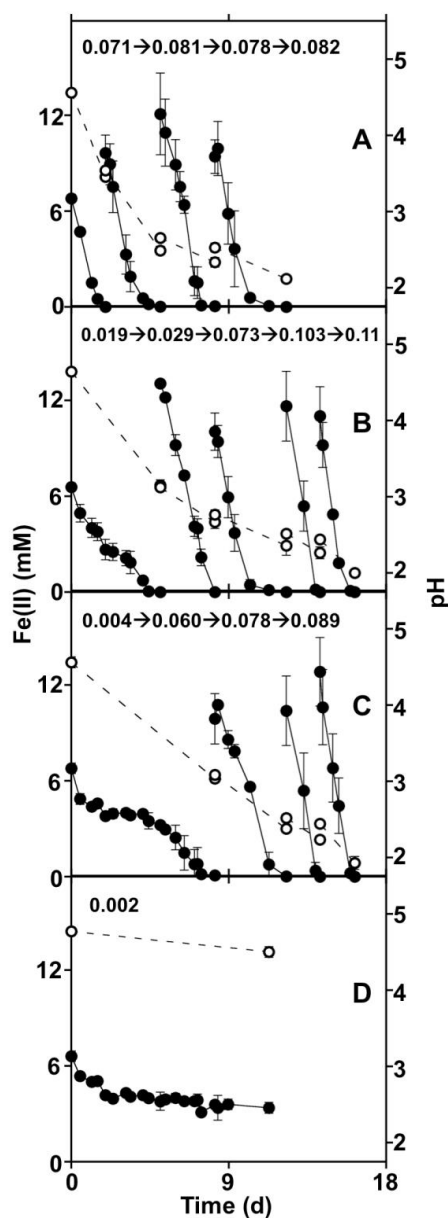


Figure 2.3: (●) Fe(II) concentrations and (○) pH values for semicontinuous incubations consisting of 'pristine' soil and AMD (A), 'pristine' soil and filter-sterilized AMD (B), heat-deactivated soil and AMD (C), and heat deactivated soil and filter-sterilized AMD (D). Numbers at the top of each panel correspond to first-order rate constants (k) of Fe(II) oxidation (d^{-1}) following SAMD replacements. Error bars represent \pm one standard deviation. [Reprinted (adapted) with permission from **Brantner, J.S. & Senko, J.M.** 2014. Response of soil-associated microbial communities to intrusion of coal mine-derived acid mine drainage. *Environmental Science and Technology* **48**:8556-8563. Copyright © 2014, American Chemical Society.] (27)

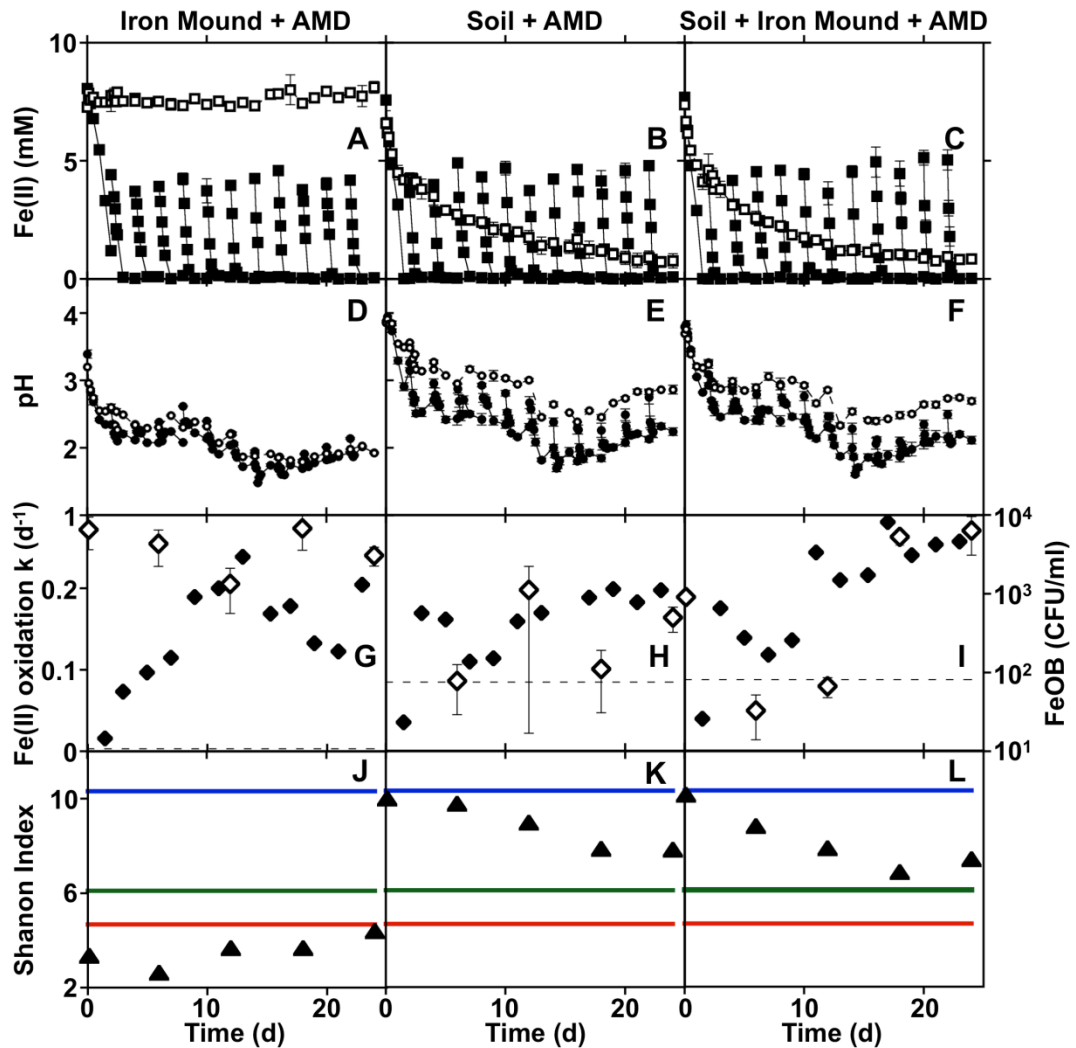


Figure 2.4: Fe(II) concentrations, pH values, Fe(II)-oxidizing bacteria (FeOB) counts, and Shannon species diversity index for long-term microcosm incubations to evaluate microbial activity in response to AMD intrusion. Microcosm incubation types are listed above each column. Fe(II) concentrations for non-sterile (■) and formaldehyde-deactivated controls (□) (Panels A-C). pH values corresponding to non-sterile (●) and formaldehyde-deactivated controls (○) (Panels D-E). First-order rate constants for Fe(II) oxidation (◆) after each microcosm exchange with AMD, and culturable FeOB abundances (◇) (Panels G-I). Shannon indices of species diversity for each microcosm environment at various time points of incubation (▲), and Shannon indices for 'pristine' soil (blue lines), AMD (green lines) and iron mound sediment (red lines) (Panels J-K). [Reprinted (adapted) with permission from **Brantner, J.S. & Senko, J.M.** 2014. Response of soil-associated microbial communities to intrusion of coal mine-derived acid mine drainage. *Environmental Science and Technology* **48**:8556-8563. Copyright © 2014, American Chemical Society.] (27)

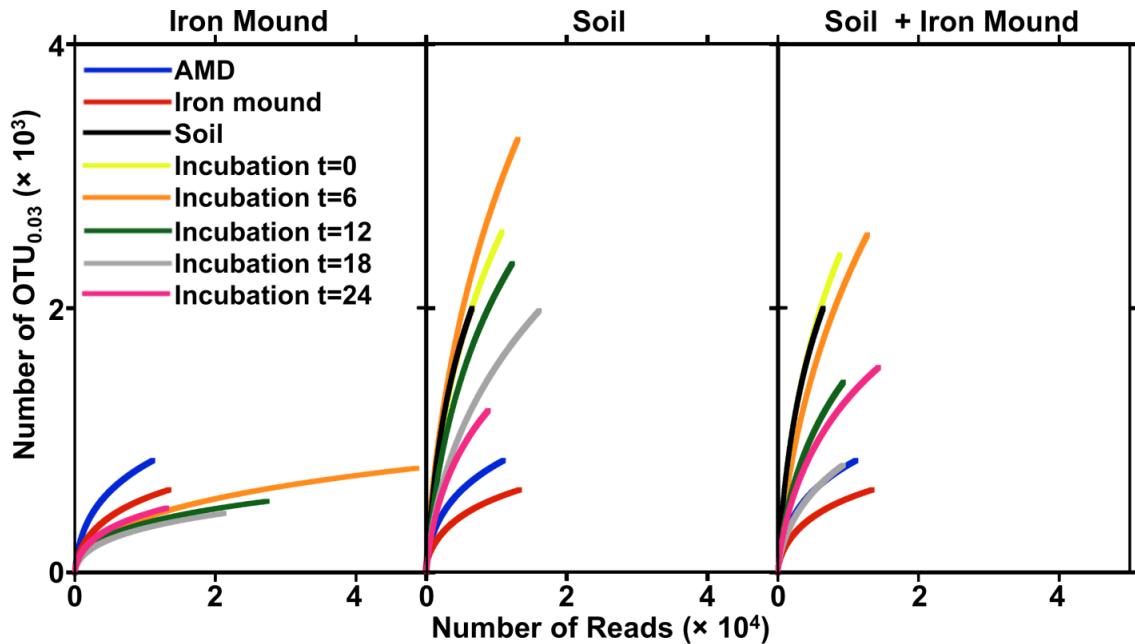


Figure 2.5: Ninety seven percent (97%) sequence similarity standard rarefaction curves of 16S rRNA gene sequence libraries obtained from AMD, iron mound sediment, 'pristine' soil, as well as for each long-term microcosm incubation type (iron mound sediment and AMD, 'pristine' soil and AMD, and 'pristine' soil supplemented with iron mound sediment and AMD) at incubation days 0, 6, 12, 18, and 24. Rarefaction curves were generated using the Ribosomal Database Project Pyrosequencing Pipeline (RDP-II) (40). [Reprinted (adapted) with permission from **Brantner, J.S. & Senko, J.M.** 2014. Response of soil-associated microbial communities to intrusion of coal mine-derived acid mine drainage. *Environmental Science and Technology* **48**:8556-8563. Copyright © 2014, American Chemical Society.] (27)

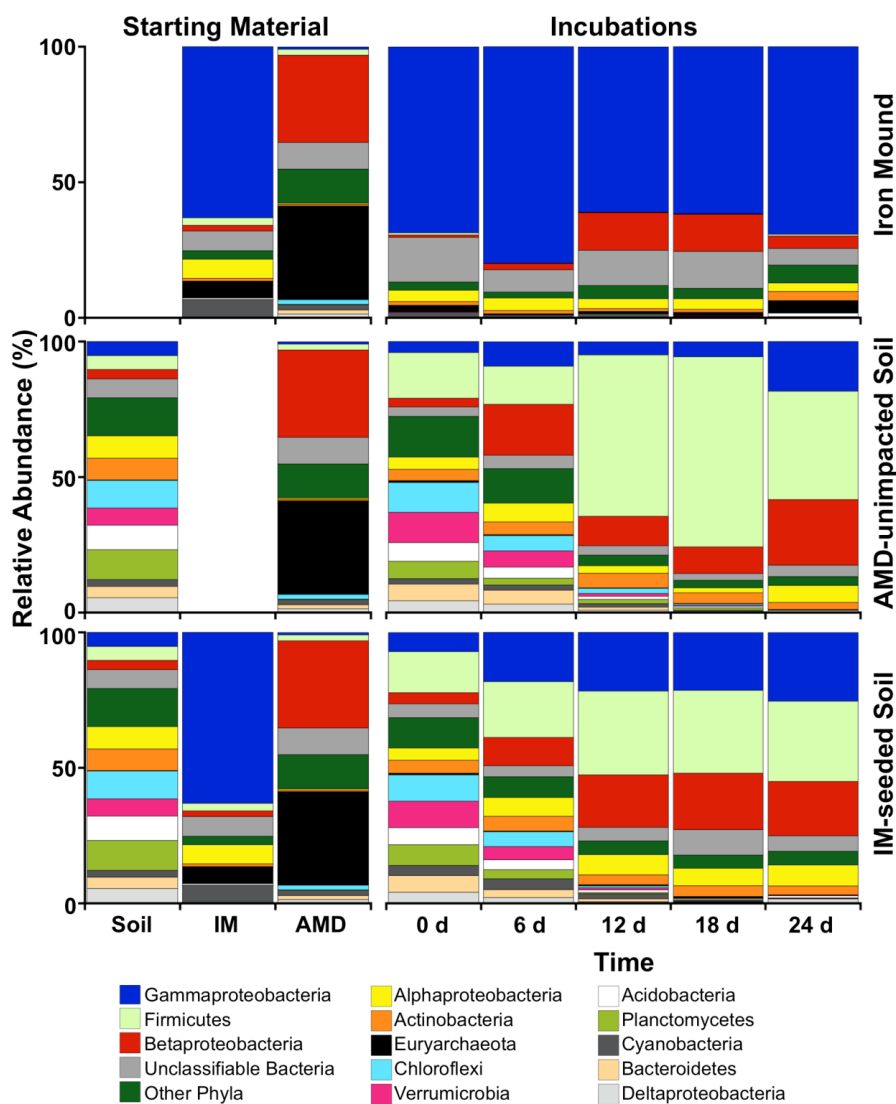
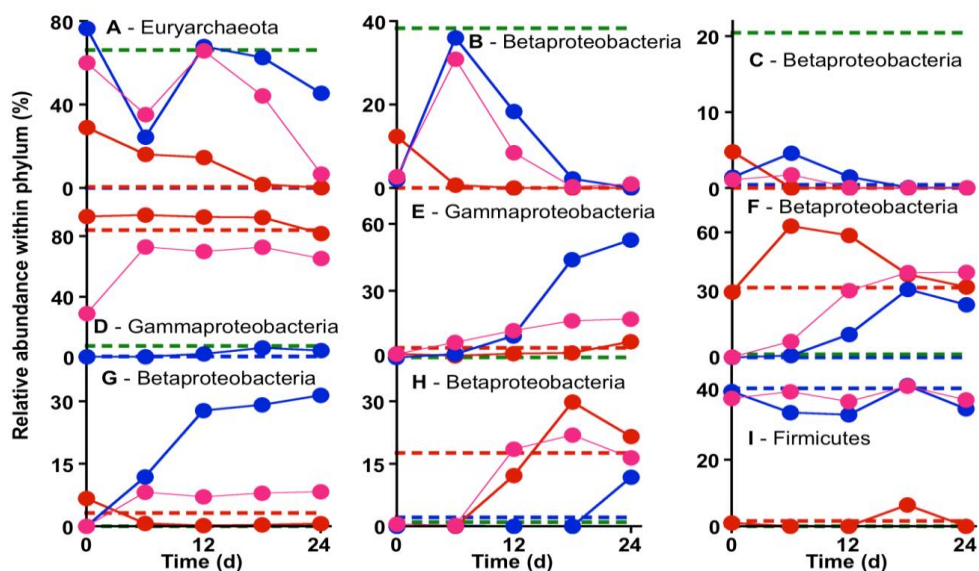


Figure 2.6: Relative phylum level (and class-level for the Proteobacteria) abundances of 16S rRNA gene OTU_{0.03} from gene sequence libraries of 'pristine' soil, iron mound sediment, AMD (all shown to the left of all three microcosm incubation types for clarity), and for each long term AMD microcosm incubation type (iron mound sediment, 'pristine' soil, and 'pristine' soil seeded with iron mound sediment) at incubation days 0, 6, 12, 18, and 24. [Reprinted (adapted) with permission from **Brantner, J.S. & Senko, J.M.** 2014. Response of soil-associated microbial communities to intrusion of coal mine-derived acid mine drainage. *Environmental Science and Technology* **48**:8556-8563. Copyright © 2014, American Chemical Society.] (27)



Panel	Cultured	Environmental
A (1 OTU _{0.03})	n/a	95% AMD-impacted Rio Tinto (8)
B (1 OTU _{0.03})	99% FeOB <i>Leptothrix ochracea</i> (75)	99% AMD-impacted Rio Tinto (8)
C (1 OTU _{0.03})	99% neutrophilic FeOB <i>Sideroxydans lithotrophicus</i> (239)	99% neutral Fe(II) seep (187)
D (3 OTU _{0.03})	98-100% acidophilic FeOB/FeRB <i>Metallibacterium</i> sp. X11 (54)	99-100% AMD-impacted sediment (72, 92)
E (2 OTU _{0.03})	97-99% acidophilic FeOB A4F5 (242)	99% AMD-impacted sediment (197)
F (1 OTU _{0.03})	99% acidophilic FeOB <i>Ferrovum myxofaciens</i> (117)	99% AMD-impacted sediment (72)
G (1 OTU _{0.03})	96% acidophilic FeOB C4C6 (242)	99% acidic hot spring (20)
H (2 OTU _{0.03})	99% <i>Herbispirillum</i> sp. T59 (108); <i>H. huttiense</i> (59)	97-99% agricultural soil (48)
I (6 OTU _{0.03})	99% <i>Bacillus</i> spp. (KF857221) (unpubl., (1, 109, 140, 161))	99% circumneutral soil/sediment (65, 129, 178)

Figure 2.7: Relative abundances of select OTU_{0.03} that belong to Euryarchaeota, Betaproteobacteria, Gammaproteobacteria, or Firmicutes in long-term AMD microcosm incubations that consisted of 'pristine' soil (solid blue lines), iron mound sediment (solid red lines), or 'pristine' soil supplemented with iron mound sediment (solid pink lines). OTU_{0.03} were selected for comparative purposes due to representing relatively abundant taxa from phyla found in high proportions in 'pristine' soil (red dashed lines), iron mound sediment (green dashed lines), or AMD (blue dashed lines). The table below the figure shows BLASTn sequence similarity results for OTU_{0.03} sequence with both cultured microorganism sequences and sequences obtained from environmental surveys that used culture-independent techniques. GenBank accession numbers for comparative sequences are located in Table 2.3. Numbers in parentheses represent

references corresponding to the References section. [Reprinted (adapted) with permission from **Brantner, J.S. & Senko, J.M.** 2014. Response of soil-associated microbial communities to intrusion of coal mine-derived acid mine drainage. *Environmental Science and Technology* **48**:8556-8563. Copyright © 2014, American Chemical Society.] (27)

Figure 2.7 Panel	Phylum	GenBank Accession Numbers (Cultured Organisms)	GenBank Accession Numbers (Environmental Sequences)
A	Euryarchaeota (1 OTU _{0.03})	n/a	(FN866063) (8)
B	Betaproteobacteria (1 OTU _{0.03})	(HQ290506) (75)	(FN866285) (8)
C	Betaproteobacteria (1 OTU _{0.03})	(DQ386859) (239)	(JQ906405) (187)
D	Gammaproteobacteria (3 OTU _{0.03})	(FR874227) (54)	(JX297618) (92) (JQ217580) (72)
E	Gammaproteobacteria (2 OTU _{0.03})	(JX869414) (242)	(KC619571, KC619557) (197)
F	Betaproteobacteria (1 OTU _{0.03})	(HM044161) (117)	(JQ217544) (72)
G	Betaproteobacteria (1 OTU _{0.03})	(JX869445) (242)	(JF280609) (20)
H	Betaproteobacteria (2 OTU _{0.03})	(FJ719318) (108) (EU046556) (59)	(KF189069) (48)
I	Firmicutes (1 OTU _{0.03})	(KF857221) (unpubl.) (FN397515) (109) (JX157878) (1) (KF836361) (unpubl.) (JX154374) (140) (HF584919) (161)	(JQ368731, JQ368847, JQ369143, JQ368916) (65) (KC433147) (129) (FN667397) (178)

Table 2.3: GenBank accession numbers for cultured organisms and environmental samples of 16S rRNA gene sequences to which Figure 2.7 OTU_{0.03} are most closely related. Numbers in parentheses following accession numbers correspond to references found in the References section. [Reprinted (adapted) with permission from **Brantner, J.S. & Senko, J.M.** 2014. Response of soil-associated microbial communities to intrusion of coal mine-derived acid mine drainage. *Environmental Science and Technology* **48**:8556-8563. Copyright © 2014, American Chemical Society.] (27)

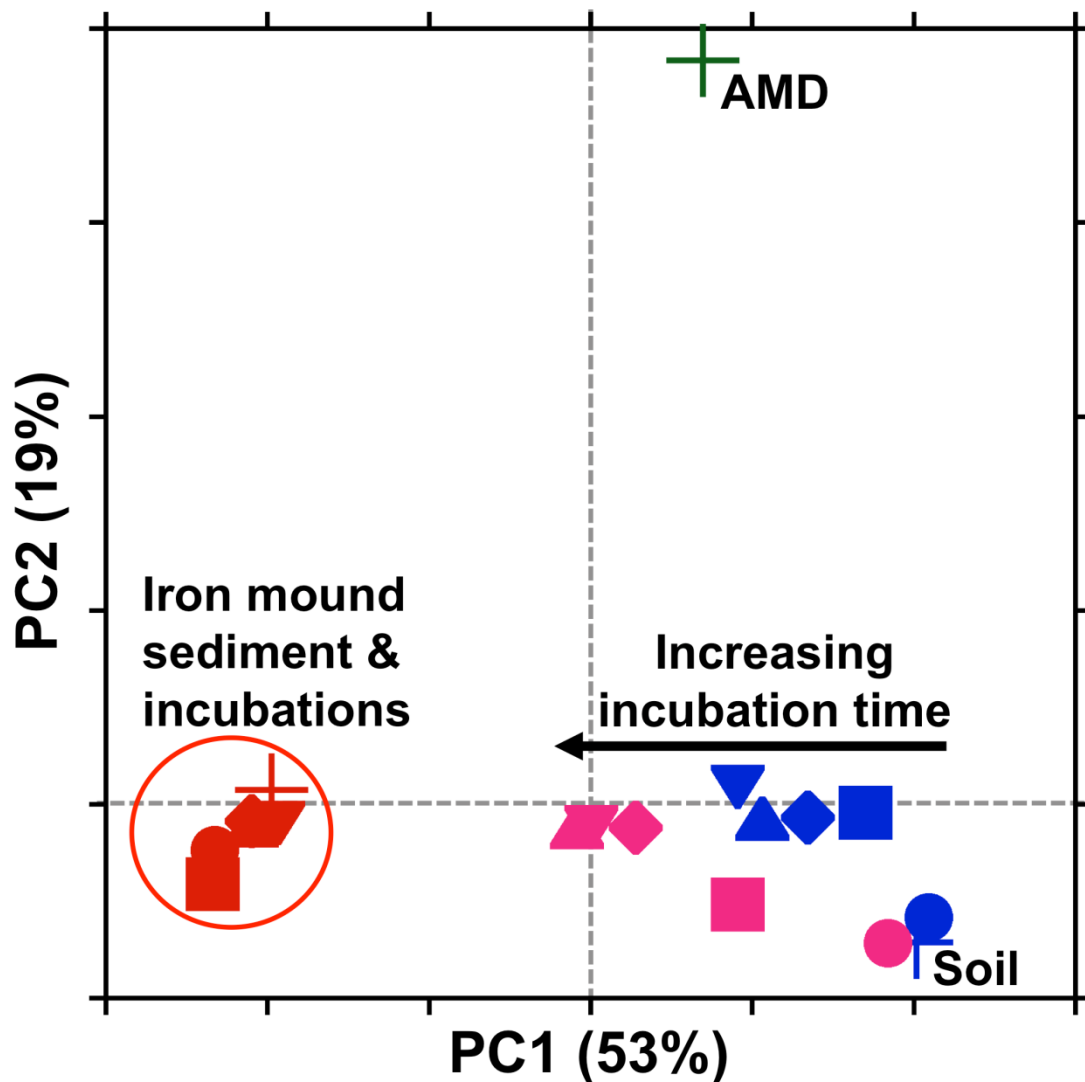


Figure 2.8: Principal coordinate analysis (PCoA) of ‘pristine’ soil (blue cross), iron mound sediment (red cross), or AMD (green cross) microbial communities and long term microcosm incubations consisting of ‘pristine’ soil (blue shapes), ‘pristine’ soil supplemented with iron mound sediment (pink shapes), and iron mound sediment (red shapes) after 0 (●), 6 (■), 12 (◆), 18 (▲), and 24 (▼) days of incubation using the weighted UniFrac metric (151, 152). Arrow designates increasing time with respect to microcosm incubation (days). Red circle indicates clustering of microbial communities associated with iron mound sediment material. [Reprinted (adapted) with permission from **Brantner, J.S. & Senko, J.M.** 2014. Response of soil-associated microbial communities to intrusion of coal mine-derived acid mine drainage. *Environmental Science and Technology* **48**:8556-8563. Copyright © 2014, American Chemical Society.] (27)

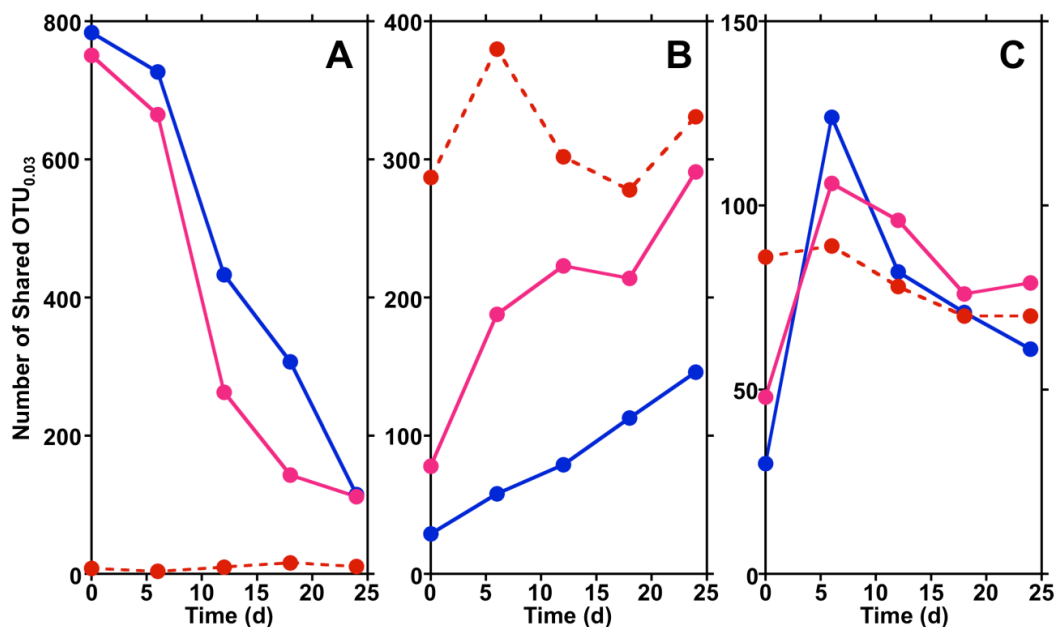


Figure 2.9: Shared OTU_{0.03} over the course of 24 day long term AMD microcosm incubation experiments between 'pristine' soil (A), iron mound sediment (B), or AMD (C) and incubations consisting of either 'pristine' soil (blue lines), 'pristine' soil seeded with iron mound sediment (pink lines), and iron mound sediment (red lines). [Reprinted (adapted) with permission from **Brantner, J.S. & Senko, J.M.** 2014. Response of soil-associated microbial communities to intrusion of coal mine-derived acid mine drainage. *Environmental Science and Technology* **48**:8556-8563. Copyright © 2014, American Chemical Society.] (27)

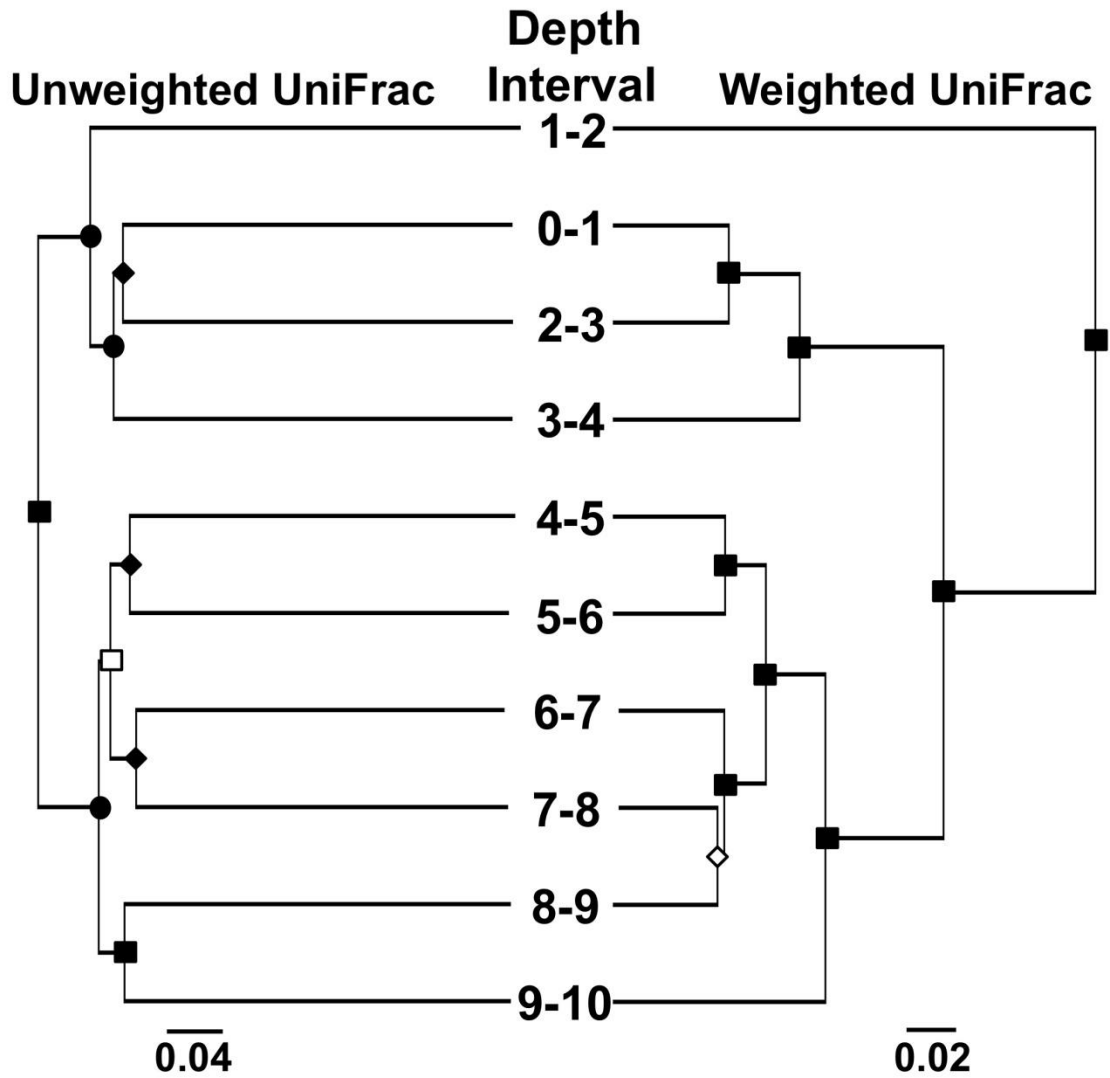


Figure 2.10: UPGMA trees constructed using the weighted and unweighted UniFrac metrics to illustrate microbial community clustering associated with each 1 cm depth interval through a core sample of iron mound material taken from the MF. Symbols on UPGMA trees designate jackknife support of $\geq 99\%$ (■), 90-99% (●), 80-89% (◆), 70-79% (□), 50-59% (◇). [Copyright © 2014 Brantner, Haake, Burwick, Menge, Hotchkiss and Senko.] (26)

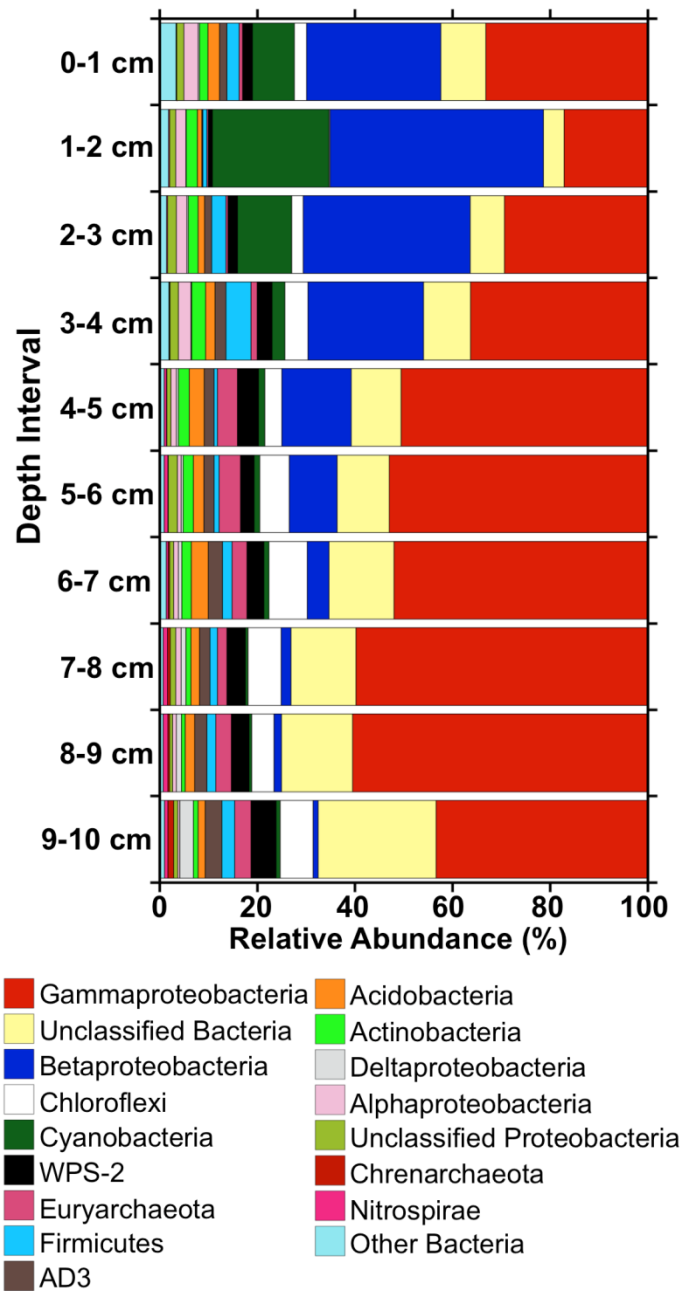


Figure 2.11: Phylum-level (and class-level in the case of the Proteobacteria) taxonomic resolutions for relative abundances of 16S rRNA gene sequences in libraries generated from sequences recovered from 1 cm depth intervals of iron mound core collected from the MF. [Copyright © 2014 Brantner, Haake, Burwick, Menge, Hotchkiss and Senko.] (26)

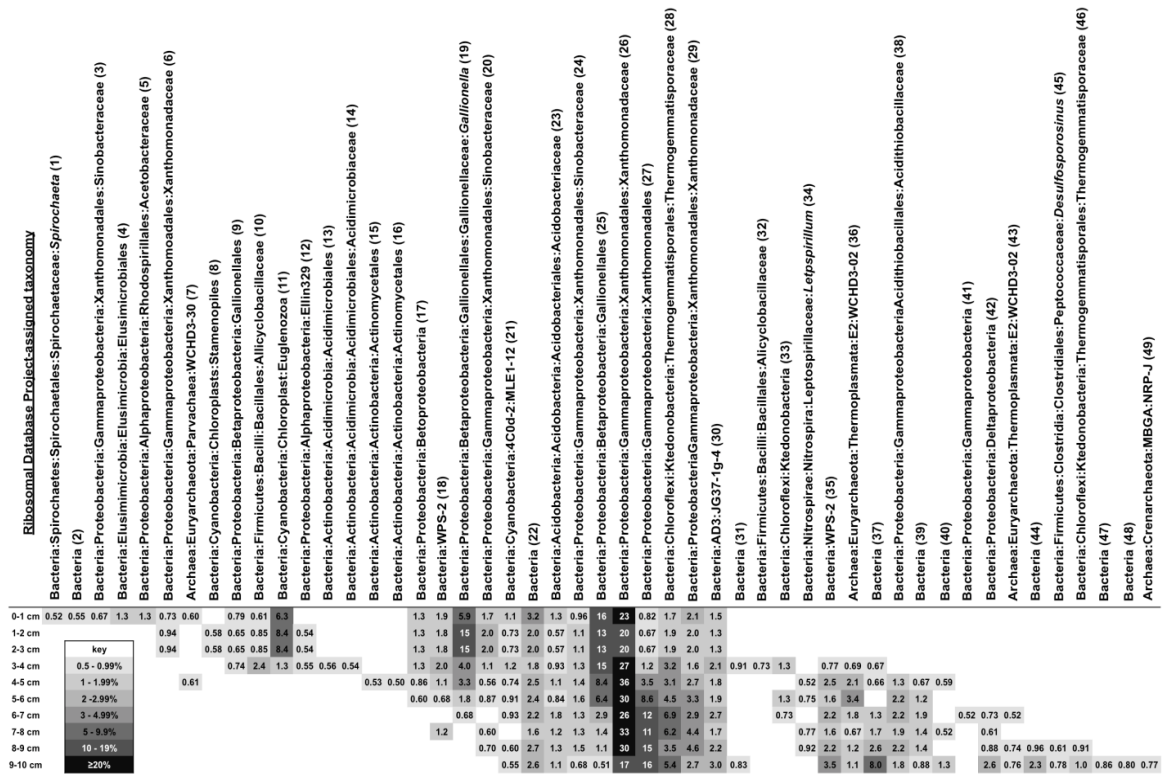


Figure 2.12: Heatmap projection illustrating relative abundances of OTU_{0.03} that make up $\geq 0.5\%$ of total OTU_{0.03} recovered from various depths (1 cm intervals) of MF iron mound sediment, and associated Ribosomal Database Project (RDP) taxonomic identities. Numbers following taxonomic identities correspond to numbers found in Table 2.4, which shows BLASTn search results for each OTU_{0.03} in Figure 2.12 and the nearest environmental 16S rRNA gene sequences and nearest culturable 16S rRNA gene sequences yielded from the BLASTn search. [Copyright © 2014 Brantner, Haake, Burwick, Menge, Hotchkiss and Senko.] (26)

OTU #	Nearest environmental 16S rRNA gene sequence	Nearest cultured 16S rRNA gene sequence
1	AMD-impacted Río Tinto (99%; FN867143; (8))	<i>Spirochaeta aurantia</i> from freshwater (94%; AJ565432; (93))
2	AMD-impacted Río Tinto (98%; FN863828; (8))	None found
3	"Iron snow" in acidic mine lake (99%; HE604017; (153))	<i>Steroidobacter denitrificans</i> FS, NO ₃ ⁻ reducer from anoxic sludge (94%; NR_044309; (71))
4	Abandoned Cu mine (99%; JQ217995; (72))	<i>Halothiobacillus kellyi</i> BII-1, thermophilic S oxidizer (84%; NR_025030; (205))
5	"Iron snow" in acidic mine lake (99%; HE604030; (153))	Acidophilic FeOB C4H7 (99%; JX869450; (242))
6	Abandoned Cu mine (99%; JQ217802; (72))	<i>Metallibacterium</i> X11 acidophilic S ₂ O ₃ ²⁻ oxidizer (95%; HE858262; (54))
7	AMD-impacted Río Tinto (96%; FN866063; (8))	None found
8	Arctic stream epilithon (97% FJ849138; (135))	<i>Elphidium aculeatum</i> A75.46 chloroplast (85%; HM213365; (180))
9	Abandoned Cu mine (99%; JQ217544; (72)); AMD iron mound (99%; HQ420151; (29))	<i>Ferrovum myxofaciens</i> EHS8, acidophilic FeOB (97%; KC155322; (98)); <i>Ferrovum myxofaciens</i> PSTR, acidophilic FeOB (97%; EF133508; (94))
10	AMD-impacted sediment (99%; EF409850; (247))	Acidophilic FeOB/FeRB iFeo-D4-31-CH (94%; FN870336; (154))
11	AMD-impacted Río Tinto (99%; FN862195; (8))	<i>Euglena mutabilis</i> SAG 1224-9b chloroplast (96%; AY626044; (165))
12	Metal sulfide mine AMD (99%; GU979565; (96))	<i>Rhizobiales</i> strain A48, neutrophilic FeRB (94%; AB081581; (198))
13	AMD-impacted Río Tinto sediment (99%; JF737887; (84))	<i>Aciditerrimonas ferrireducens</i> , thermoacidophilic FeRB (92%; AB517669; (112))
14	Acidic mine lake (99%; KC619609; (197))	Acidophilic heterotrophic FeOB Py-F3 (96%; KC208497; (121))
15	Acidic wetland soil (99%; GQ203360; (128))	<i>Actinoallomurus</i> sp. 645152, acidophilic organotroph (96%; AB604840; (169))
16	Acidic mine lake sediments (99%; FN870199; (154))	Acidophilic FeOB A4F6 (93%; JX869415; (242))
17	AMD iron mound (97%; HQ420151; (29)); AMD-impacted Río Tinto (97%; FN867145; (8))	<i>Ferrovum myxofaciens</i> EHS8, acidophilic FeOB (97%; KC155322; (98)); <i>Ferrovum myxofaciens</i> PSTR, acidophilic FeOB (97%; EF133508; (94))

OTU #	Nearest environmental 16S rRNA gene sequence	Nearest cultured 16S rRNA gene sequence
18	"Iron snow" in acidic mine lake (99%; HE604029; (153))	<i>Arhodomonas</i> sp. Seminole, aerobic halophile (84%; JX099567; (50))
19	Abandoned Cu mine (99%; JQ217975; (72))	<i>Leptothrix ochracea</i> SCGC AAA018-M4 FeOB (98%; HQ290506; (75))
20	AMD-impacted Río Tinto (99%; FN860398; (8))	Acidophilic FeOB A4F5 (98%; JX869415; (242))
21	Acidic hot spring (97%; JF280561; (20))	Anaerobic bacterium BSV83 (86%; AJ229227; (101))
22	AMD-impacted Río Tinto (99%; FN866617; (8))	<i>Lysobacter</i> sp. AP7 (82%; EU374884; (6))
23	Abandoned Cu mine (99%; JQ218102; (72))	Acidophilic, organotrophic Acidobacteriaceae CH1 from AMD (97%; DQ355184; (58))
24	AMD-impacted Río Tinto sediment (99%, HQ730615; (196))	Acidophilic FeOB A4F5 (98%; JX869414; (242))
25	Abandoned Cu mine (99%; JQ217544.1; (72))	<i>Ferroplasma myxofaciens</i> EHS8, acidophilic FeOB (99%; KC155322; (98)); <i>Ferroplasma myxofaciens</i> PSTR, acidophilic FeOB (99%; EF133508; (94))
26	AMD biofilm (99%; JX297618.1; (92))	<i>Metallibacterium</i> X11 acidophilic S2O32- oxidizer (99%; HE858262; (54)); <i>Metallibacterium scheffleri</i> DKE6, acidophilic facultative FeRB (98%; HQ909259.1; (251))
27	AMD-impacted Río Tinto (99%; FN862147; (8))	<i>Thiohalophilus thiocyanatoxydans</i> HRhD 2, halophilic S oxidizer (91%; NR_043875; (211))
28	Volcanic deposits (88%; AY917857; (88))	<i>Thermogemmatispora onikobensis</i> , thermophilic organotroph (86%; AB547912; (243))
29	Abandoned Cu mine (100%; JQ217580; (72))	<i>Metallibacterium</i> X11 acidophilic S2O32- oxidizer (100%; HE858262; (54)); Acidophilic Fe(II) oxidizer C4C8 (97%; JX869446; (242)); <i>Metallibacterium scheffleri</i> DKE6, acidophilic facultative FeRB (97%; HQ909259.1; (251))
30	"Iron snow" in acidic mine lake (99%; HE604014; (153))	Acidophilic FeOB A10G4 (99%; JX869422; (242))
31	Reject coal-impacted soil (97%; AF523920; (28))	<i>Moorella</i> sp. 64_FGQ, thermophilic FeRB (87%; GQ872425; (170))
32	Metal sulfide mine AMD (99%; GU979565; (96))	<i>Alicyclobacillus acidoterrestris</i> C-ZJB-12-17, thermoacidophilic (96%; KC193190; (250))
33	Volcanic deposits (90%; AY425781; (88))	<i>Thermogemmatispora onikobensis</i> , thermophilic organotroph (85%; AB547912; (243))
34	AMD-impacted Río Tinto (99%; FN863733; (8))	<i>Leptospirillum ferrooxidans</i> C2-3 acidophilic FeOB (99%; NR_074963) (80))

OTU #	Nearest environmental 16S rRNA gene sequence	Nearest cultured 16S rRNA gene sequence
35	AMD-impacted Río Tinto sediment (100%; JF737887; (84))	<i>Chloroflexi</i> SCGC AAA007-G23, marine S oxidizer (82%; HQ675468; (223))
36	AMD-impacted creek (99%; HE653802; (233))	<i>Methanomassiliicoccus luminyensis</i> B10, methanogen (85%; HQ896499; (64))
37	Anoxic rice field soil (89%; FM956256; (83))	<i>Thermoactinomyces vulgaris</i> 55N1-5, thermophilic organotroph (88%; JN366723; (145))
38	AMD-impacted Río Tinto (99%; FN862217; (8))	<i>Acidithiobacillus ferrivorans</i> SS3, FeOB/facultative FeRB (99%; NR_074660; (144))
39	Abandoned Cu mine (99%; JQ218054; (72))	<i>Clostridium ghonii</i> 2447_6, fermentative anaerobe (76%; JN048963; (194))
40	Deep granitic fracture water (88%; 7150D1B75; (195))	<i>Pelotomaculum terephthalicum</i> JT strain J, syntroph (85%; NR_040948; (183))
41	AMD biofilm (95%; JX297618.1; (92))	<i>Metallibacterium</i> X11 acidophilic S2O32- oxidizer (94%; HE858262; (54)); Acidophilic FeOB C4C8 (94%; JX869446; (242)); <i>Metallibacterium scheffleri</i> DKE6, acidophilic facultative FeRB (94%; HQ909259.1; (251))
42	Alpine tundra soil (94%; FJ570063; (253))	<i>Myxobacterium</i> sp. KC, humic substance oxidizer (93%; AF482687; (39))
43	AMD-impacted creek (99%; HE653802; (233))	<i>Methanomassiliicoccus luminyensis</i> B10, methanogen (85%; HQ896499; (64))
44	Anoxic rice field soil (87%; FM956256; (83))	<i>Thermoactinomyces vulgaris</i> 55N1-5, thermophilic organotroph (86%; JN366723; (145))
45	Acidic mine lake (93%; KC619609; (197))	<i>Desulfosporosinus</i> sp. GBSRB4.2 (99%; EU839714; (201))
46	Arctic fell-field soil (94%; EF221592; (246))	<i>Ktedobacter racemifer</i> SOSP1-21, aerobic organotroph (88%; AM180160; (36))
47	AMD-impacted Río tinto (97%; FN860399; (8))	<i>Chloroflexi</i> SCGC AAA007-G23, marine S-oxidizer (79%; HQ675468; (223))
48	AMD-impacted Río Tinto (99%; FN860359; (8))	<i>Lysobacter</i> sp. AP7 (80%; EU374884; (6))
49	Acidic bog (99%; JQ807564; (146))	<i>Crenarchaeote</i> OS70 (87%; EU239962; (53))

Table 2.4: Nearest 16S rRNA gene sequences from environmental surveys and cultured microorganisms resulting from BLASTn searches of OTU_{0.03} representing ≥0.5% of sequences found in libraries derived for each 1 cm depth interval of MF iron mound sediment shown in Figure 2.12. OTU numbers

correspond to numbers found in Figure 2.12. Environment type is provided for each nearest environmental 16S rRNA gene sequence obtained from BLASTn. Associated GenBank accession numbers, percent similarities, and corresponding references are shown for each OTU_{0.03}. Numbers appearing in parentheses after accession numbers represent references (see References section). [Copyright © 2014 Brantner, Haake, Burwick, Menge, Hotchkiss and Senko.] (26)

NOTE: Data and figures/tables presented in this chapter have been published, and were reprinted (adapated) with appropriate written approval (see Appendix (26, 27)).

CHAPTER III
THE INFLUENCE OF MUCIN AND SYNTHETIC CYSTIC FIBROSIS MEDIUM
ON THE *IN VITRO* BIOACTIVITY OF SILVER CARBENE COMPLEXES AND
SELECT ANTIMICROBIALS

Introduction

As a direct result of defective mucociliary clearance mechanisms (22, 77, 85, 132, 157, 166, 209, 234), the CF lung is often found to contain a thickened, semi-viscous mucus layer that is rich with various glycoproteins (mucins), DNA, salts, ions, proteins, carbohydrates, specific concentrations of amino acids, and water (22, 85, 132, 163, 175, 176, 190, 192, 212, 213, 234). This layer of dense, purulent mucus is highly susceptible to colonization, and in turn, infection by the opportunistic pathogen *Pseudomonas aeruginosa*, which has been documented to be responsible for respiratory complications that lead to high incidence of morbidity and mortality rates among CF patients (10, 77, 156, 157, 179, 245). Population densities of *P. aeruginosa*, once established, have been suggested to range as high as $10^8 - 10^{10}$ CFU/mL within the CF lung (175, 176, 208). This number becomes increasingly startling when viewed in light of evidence that suggests hypermutable strains of *P. aeruginosa* can exist in the CF lung that are prone to higher mutation rates that can in turn confer an accelerated antibiotic

resistance rate (173, 174). While it has become increasingly evident that *P. aeruginosa*, specifically CF isolates (103), have developed resistance to a myriad of antibiotics (79, 103, 157, 181, 184, 185, 203, 230), resistance alone may not be the only driving force for antimicrobial ineffectiveness against this pathogen in the CF lung environment. The viscous, mucin-laden sputum that builds up in the CF lung provides an even further layer of protection to the colonized bacteria by acting as an antibiotic antagonist (110, 142, 158, 164). It has been suggested that *P. aeruginosa* interacts with mucin (a key component of CF sputum) in such a way that it is capable of conferring an extra level of evasion for *P. aeruginosa* against antimicrobial therapies (133). Antimicrobial penetration and bioactivity in respiratory secretions of the CF lung have traditionally been viewed as hallmarks of antibiotic activity within CF sputum (141). Despite this fact, very few studies have examined the bioactivity of antimicrobial compounds in patient CF sputum (30, 110, 141, 142, 164), and even fewer studies have examined the potential effects that mucin concentration in artificial CF sputum specifically plays on impacting the bioactivity of antimicrobial compounds under CF relevant conditions (166). Due to the complex nature of the infected CF lung environment, it becomes increasingly evident that more data is needed with regard to antimicrobial effectiveness in situations that better approximate the CF lung environment.

Standard, widely acceptable susceptibility tests have been adopted over the years as a means to evaluate antibiotic effectiveness against various strains

of microorganisms. However, these standard methodologies often fail to accurately reflect the growth environment *in vitro* of that which microorganisms are exposed to *in vivo*. As such, recent studies have questioned susceptibility testing as it relates to clinical relevance (209), and some studies have developed novel methods for testing antimicrobial effectiveness in conditions that better approximate those of the CF lung environment (124, 166). For cystic fibrosis, utilizing a defined medium would help to elucidate the effects that sputum (and more specifically mucin concentration) has on the bioactivity of both novel and current clinically relevant antimicrobial compounds. One such medium that attempts to nutritionally mimic aspects of the early CF lung environment is Synthetic Cystic Fibrosis sputum Medium (SCFM) (175, 176). SCFM is a chemically defined medium that consists of iron, various salts, carbon sources, and amino acids all in concentrations mimicking levels found in the sputum of the early CF lung (175). This medium has been previously shown to not only mimic nutritional cues of the CF lung, but it has also been documented to accurately reflect *in vitro* key physiological behavior of *P. aeruginosa* as that seen in patient CF sputum (175, 176). One key ingredient missing however from SCFM is mucin (175). As mucins are key components found in CF sputum (22, 132, 158, 163, 190, 192, 234), augmentation of SCFM with mucin could provide a further realistic understanding of the efficiency and efficacy of antimicrobial compounds in an environment that more accurately attempts to mimic the CF lung.

In order to gain a better understanding of the effectiveness and bioactivity of various antimicrobials against *P. aeruginosa* grown in conditions (and to population densities) that better approximate the CF lung environment, a defined Synthetic Cystic Fibrosis sputum Media (SCFM) (175) was selected and augmented with varying concentrations of mucin. Various clinically relevant antimicrobial compounds from multiple antibacterial classes were selected including Tobramycin (an aminoglycoside), Ciprofloxacin (a fluoroquinolone), and Meropenem (a β -lactam). In addition, two novel silver carbene complexes (SCCs) were utilized. These included both SCC-1 (silver acetate bound to methylated caffeine), and SCC-22 (hydroxylated 4,5 dichloroimidazole bonded with silver acetate). These compounds were selected as candidate silver antimicrobials due to previous reports that found both to be water soluble/stable and highly effective as broad-spectrum antimicrobials (31, 119, 139, 166, 177). The research projects contained herein aimed to address three primary research goals:

- Determine the growth curves for various strains of *P. aeruginosa* using a defined growth medium (SCFM) that has been augmented with varying concentrations of mucin.
- Using the growth curve data, grow *P. aeruginosa* strains to population densities common in the CF lung environment, and test/determine inhibitory and killing concentrations of novel, broad spectrum silver

carbene complexes and other clinically relevant antibiotics against multiple strains of *P. aeruginosa*.

- Determine the effects that varying mucin concentration in SCFM has on the inhibitory/killing efficacy for high population densities ($\sim 10^8$ CFU/mL) of *P. aeruginosa* during log growth phase using multiple antimicrobial compounds.

Based on these research aims, it was hypothesized that addition of mucin to SCFM will increase the growth rates of *P. aeruginosa* strains based on evidence that suggests some bacterial communities utilize mucin as a carbon/nitrogen source (86). Further, it was predicted that all antimicrobials tested in SCFM would show low inhibiting and killing concentrations when used against *P. aeruginosa*. More specifically, it was hypothesized that SCC-1 and SCC-22 would have lower inhibitory and bactericidal concentrations compared to common, clinically relevant broad spectrum antibiotics. Lastly, it was hypothesized that an increase in mucin concentration (up to 1% wt/vol) in SCFM would significantly reduce bioactivity for all antimicrobials tested, and therefore would result in higher killing concentrations necessary to reduce CF relevant population densities of various strains of *P. aeruginosa*.

Materials and Methods

Pseudomonas aeruginosa Strains and Cystic Fibrosis Medium

Four *Pseudomonas aeruginosa* strains with differing phenotypes were obtained. These strains included a standard PAO1 isolate (ATCC BAA-47), a green fluorescent protein (*gfp*) expressing PAO1 strain (244) generously provided by Dr. Søren Molin, as well as an engineered alginate overproducing strain of *P. aeruginosa* PAO1 (PDO300 Δ *mucA*) (162) and a clinical CF mucoid *P. aeruginosa* isolate (designated strain 7119) generously provided by Dr. Jeff Leid. Freezer stocks (-80 °C) for all strains were generated using Tryptic Soy Broth (TSB) and 20% sterile glycerol. As needed, freezer stocks were removed and streaked onto Tryptic Soy Agar (TSA) plates. Plates containing each strain intended for experiments (see below) were stored in a 4°C refrigerator for no longer than two weeks before being discarded, upon which fresh stock plates were restreaked.

Synthetic Cystic Fibrosis Medium (SCFM) developed by Palmer et al. (175) was used as a base growth medium for *P. aeruginosa* strains in conditions that better approximate the nutritional aspects of the early CF lung environment. Each one liter of SCFM (175) consisted of the following concentrations of amino acids (in mM) achieved by adding appropriate amounts from sterile 100 mM stock solutions (prepared in sterile deionized (DI) water unless otherwise specified): 1.78 mM L-alanine, 0.306 mM L-arginine · HCl, 0.827 mM L-aspartate (prepared in 0.5 M NaOH), 0.16 mM L-cysteine · HCl, 1.549 mM L-glutamate ·

HCl, 1.203 mM L-glycine, 0.519 mM L-histidine · HCl, 1.12 L-isoleucine, 1.609 mM L-leucine, 2.128 mM L-lysine · HCl, 0.633 mM L-methionine, 0.676 mM L-ornithine · HCl, 0.53 mM L-phenylalanine, 1.661 mM L-proline, 1.446 mM L-serine, 1.072 mM L-threonine, 0.013 mM L-tryptophan (prepared in 0.2 M NaOH), 0.802 mM L-tyrosine (prepared in 1 M NaOH), and 1.117 mM L-valine. All amino acids were directly added to a buffered base that consisted of 6.5 mL of a 0.2 M NaH₂PO₄ solution, 6.25 mL of a Na₂HPO₄ solution, 0.348 mL of a 1 M KNO₃ solution, 1.084 mL of a 0.25 M K₂SO₄ solution, 0.122 g NH₄Cl, 1.114 g KCl, 3.03 g NaCl, and 2.09 g MOPS (10 mM final concentration), and the solution was adjusted to pH 6.8. Next, 779.6 mL of sterile DI water was added, and the resulting solution was filter-sterilized into a sterile 1 L bottle. Next, the following filter-sterilized components were directly added: 1.754 mL of a 1 M CaCl₂ solution, 0.606 mL of a 1 M MgCl₂ solution, 1.0 mL of a 3.6 mM FeSO₄ · 7H₂O solution, 9.3 mL of a 1 M lactate solution, and 3.0 mL of a 1 M D-glucose solution.

While SCFM attempts to mimic the nutritional aspects of the early CF lung environment, a key component found in the sputum of CF patients, though lacking in the SCFM base medium, is mucin. Although mucin concentrations vary in the non-CF and CF lung environment, differential refractometry has shown that mucin dry weight can range between 1-4% in 'normal' and CF-like mucus respectively (163). As such, in order to better approximate the early CF lung environment nutritionally for various experiments, SCFM was augmented with

mucin to various final concentrations (0%, 0.1%, and 1% wt/vol) using Type III mucin from porcine stomach, bound sialic acid 0.5-1.5%, partially purified powder (Sigma Aldrich, M1778). Ten percent mucin (wt/vol) stocks (the highest concentration that was able to be completely dissolved and sterilized) were made by adding 10 g of Type III mucin to 100 mL of DI water, vigorously mixed, and autoclaved for 30 minutes at 121°C.

Bacterial Growth Curves

To determine growth dynamics of PAO1, PAO1/*gfp*, PDO300, and 7119 in SCFM with varying concentrations of mucin, growth curve experiments were carried out. The four different growth conditions included: 100% SCFM (no mucin added), 90% SCFM + 0.1% mucin (final wt/vol), 90% SCFM + 1% mucin (final wt/vol), and 90% SCFM. The 100% SCFM was prepared as previous described (see above). The 90% SCFM + 0.1% mucin (final wt/vol) was prepared by taking 100% SCFM and diluting it to 90% using a 1% (final wt/vol) mucin stock solution (made by taking 10% mucin (wt/vol) stock and diluting it down to 1% (wt/vol)). The 90% SCFM + 1% mucin (final wt/vol) was prepared by diluting 100% SCFM to 90% using the 10% mucin (wt/vol) stock solution. The 90% SCFM solution was used as a control by taking 100% SCFM and diluting it to 90% with sterile DI water. Triplicate overnight cultures were prepared by inoculating 5 mL of corresponding medium with single colonies from refrigerated plates of PAO1, PAO1/*gfp*, PDO300, or 7119. Cultures were then placed on an orbital shaker at

250 rpm and incubated at 37°C for approximately 12 hours. Overnight cultures were diluted (1:1000) by placing 100µL of overnight culture into 99.9 mL of fresh corresponding medium in triplicate 250 mL Erlenmeyer flasks. Flasks were placed into an incubator (37°C) and shaken at 250 rpm for 48 hours. One milliliter samples were taken from each flask at 0, 1, 2, 3, 4, 5, 6, 7, 8, 9, 10, 11, 12, 24, and 48 hours after being placed in the incubator. When possible, optical densities (OD₆₀₀) were measured for each sample by spectrophotometry using an Eppendorf® (Eppendorf North America, Hauppauge, NY, USA) BioPhotometer spectrophotometer. Samples were then diluted accordingly using sterile DI water, and then triplicate plated onto TSA plates using an Autoplate® 4000 automated spiral plater (Spiral Biotech, Inc., Bethesda, MD, USA) according to manufacturer protocols. TSA plates were incubated (37°C) until the appearance of colonies, and colonies were counted as colony forming units (CFU) and CFU/mL were determined.

Treatment of Planktonic P. aeruginosa Strains with Various Antimicrobial Compounds Using Conditions that Approximate the CF Lung Environment

A modified protocol of treating *P.aeruginosa* strains grown in SCFM to a population density of $\sim 10^8$ CFU/mL was used (166). Briefly, *P. aeruginosa* strains PAO1, PAO1/*gfp*, PDO300, and 7119 cultures were prepared by inoculating 5 mL of medium (100% SCFM, 90% SCFM + 0.1% mucin (final wt/vol), or 90% SCFM + 1% mucin (final wt/vol)), and grown overnight (approximately 12 hours)

at 37°C with agitation (250 rpm). Overnight cultures were diluted the next day (1:1000) in 250 mL Erlenmeyer flasks using fresh corresponding medium. Flasks were placed on an orbital shaker (250 rpm) in an incubator (37°C) and allowed to grow to a population density of approximately 10^8 CFU/mL based on growth curve times for each strain (confirmed by dilution and spiral plating). Upon reaching a population density of approximately 10^8 CFU/mL, cultures were aliquoted (3.9 mL each) into sterile 15 mL culture tubes. Fresh antimicrobial stock solutions (10 mg/mL) were prepared as needed first by adding 0.1 g of compound into 10 mL of sterile dissolvent. Tobramycin (Sigma Aldrich, T4014) was dissolved in sterile DI water, Ciprofloxacin (Sigma Aldrich, 17850) was dissolved in 0.1N HCl, Meropenem (Hospira, NDC 0409-3506-01) was dissolved in sterile 5% KH_2PO_4 . Both SCC-1 and SCC-22 were synthesized as previously described (119, 177), and were prepared by dissolving the compounds in sterile DI water stabilized with 0.0075 mL glacial acetic acid as previously described (166). Antimicrobial stocks were then diluted in corresponding dissolvents to 40x final desired antibiotic concentrations. From these dilutions, 100 μL was added to the aliquoted cultures to achieve final treatment concentrations of 0 (no treatment), 1, 2, 4, 6, 8, 12, 16, 24, 32, 64, 128, and 250 $\mu\text{g}/\text{mL}$. As controls, 100 μL of corresponding dissolvent was added to 3.9 mL of culture for each antibiotic tested in each growth condition. Culture tubes were placed on an orbital shaker at 250 rpm in a 37°C incubator for a treatment length of approximately 24 hours. After 24 hours, culture tubes were removed and diluted using sterile DI water.

Dilutions were spiral plated onto TSA plates using an Autoplate® 4000 automated spiral plater (Spiral Biotech, Inc., Bethesda, MD, USA). Plates were incubated in a 37°C incubator. Upon appearance of visible colonies, plates were counted and CFU/mL values were determined. Minimum inhibitory concentrations (MICs) were calculated based on failure to grow beyond that of the starting population density ($\sim 10^8$ CFU/mL). Minimum bactericidal concentrations (MBC) were also calculated based on $\geq 99.9\%$ killing of initial starting bacterial load of approximately 10^8 CFU/mL. All experiments were carried out in triplicate.

Statistical Analysis

Statistical analysis for both MIC and MBC values looking for significant interactions with respect to multiple variables including bacterial strain (PAO1, PAO1/*gfp*, PDO300, and 7119), growth medium (100% SCFM, 90% SCFM + 0.1% mucin (final wt/vol), or 90% SCFM + 1% mucin (final wt/vol)), and antibiotics (Tobramycin, Ciprofloxacin, Meropenem, SCC-1, and SCC-22) was performed using SAS version 9.3 (SAS Institute Inc., Cary, NC, USA) by a biostatistician (Mirades Brown) at Akron Children's Hospital. Categorical variables (i.e., growth medium, antibiotics, and strains) were treated as counts and percentages, while quantitative variables (MIC and MBC values based on CFU/mL counts) were represented as means and standard deviations and/or medians and 1st and 3rd quartiles. Kolmogorov Smirnov test was used to

determine the normality of the data. Resulting non-normally distributed nature of the data prompted the use of non-parametric statistics. Friedman's test was used to assess non-normally repeated measures of MIC and MBC values between levels of bacterial strain, growth medium, and antibiotic type, followed by subsequent post-hoc analysis using Wilcoxon signed-rank test with Bonferroni correction. In addition, Friedman's test was used to compare MIC and MBC values between the various growth conditions while controlling for antibiotic, and subsequent post-hoc analysis was performed using the Wilcoxon signed-rank test with Bonferroni correction. All tests performed were two-sided with statistical significance being determined at p -values less than 0.05 unless otherwise noted.

Results

Growth Curves for Multiple P. aeruginosa Strains Grown Using CF relevant Media Conditions.

In order to assess the growth dynamics of the four selected strains of *P. aeruginosa* (PAO1, PAO1/*gfp*, PDO300, and 7119) in conditions that better approximate the CF lung environment, growth curves were established. The four strains were grown in 100% SCFM with no mucin added, 90% SCFM + 0.1% mucin (final wt/vol) and 90% SCFM + 1% mucin (final wt/vol). In addition, in order to check for any aberrance in growth dynamics due to the dilution of 100% SCFM to 90% SCFM in the cases that mucin was added, growth curves were also established whereby 100% SCFM was diluted to 90% SCFM using sterile DI water. In all four medium conditions, *P. aeruginosa* strains PAO1, PAO1/*gfp*, and

PDO300 remained in lag phase until approximately two hours after the initial dilution of the overnight culture, whereby all three of these strains entered the log phase between two to three hours post inoculation (Figure 3.1A-C). In the case of *P. aeruginosa* strain 7119, the lag phase was relatively short such that this strain seemed to begin log growth beginning between one and two hours (Figure 3.1D). For all four *P. aeruginosa* strains under investigation, log phase appeared to taper into stationary phase beginning around seven hours after the initial overnight cultures were diluted, with no noticeable differences between the four different medium conditions (Figure 3.1A-D). One specific factor from the growth curves of *P. aeruginosa* strains PAO1, PAO1/*gfp*, PDO300, and 7119 that was obtained is the time points at which the four strains reach $\sim 10^8$ CFU/mL.

Pseudomonas aeruginosa strain PAO1 achieved $\sim 10^8$ CFU/mL in all growth media tested between approximately four and six hours after the start of the growth curves (Figure 3.1A). For *P. aeruginosa* strains PAO1/*gfp* and PDO300, $\sim 10^8$ CFU/mL was reached in all growth conditions between five and six hours after the growth curves were started (Figure 3.1B,C). Lastly, *P. aeruginosa* strain 7119 reached $\sim 10^8$ CFU/mL in all growth conditions between five and seven hours post the start of the growth curves (Figure 3.1D). Understanding the time points at which these four strains of *P. aeruginosa* reach a bacterial population density of $\sim 10^8$ CFU/mL was critical in order to grow bacterial populations to a specific CF relevant population density for *in vitro* experiments targeted at better understanding antimicrobial effectiveness. Therefore, the data from the growth

curves of *P. aeruginosa* grown in 100% SCFM with no mucin, 90% SCFM + 0.1% mucin (final wt/vol), and 90% SCFM + 1% mucin (final wt/vol) was critical in establishing the necessary time points to grow up large batch cultures of each *P. aeruginosa* strain to reach CF relevant bacterial population densities to be used in experiments examining the effects that CF relevant conditions have on antibiotic effectiveness.

Killing Curves to Establish MIC and MBC Values

In order to better approximate antimicrobial effectiveness using CF relevant conditions, four *P. aeruginosa* strains (PAO1, PAO1/*gfp*, PDO300, and 7119) were grown to a population density of $\sim 10^8$ CFU/mL in three different media (100% SCFM with no mucin added, 90% SCFM + 0.1% mucin (final wt/vol) and 90% SCFM + 1% mucin (final wt/vol)) and subsequently treated with various antibiotics (Tobramycin, Ciprofloxacin, Meropenem, or one of two novel silver carbene complexes; SCC-1 or SCC-22) for 24 hours. Killing curves for all strains, media, and antibiotic concentrations were generated (Figures 3.2-3.6) and MIC and MBC values were determined from the killing curves (see Chapter 3 methods section) (Tables 3.1, 3.2). In general, CFU/mL counts for each strain tested (PAO1/ PAO1/*gfp*, PDO300, and 7119) were lowest when antibiotics were tested against bacteria grown in 100% SCFM, and were higher when antibiotics were used against bacteria grown in 90% SCFM + 1% mucin (final wt/vol) (Figures 3.2-3.6). Further, it was noticed that increasing the concentration of

mucin to 0.1% (wt/vol) in SCFM did not appear to affect CFU/mL counts overall compared to those values from using 100% SCFM with no mucin as a growth medium. In addition, it was observed that MIC values (determined from killing curve data) were higher for both SCC-1 and SCC-22 when compared to the other three antibiotics (Tobramycin, Ciprofloxacin, and Meropenem) regardless of medium (Figures 3.2-3.6, Table 3.1). Also, regardless of *P. aeruginosa* strain and level of mucin added to SCFM, Ciprofloxacin and Meropenem were shown to have the greatest inhibitory effect among antibiotics tested against *P. aeruginosa* population densities of $\sim 10^8$ CFU/mL (Figures 3.2-3.6, Table 3.1). Trends noticed for inhibitory concentrations (Table 3.1) were also similar for bactericidal values with a few noticeable exceptions (Figures 3.2-3.6, Table 3.2). First, minimum bactericidal concentration values were lowest for all four *P. aeruginosa* strains tested using 100% SCFM as a growth medium and highest when using 90% SCFM + 1% mucin (final wt/vol) (Figures 3.2-3.6, Table 3.2). Further, aside from SCC-1 and SCC-22, the increase in mucin concentration in SCFM from 0 to 0.1% (wt/vol) did not alter MBC values by any appreciable amount (Figures 3.2-3.6, Table 3.2), though MBC values for all antibiotics tested (specifically Meropenem, SCC-1, and SCC-22) were dramatically greater (reaching as much as ≥ 250 $\mu\text{g/mL}$ in some strains) when mucin concentration in SCFM was at 1% (final wt/vol) (Figures 3.2-3.6, Table 3.2). These MBC values for all four *P. aeruginosa* strains grown in 90% SCFM + 1% mucin (final wt/vol), were lowest for Tobramycin and Meropenem (Table 3.2). This is interesting, as MIC values

for the four *P. aeruginosa* strains tested were lowest for Ciprofloxacin and Meropenem, while the MBC values were actually lowest for Meropenem and Ciprofloxacin (Table 3.1, 3.2). Further, the addition of 1% mucin (final wt/vol) greatly affected the antibiotic efficacy of Meropenem against all four *P. aeruginosa* strains (Figure 3.4, Table 3.1, 3.2). Lastly, the CF clinical isolate *P. aeruginosa* strain 7119 had the lowest within strain difference in bactericidal concentration when SCC-22 was used in 90% SCFM + 1% mucin (final wt/vol) (Figure 3.6, Table 3.2). While general trends amidst antimicrobial efficacy were noted for the four strains of *P. aeruginosa* under investigation in the three different growth conditions, a more rigorous statistical approach was taken in order to determine any significant interaction amidst the various variables.

Effect of P. aeruginosa Strain Type on MIC/MBC Values

Using the data collected from the killing curves to determine MIC/MBC values (Figures 3.2-3.6, Tables 3.1-3.2), comparisons were conducted using the MIC/MBC values and checking for significant interactions with respect to bacterial strain, growth condition, and antibiotics, and any associated pairwise comparisons where appropriate.

In order to determine if *P. aeruginosa* strain had an effect on the determined MIC and MBC values for all antibiotics in all three grown conditions, all MIC or MBC values were pooled for each strain (Figures 3.7-3.8). Using Friedman's test, it was determined that no statistical difference existed for both

median MIC values ($p = 0.1359$) and median MBC values ($p = 0.2969$) among the four different strains. It was observed that *P. aeruginosa* strain PAO1/*gfp* had the highest median MIC and MBC values compared to PAO1, PDO300, and 7119, but also had the greatest interquartile range from 4-250 $\mu\text{g/mL}$ (Figures 3.7-3.8). In addition, *P. aeruginosa* had the lowest median MIC and MBC values of the four strains for all growth conditions and antibiotics tested (Figures 3.7-3.8). Based on the lack of statistical significance for median MIC and median MBC values between bacterial strains, other comparisons were made by grouping together all MIC or MBC data respectively for the four *P. aeruginosa* strains investigated.

Effect of CF Relevant Growth Medium on MIC/MBC Values

In order to determine if growth medium had a significant effect on antimicrobial efficacy, the MIC or MBC values for all four *P. aeruginosa* strains treated with all five of the antibiotics (Tobramycin, Ciprofloxacin, Meropenem, SCC-1, and SCC-22) were grouped by growth medium conditions (i.e., 100% SCFM with no mucin, 90% SCFM + 0.1% mucin (final wt/vol) and 90% SCFM + 1% mucin (final wt/vol)) (Figures 3.9 – 3.10). Again, Friedman's test was used to initially compare all three medium conditions for any significant interaction. It was found that indeed growth medium had a significant effect on the median MIC ($p = 0.0039$) and median MBC ($p = <0.0001$) values (Figures 3.9-3.10). Using a post-hoc pairwise analysis (Wilcoxon signed-rank test) with Bonferroni adjustment

(adjusted $\alpha = 0.0167$), median MIC and median MBC values were compared among the different growth conditions. It was found that no statistical difference existed for median MIC or median MBC values between 100% SCFM vs. 90% SCFM + 0.1% mucin (final wt/vol) ($p = 0.5078$ and $p = 0.1064$ respectively). However, median MIC and median MBC values were statistically significant between 100% SCFM and 1% mucin (final wt/vol) (MIC $p = 0.0006$, MBC $p = <0.0001$), and median MIC and median MBC values between 90% SCFM + 0.1% mucin (final wt/vol) and 90% SCFM + 1% mucin (final wt/vol) (MIC $p = 0.0010$, MBC $p = <0.0001$). Median MIC values ranged from 3 $\mu\text{g/mL}$ (100% SCFM) up to 8 $\mu\text{g/mL}$ (90% SCFM + 1% mucin (final wt/vol)) (Figures 3.9-3.10). Mean MIC values for all three growth conditions ranged from 4.5 $\mu\text{g/mL}$ (100% SCFM) – 9.8 $\mu\text{g/mL}$ (90% SCFM + 1% mucin (final wt/vol)), while mean MBC values for all three growth conditions ranged from 9.3 $\mu\text{g/mL}$ (100% SCFM) – 144.8 $\mu\text{g/mL}$ (90% SCFM + 1% mucin (final wt/vol)) (Figures 3.9-3.10).

Effect of Antibiotic on MIC/MBC Values

In order to determine if there was a significant difference in median MIC and median MBC values among the five antibiotics investigated, a comparison between median MIC and median MBC values was done using Friedman's test in both cases. Indeed, there was a significant difference for both median MIC values ($p = <0.0001$) and median MBC values ($p = 0.0001$) based on antibiotic used. Median MIC values for all five antibiotics combining MIC values for all four

strains in all three growth medium conditions were 4 µg/mL (Tobramycin), 1 µg/mL (Ciprofloxacin), 1 µg/mL (Meropenem), 12 µg/mL (SCC-1), and 12 µg/mL (SCC-22), while median MBC values based on each antibiotic type were 6 µg/mL (Tobramycin), 4 µg/mL (Ciprofloxacin), 8 µg/mL (Meropenem), 28 µg/mL (SCC-1), and 28 µg/mL (SCC-22) (Figures 3.11-3.12). Mean MIC values for all four *P. aeruginosa* strains grown in all three growth medium conditions were 4.67 µg/mL (Tobramycin), 1.17 µg/mL (Ciprofloxacin), 1.17 µg/mL (Meropenem), 13.33 µg/mL (SCC-1), and 12.0 µg/mL (SCC-22), while mean MBC values were 10.17 µg/mL (Tobramycin), 5.33 µg/mL (Ciprofloxacin), 86.83 µg/mL (Meropenem), 113.5 µg/mL (SCC-1), and 81.67 µg/mL (SCC-22) (Figures 3.11-3.12). To investigate if any significant interactions existed between median MIC/MBC values for the various antibiotics under investigation, Wilcoxon signed-rank test was used with a Bonferroni adjustment (with an adjusted $\alpha = 0.005$). Comparing MIC values between antibiotic pairs, it was noted that significant differences in MIC values existed between Tobramycin and each of the other four antibiotics (Ciprofloxacin, Meropenem, SCC-1 and SCC-22) (with each interaction consisting of $p = 0.0010$), and significant differences also existed between Ciprofloxacin and both SCC complexes (SCC-1 and SCC-22) (with each interaction consisting of $p = 0.0005$) and Meropenem and SCC-1 and SCC-22 ($p = 0.0005$ for each). No significant differences existed between median MIC values of Ciprofloxacin vs. Meropenem, nor was there any significant difference in median MIC values between SCC-1 and SCC-22. Comparisons between

median MBC values for the different antibiotics showed that median MBC values for Tobramycin were statistically significant for SCC-1 ($p = 0.0005$) and SCC-22 ($p = 0.0029$). Further, median MBC values for Ciprofloxacin were statistically significant from both SCC-1 ($p = 0.001$) and SCC-22 ($p = 0.002$). No other significant pairwise interactions were noted in median MBC values among pairs of antibiotics under investigation.

Effect of CF Relevant Growth Medium (Controlling for Antimicrobial) on MIC/MBC Values

One last statistical comparison that was examined included looking for significant interactions between median MIC/MBC values for different growth conditions while controlling for antimicrobial (Figures 3.13-3.14). This comparison was done to determine how medium would individually affect each antibiotic tested, and whether or not significant interactions existed. Using Friedman's test, it was determined that a significant difference did exist between the median MIC values of growth conditions controlling for antibiotic ($p = 0.0011$). In addition, a significant difference was also found to exist between MBC values of growth conditions while controlling for antibiotics ($p = 0.0011$). However, post-hoc analysis using Wilcoxon signed-rank test with Bonferroni correction resulted in a significance level being set at $p < 0.0033$. Based on this corrected significance level, all p -values for median MIC/MBC values for each antibiotic comparing growth medium conditions were greater than the 0.0033 significance

threshold. As a result, no pairwise comparison was significant when comparing median MIC/MBC values among growth conditions while controlling for antibiotic. However, each pairwise comparison only consisted of 4 median MIC or 4 median MBC values per growth medium condition for each antibiotic (i.e., the four *P. aeruginosa* strains). Thus, this small sample for each growth condition within each antibiotic type affected the power of such a statistical test. Yet, some observations are still abundantly clear based on these comparisons. Noticeably, median and mean MIC and MBC values for Ciprofloxacin were relatively low and close in value range regardless of growth medium (Figures 3.13-3.14). Meropenem maintained low median and mean MIC values in all three growth medium conditions. However, while median MIC and MBC values were low for 100% SCFM and 90% SCFM + 0.1% mucin (final wt/vol), median and mean MBC values were far greater in the 90% SCFM + 1% mucin (final wt/vol) condition (Figures 3.13-3.14). Tobramycin displayed the greatest median and mean MIC/MBC values in 90% SCFM + 1% mucin (final wt/vol) of the three different growth conditions (Figures 3.13-3.14). This trend was also noticed for median and mean MIC values of both SCC-1 and SCC-22, with the lowest MIC/MBC values existing when either 100% SCFM or 90% SCFM + 0.1% mucin (final wt/vol) was used as a growth medium, and the highest median MIC/MBC values existing when 90% SCFM + 1% mucin (final wt/vol) was used as a growth medium (Figure 3.14). However, while median MBC values for SCC-1 and SCC-22 compare to MBC values for Tobramycin, Ciprofloxacin, and Meropenem when

grown in 100% SCFM, the greatest disparity exists when SCC-1 and SCC-22 are used under growth conditions that include 90% SCFM + 1% mucin (final wt/vol) (Figure 3.14).

Discussion/Conclusions

The nutrient rich environment found within the lungs of patients diagnosed with cystic fibrosis represents a complex niche in which microorganisms are able to thrive (249). Unique to the lungs of CF patients is the high colonization rate by *P. aeruginosa* (22, 157), due in part to the mucin laden material that becomes trapped in the lungs from defective mucociliary clearance mechanisms (22, 85, 132, 157, 175, 176, 190, 234). As a result, *P. aeruginosa* is afforded an ideal environment to reach very high population densities (175, 176, 208). While previous work has focused on developing a synthetic medium to better approximate the early CF lung environment (175), little work has been done using this synthetic cystic fibrosis medium with the addition mucin (166). As illustrated by the growth of *P. aeruginosa* strains PAO1, PAO1/*gfp*, PDO300, and 7119, the growth dynamics of all four strains are very similar to those of a different *P. aeruginosa* strain grown in 100% SCFM and also actual patient CF sputum (175). While the growth medium presently under investigation (i.e., SCFM) was used initially at 100% and did not contain mucin (175), the present data suggests that the dilution of 100% SCFM to 90% in general (and even more specifically with mucin) does not affect the overall growth dynamics of *P.*

aeruginosa. This is somewhat surprising as mucins, which are members of the O-linked glycosylated protein family (227) have been shown previously to be used by some bacteria as a carbon/nitrogen source (86). One particular note of interest with respect to adding mucin to the base SCFM formula is that upon adding mucin (specifically to a final concentration of 1% wt/vol), the solution becomes very turbid, thereby rendering the use of spectroscopy (i.e., OD₆₀₀ values) useless when trying to approximate bacterial population densities. Therefore, an understanding of the growth dynamics is critical in order to assess bacterial population density levels at various time points. The growth for *P. aeruginosa* strains PAO1, PAO1/*gfp*, PDO300, and 7119 all reached a population density of $\sim 10^8$ CFU/mL at time points that ranged around the same time point observed for the *P. aeruginosa* grown in SCFM and CF sputum by Palmer et al. (175). As already noted, population densities of *P. aeruginosa* have been demonstrated to reach as high as $10^8 - 10^{10}$ CFU/mL in the lungs of CF patients (175, 176, 208). Therefore, in order to develop more effective antimicrobial treatment strategies, it becomes apparent that working with bacterial density numbers more closely relevant to *in vivo* conditions is necessary. These findings on the bacterial population density growth for *P. aeruginosa* strains PAO1, PAO1/*gfp*, PDO300, and 7119 illustrate that the addition of mucin to SCFM appears to have little effect on changing growth patterns as seen by *P. aeruginosa* in actual patient CF sputum (175).

One of the hallmarks in developing an effective antimicrobial treatment strategy to combat infections caused by *P. aeruginosa* in the CF lung is the development of *in vitro* testing of antibiotics that better approximate clinically relevant conditions. In general, *in vitro* antimicrobial susceptibility tests have been called into question with regards to clinical significance (209). As it relates to cystic fibrosis specifically, testing antimicrobials *in vitro* using CF relevant conditions has remained somewhat sparse (124, 166). As such, by utilizing the growth curve dynamics for *P. aeruginosa* strains PAO1, PAO1/*gfp*, PDO300, and 7119 grown in SCFM and SCFM augmented with mucin, multiple clinically relevant antibiotics as well as two novel silver antimicrobials were examined for their antimicrobial effectiveness against high bacterial population densities ($\sim 10^8$ CFU/mL) in an attempt to better approximate the CF lung environment. Overall, the strain of *P. aeruginosa* did not have a significant effect on any of the inhibiting or killing concentrations of the five antibiotics tested in any of the growth conditions. This is particularly promising for both SCC-1 and SCC-22 as novel antimicrobial candidates specifically due to the rise in reports of multiple antibiotic resistant strains of *P. aeruginosa* (79, 103, 157, 181, 184, 185, 203, 230). The three antibiotics Tobramycin, Ciprofloxacin, and Meropenem are currently used by clinicians in the treatment of CF infections (131, 157). All three displayed very low inhibiting and killing concentrations when used in 100% SCFM without the addition of mucin. Both SCC-1 and SCC-22 also had low inhibiting concentrations, with slightly higher minimum bactericidal concentrations

compared to the other three antibiotics. This is not particularly surprising as SCFM contains multiple halide salts at varying concentrations (175). It is well known that one of the drawbacks to utilizing silver based compounds is the affinity for the silver(I) cation (the actual agent that affects bacterial physiology) to various halide species (206). As such, these slightly elevated MIC/MBC values for both SCC-1 and SCC-22 in 100% SCFM with no mucin are most likely attributed to the high amount of halides found in the medium. The addition of 0.1% mucin (final wt /vol) to SCFM did not appear to affect the overall inhibitory capabilities of Tobramycin, Ciprofloxacin, Meropenem, SCC-1 or SCC-22. However, there were some increases in MBC values (most noticeably for SCC-1 and SCC-22).

Perhaps the most noticeable effect on antimicrobial efficacy was when the mucin concentration in SCFM was increased to a final concentration of 1% (wt/vol). For all antibiotics tested, the addition of mucin to 1% (final wt/vol) had a significant effect on both MIC and MBC values, essentially requiring greater concentrations in all cases to inhibit and cause a bactericidal effect on *P. aeruginosa*. This is certainly consistent with other studies that have shown that patient CF sputum alters antibiotic bioactivity (30, 110, 141, 142, 164). It was observed specifically that Meropenem, SCC-1, and SCC-22 appeared to show the greatest increase in MBC values between 100% SCFM with no mucin and 90% SCFM + 1% mucin (final wt/vol) growth conditions (i.e., had the greatest reduction in antimicrobial effectiveness). Meropenem, which is a member of the

larger broad-spectrum class of antibiotics known as the Carbapenems, is widely used to treat serious infections (14, 131, 167, 185) including infections associated with cystic fibrosis (131). However, it has been shown that Meropenem stability becomes reduced by 10% at 37°C after only 1 hour in sterile DI water (231). This reduction in stability could account for the reduced antimicrobial efficacy of the drug. In fact, Meropenem had the highest MBC value in all three growth conditions when used to treat the clinical CF isolate of *P. aeruginosa* (strain 7119). Thus, the stability of Meropenem in solution could account for its reduced antimicrobial efficacy, and increasing mucin may in some way be interacting with the drug even further to account for its greatly reduced capabilities. With respect to the two novel silver carbene complexes, the substantial increase in MBC values when 1% mucin (final wt/vol) was added to SCFM could again be attributed to the reactivity of the silver(I) cation. As already stated, the silver(I) cation is highly reactive with halides that result from halide salt dissolution (206). More specifically however, it has been proposed that the silver(I) cation often interacts with amino acid chains that contain sulfhydryl groups (i.e., cysteine residues) in such a way that protein function in bacteria is rendered inert (73, 143, 193). Certain mucins (polymeric mucins) are also known to possess cysteine-rich domains that aid the mucin chains in forming disulfide bridges (227). Even though both SCC-1 and SCC-22 were designed to have greater water solubility and stability properties compared to other SCC complexes (31, 119, 139, 166, 177), it is very possible that once the silver(I)

cation dissociates from the carbene complex, it may interact with the cysteine residues on the mucin chains prior to reaching bacterial cells. This reduction in the free available silver(I) cation by binding to mucin could account for why SCC-1 and SCC-22 MIC/MBC values were much higher than either Tobramycin or Ciprofloxacin when used in 90% SCFM + 1% mucin (final wt/vol), and could also explain why MIC/MBC values were so much greater for SCC-1 and SCC-22 used in 90% SCFM + 1% mucin (final wt/vol) compared to MIC/MBC values when these compounds were used in 100% SCFM with no mucin added. Thus, although SCC-1 and SCC-22 have demonstrated exceptional antimicrobial capabilities (31, 119, 139, 166, 177), mucin levels present a potential challenge in using these compounds as agents within the CF lung environment. Possible avenues to overcome this mucin barrier could be modification to the SCC complexes and/or encapsulations of the complexes prior to delivery. Indeed, some recent work has already begun to show promise with encapsulation of SCC-22 in L-tyrosine polyphosphate (LTP) nanoparticles in order to aid in delivery and release of the antimicrobial compound (139, 166). Further, a combination approach may also be warranted, whereby free SCC-1 and/or SCC-22 is used along with the slow releasing nanoparticle encapsulated SCC-1 and/or SCC-22. This would establish an upfront reduction in the bacterial population, with the continual release of silver carbene antimicrobial overtime to continue to kill off the remaining bacterial population. Another proposed avenue that could aid SCC-1 and SCC-22 in overcoming the mucin barrier is the addition of

polyethylene glycol (PEG) side chains to SCC-1 and/or SCC-22. Recent work has already demonstrated that this “PEGylation” process greatly improves penetration through sputum/mucus by increasing diffusivity and avoiding mucoadhesivity (220, 221, 237). Regardless, the mucin barrier must be taken into account in future studies looking at the efficacy of SCC complexes in designing treatment options for CF related infections.

One other possible explanation for the reduced bioactivity of all antibiotics tested when the mucin level in SCFM was increased to 1% (final wt/vol) could be that *P. aeruginosa* has been shown to form non-surface attached microcolonies and aggregates that display characteristics of surface adhered microbial communities known as biofilms (3, 212, 213). As *P. aeruginosa* biofilms are known to possess greater resistance to antibiotics than planktonic counterparts (3, 15, 38, 62, 63, 78, 102, 133, 168, 214, 215), it is possible that microcolony or aggregate formation in the turbid, mucin laden medium may have caused a decreased sensitivity to the antimicrobial compounds under investigation. Indeed, this formation of aggregates by *P. aeruginosa* strain PAO1 has been demonstrated to be induced by environmental stress (127). As such, if complete killing of the bacterial population by each antibiotic did not occur rapidly in the 90% SCFM + 1% mucin (final wt/vol), the induced stress caused by the antibiotics could have elicited a stress response thereby promoting aggregate formation and thus protecting groups of *P. aeruginosa* from antibiotic effects.

In conclusion, the data generated suggests that the addition of mucin (up to 1% final wt/vol) to the base medium SCFM developed by Palmer et al. (175) causes bacterial growth for multiple *P. aeruginosa* strains to resemble the growth seen in both 100% SCFM with no mucin as well as similar growth patterns observed in sputum collected from CF patients (175). Also, the antimicrobial susceptibility tests used in this study more accurately reflect CF relevant conditions that allows for the production of more clinically useful MIC/MBC data. The most significant finding of this study was the effect that 1% mucin (final wt/vol) in a synthetic cystic fibrosis medium had on antimicrobial bioactivity. In a medium that consisted of 90% SCFM + 1% mucin (final wt/vol), a significant increase in MIC/MBC values was observed for Tobramycin, Ciprfloxacin, Meropenem, and two novel silver carbene complexes (SCC-1 and SCC-22). This reduction in bioactivity for all five antimicrobials under investigation suggests that mucin (a key component in the cystic fibrosis lung environment) is a major challenge that must be overcome when developing successful antimicrobial treatment strategies to combat CF related infections.

Figures/Tables

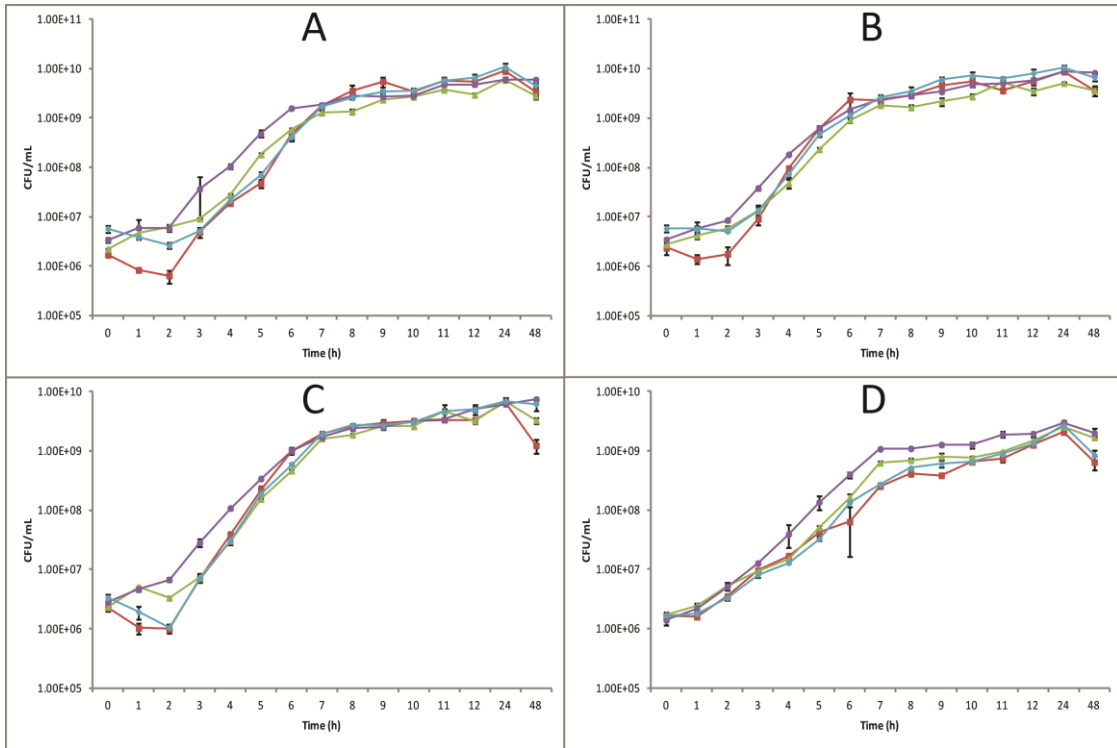


Figure 3.1: Bacterial growth curves for *P. aeruginosa* strains PAO1 (A), PAO1/*gfp* (B), PDO300 (C), and 7119 (D) grown in either 100% SCFM with no mucin (red ■), 90% SCFM + 0.1% mucin (final wt/vol) (green ▲), 90% SCFM + 1% Mucin (final wt/vol) (purple ●), or a control using 100% SCFM diluted to 90% SCFM using sterile DI water (blue ◆). Data points are presented as means with error bars representing \pm one standard deviation from the mean.

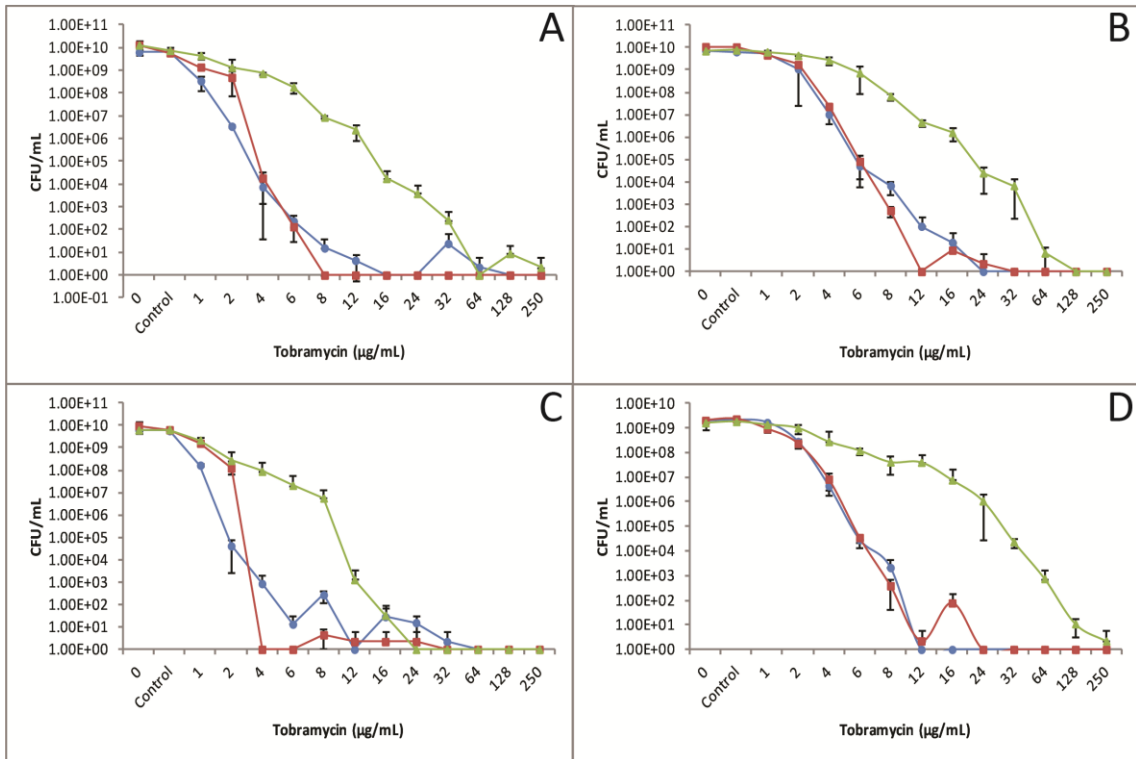


Figure 3.2: Bacterial killing curves for *P. aeruginosa* strains PAO1 (A), PAO1/gfp (B), PDO300 (C), and 7119 (D) grown in 100% SCFM (red ■), 90% SCFM + 0.1% mucin (final wt/vol) (blue ●), or 90% SCFM + 1% mucin (final wt/vol) (green ▲) and subsequently treated with various concentrations of Tobramycin for 24 hours. Data points are presented as means with error bars representing ± one standard deviation from the mean.

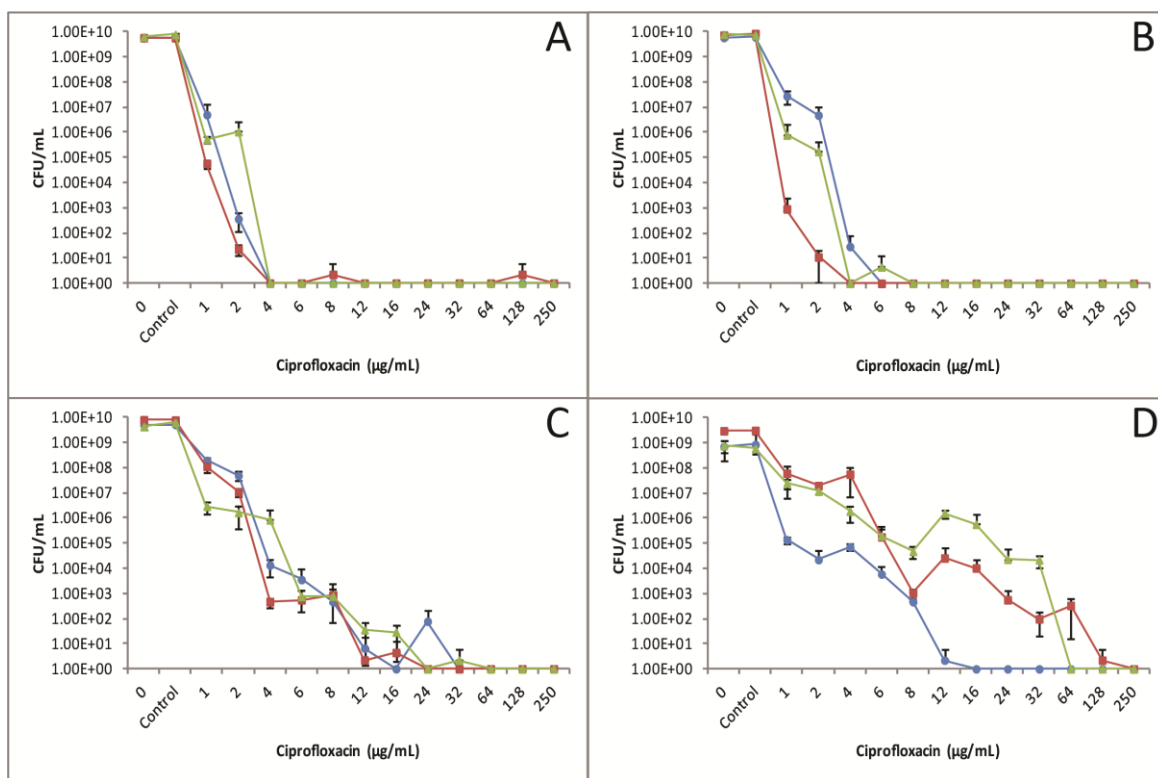


Figure 3.3: Bacterial killing curves for *P. aeruginosa* strains PAO1 (A), PAO1/*gfp* (B), PDO300 (C), and 7119 (D) grown in 100% SCFM (red ■), 90% SCFM + 0.1% mucin (final wt/vol) (blue ●), or 90% SCFM + 1% mucin (final wt/vol) (green ▲) and subsequently treated with various concentrations of Ciprofloxacin for 24 hours. Data points are presented as means with error bars representing ± one standard deviation from the mean.

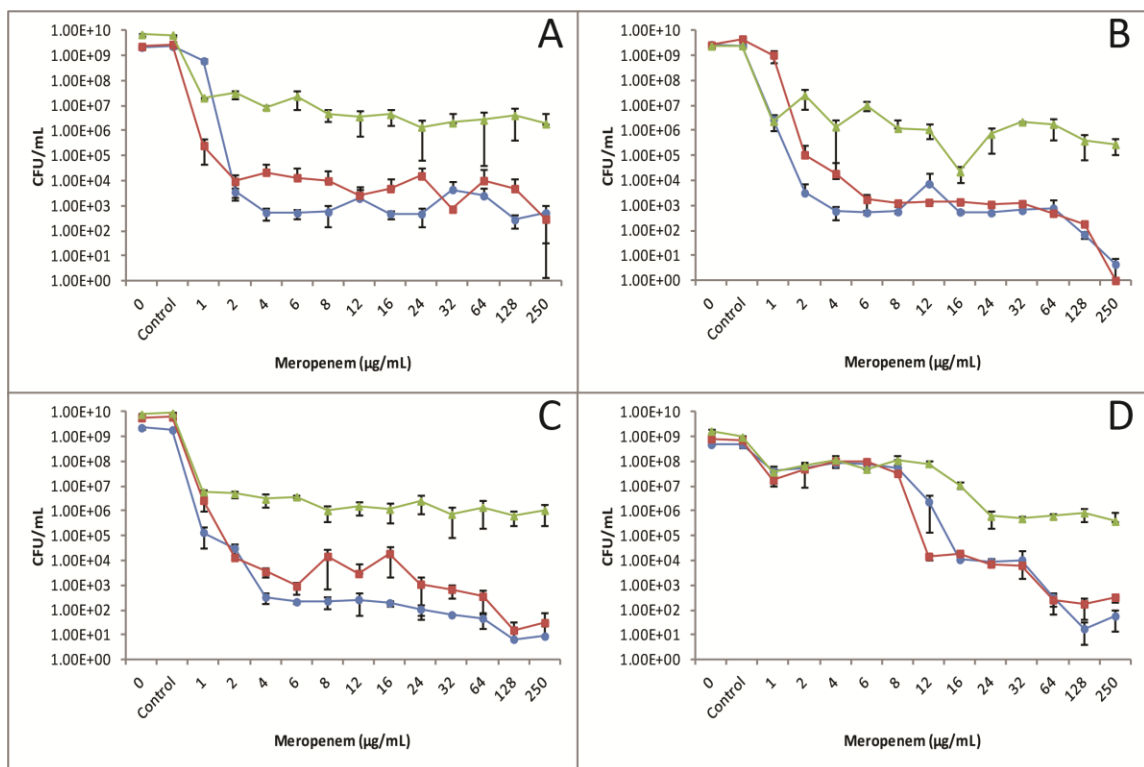


Figure 3.4: Bacterial killing curves for *P. aeruginosa* strains PAO1 (A), PAO1/gfp (B), PDO300 (C), and 7119 (D) grown in 100% SCFM (red ■), 90% SCFM + 0.1% mucin (final wt/vol) (blue ●), or 90% SCFM + 1% mucin (final wt/vol) (green ▲) and subsequently treated with various concentrations of Meropenem for 24 hours. Data points are presented as means with error bars representing ± one standard deviation from the mean.

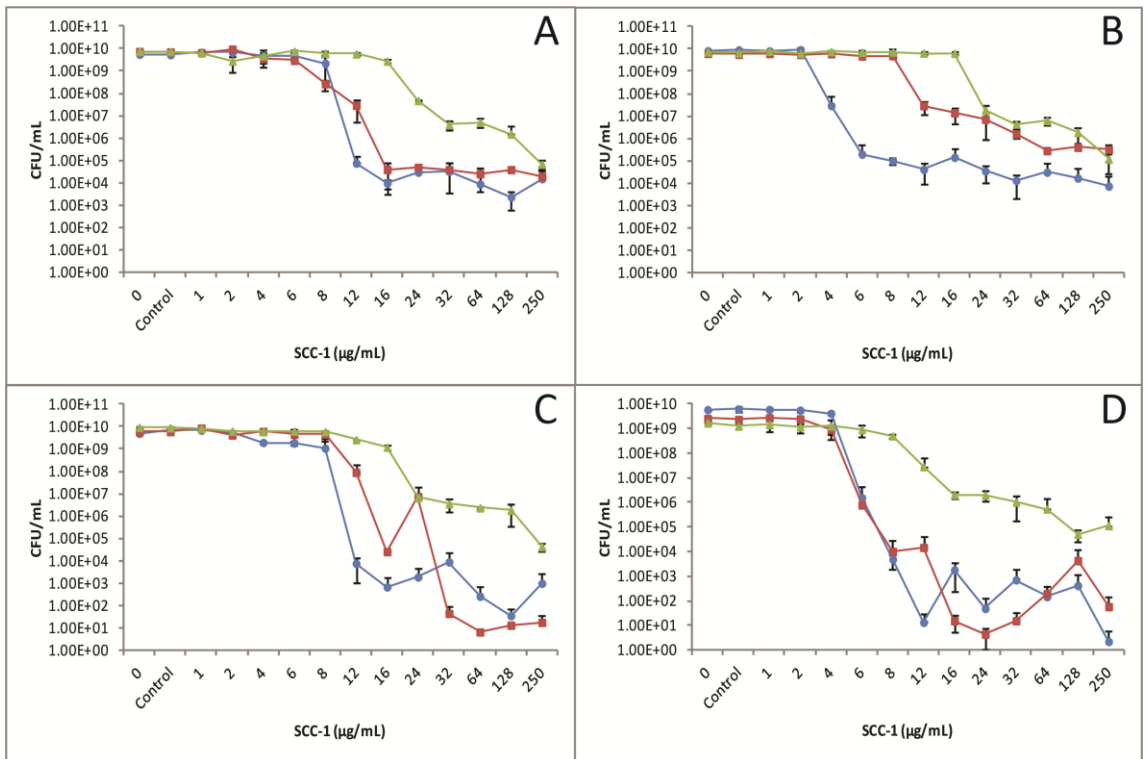


Figure 3.5: Bacterial killing curves for *P. aeruginosa* strains PAO1 (A), PAO1/*gfp* (B), PDO300 (C), and 7119 (D) grown in 100% SCFM (red ■), 90% SCFM + 0.1% mucin (final wt/vol) (blue ●), or 90% SCFM + 1% mucin (final wt/vol) (green ▲) and subsequently treated with various concentrations of SCC-1 for 24 hours. Data points are presented as means with error bars representing ± one standard deviation from the mean.

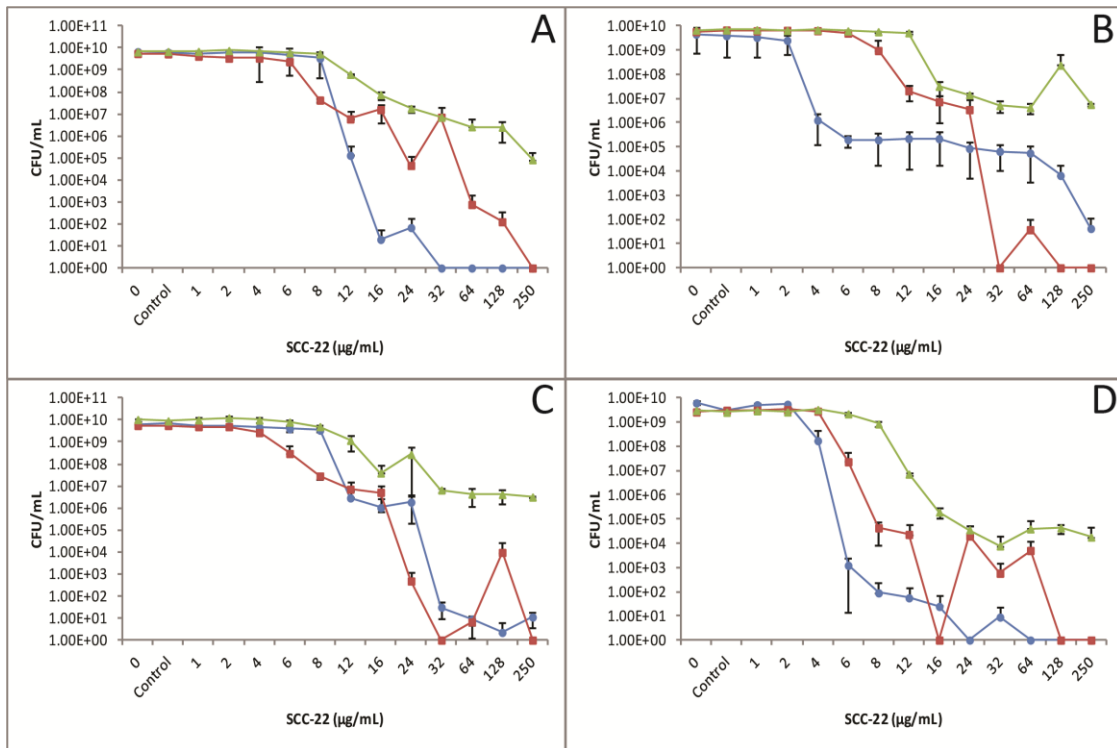


Figure 3.6: Bacterial killing curves for *P. aeruginosa* strains PAO1 (A), PAO1/*gfp* (B), PDO300 (C), and 7119 (D) grown in 100% SCFM (red ■), 90% SCFM + 0.1% mucin (final wt/vol) (blue ●), or 90% SCFM + 1% mucin (final wt/vol) (green ▲) and subsequently treated with various concentrations of SCC-22 for 24 hours. Data points are presented as means with error bars representing ± one standard deviation from the mean.

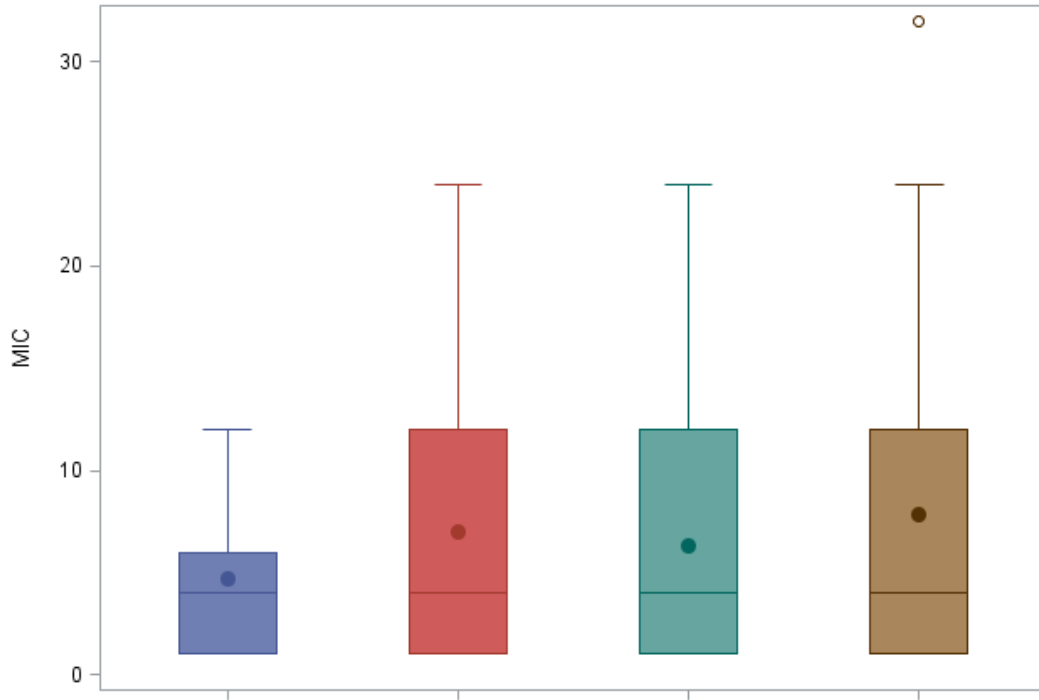


Figure 3.7: Box-and-whisker-plots of median (solid line within each box plot) and mean (shaded circles) comparing MIC ($\mu\text{g/mL}$) values for *P. aeruginosa* strains 7119 (blue), PAO1 (red), PAO1/*gfp* (green), and PDO300. Each box plot includes MICs for each strain grown in 100% SCFM with no mucin, 90% SCFM + 0.1% mucin (final wt/vol), or 90% SCFM +1% mucin (final wt/vol) and treated with Tobramycin, Ciprofloxacin, Meropenem, SCC-1, or SCC-22. Open circles represent outliers.

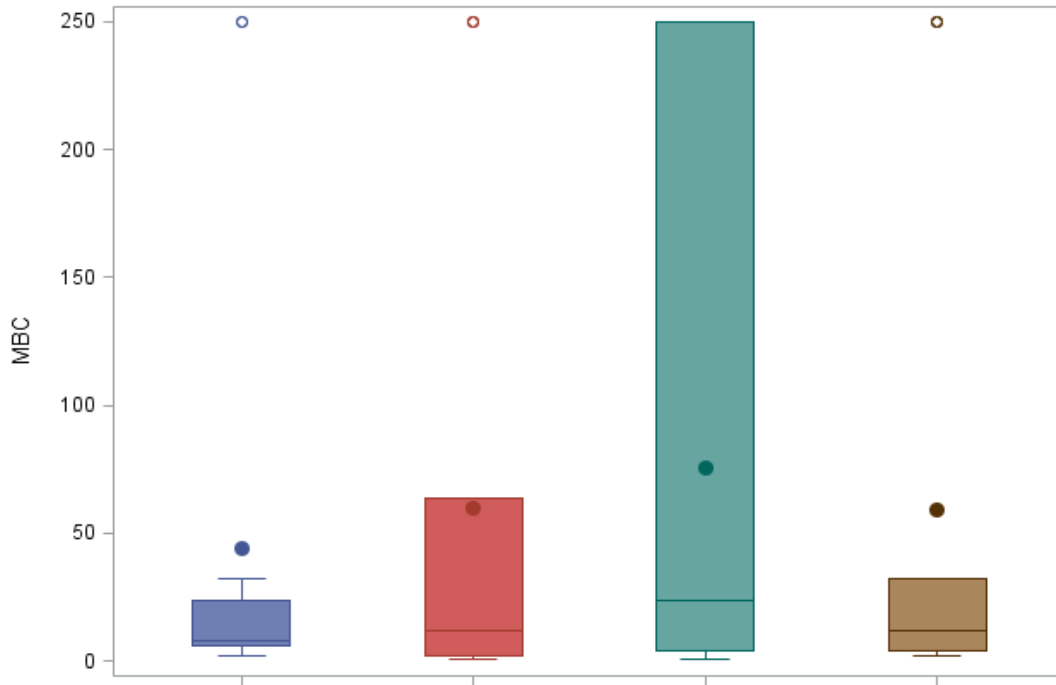


Figure 3.8: Box-and-whisker-plots of median (solid line within each box plot) and mean (shaded circles) comparing MBC ($\mu\text{g/mL}$) values for *P. aeruginosa* strains 7119 (blue), PAO1 (red), PAO1/*gfp* (green), and PDO300. Each box plot includes MBCs for each strain grown in 100% SCFM with no mucin, 90% SCFM + 0.1% mucin (final wt/vol), or 90% SCFM +1% mucin (final wt/vol) and treated with Tobramycin, Ciprofloxacin, Meropenem, SCC-1, or SCC-22. Open circles represent outliers.

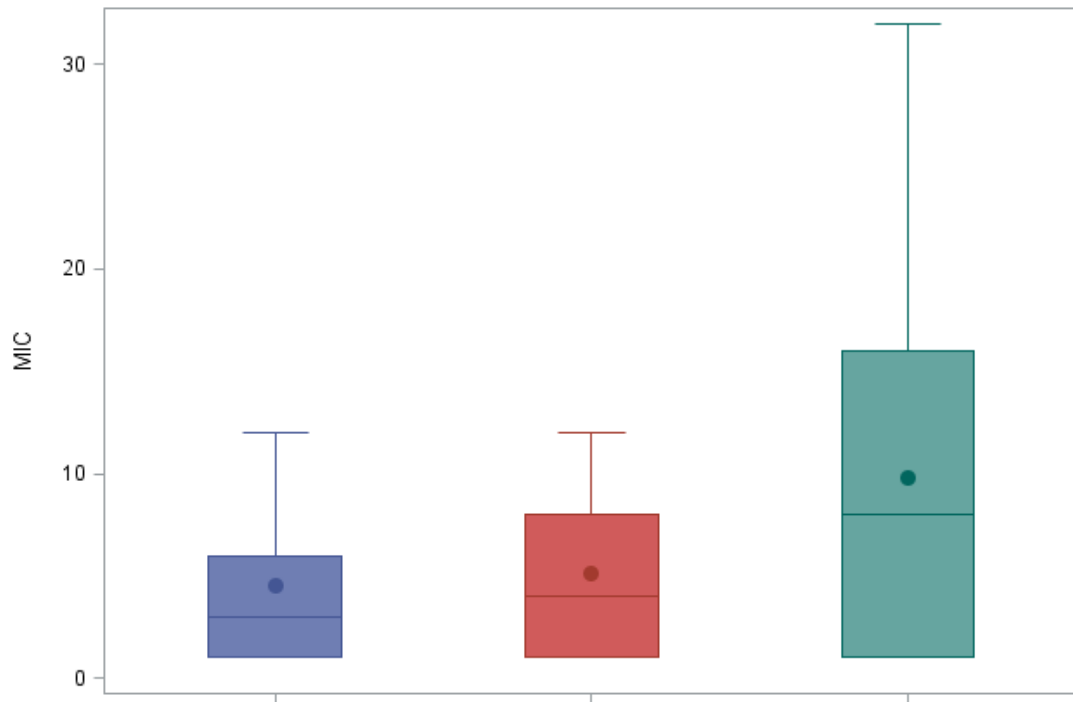


Figure 3.9: Box-and-whisker-plots of median (solid line within each box plot) and mean (shaded circles) MIC values ($\mu\text{g/mL}$) for all four *P. aeruginosa* strains (PAO1, PAO1/*gfp*, PDO300, and 7119) treated with Tobramycin, Ciprofloxacin, Meropenem, SCC-1 and SCC-22 grown in either 100% SCFM (purple), 90% SCFM + 0.1% mucin (final wt/vol) (red), or 90% SCFM + 1% mucin (final wt/vol) (green).

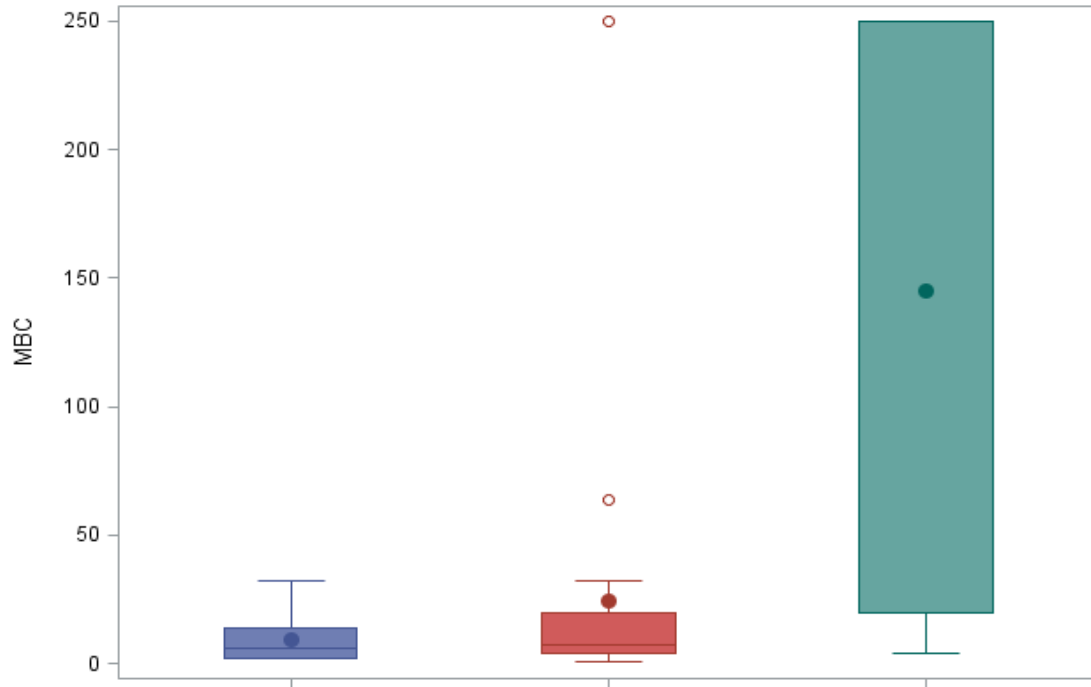


Figure 3.10: Box-and-whisker-plots of median (solid line within each box plot) and mean (shaded circles) MBC values ($\mu\text{g/mL}$) for all four *P. aeruginosa* strains (PAO1, PAO1/*gfp*, PDO300, and 7119) treated with Tobramycin, Ciprofloxacin, Meropenem, SCC-1 and SCC-22 grown in either 100% SCFM (purple), 90% SCFM + 0.1% mucin (final wt/vol) (red), or 90% SCFM + 1% mucin (final wt/vol) (green). Open circles represent outliers.

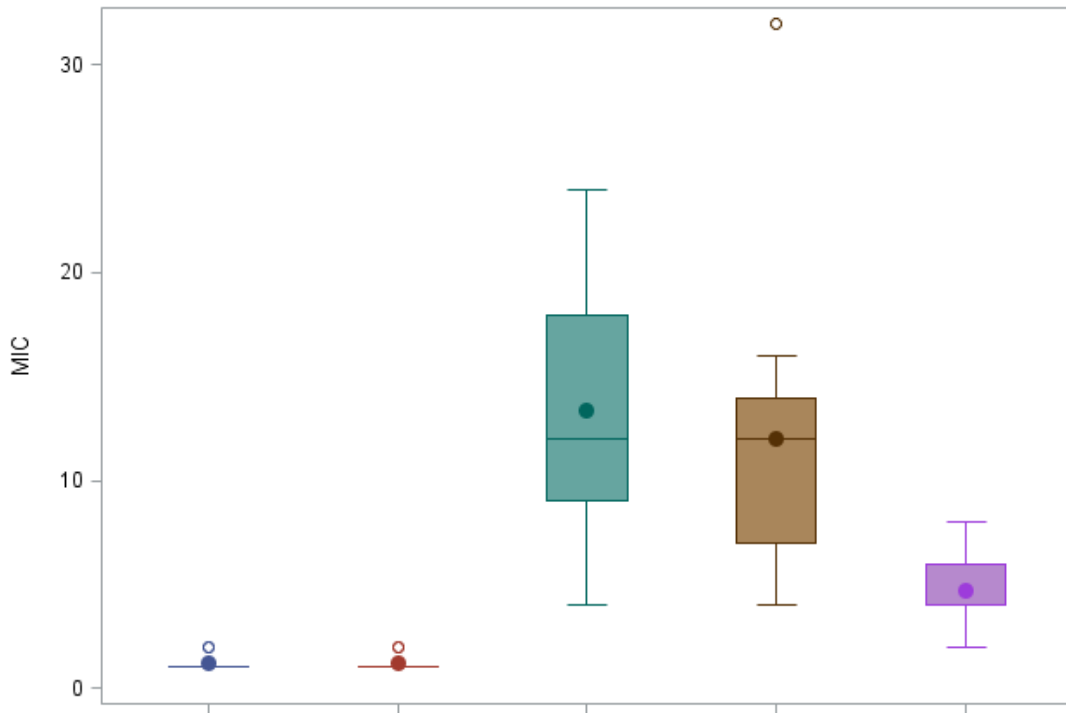


Figure 3.11: Box-and-whisker-plots of median (solid line within each box plot) and mean (shaded circles) MIC values ($\mu\text{g/mL}$) for all four *P. aeruginosa* strains (PAO1, PAO1/*gfp*, PDO300, and 7119) grown in 100% SCFM, 90% SCFM + 0.1% mucin (final wt/vol), and 90% SCFM + 1% mucin (final wt/vol) and treated with either Ciprofloxacin (blue), Meropenem (red), SCC-1 (green), SCC-22 (brown), or Tobramycin (purple). Open circles represent outliers.

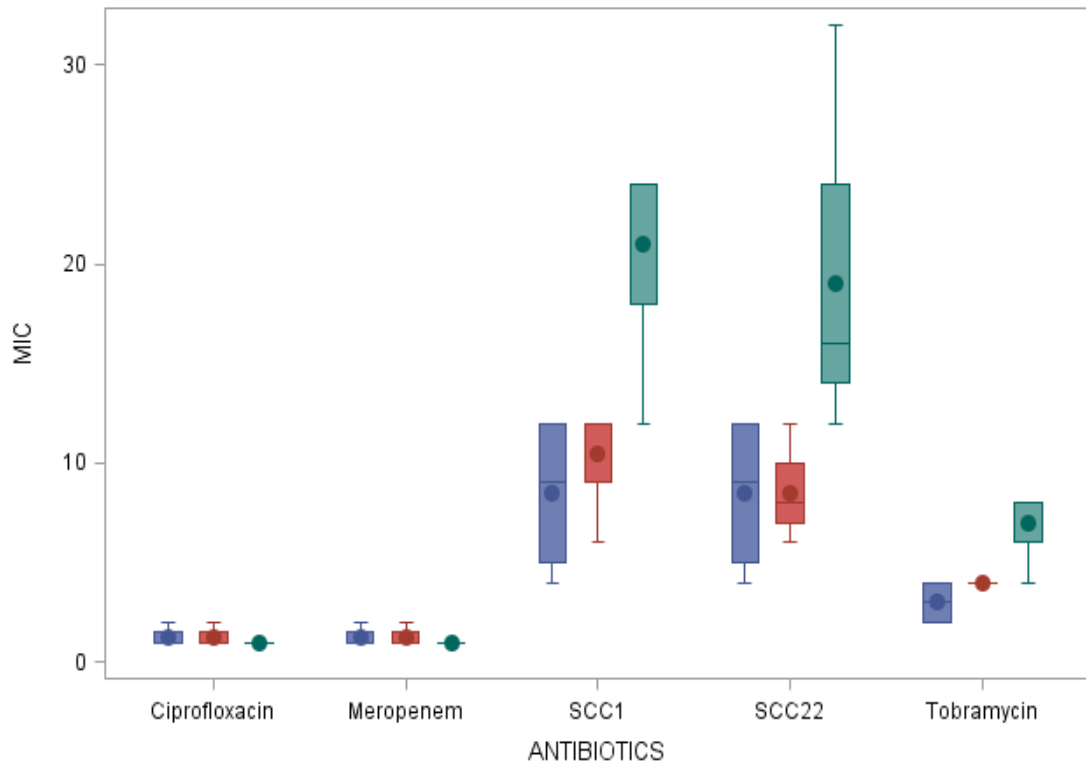


Figure 3.13: Box-and-whisker-plots of median (solid line within each box plot) and mean (shaded circles) MIC values ($\mu\text{g/mL}$) for all four *P. aeruginosa* strains (PAO1, PAO1/*gfp*, PDO300, and 7119) by growth medium (100% SCFM (blue), 90% SCFM + 0.1% mucin (final wt/vol) (red), or 90% SCFM + 1% mucin (final wt/vol) (green) and antibiotic.

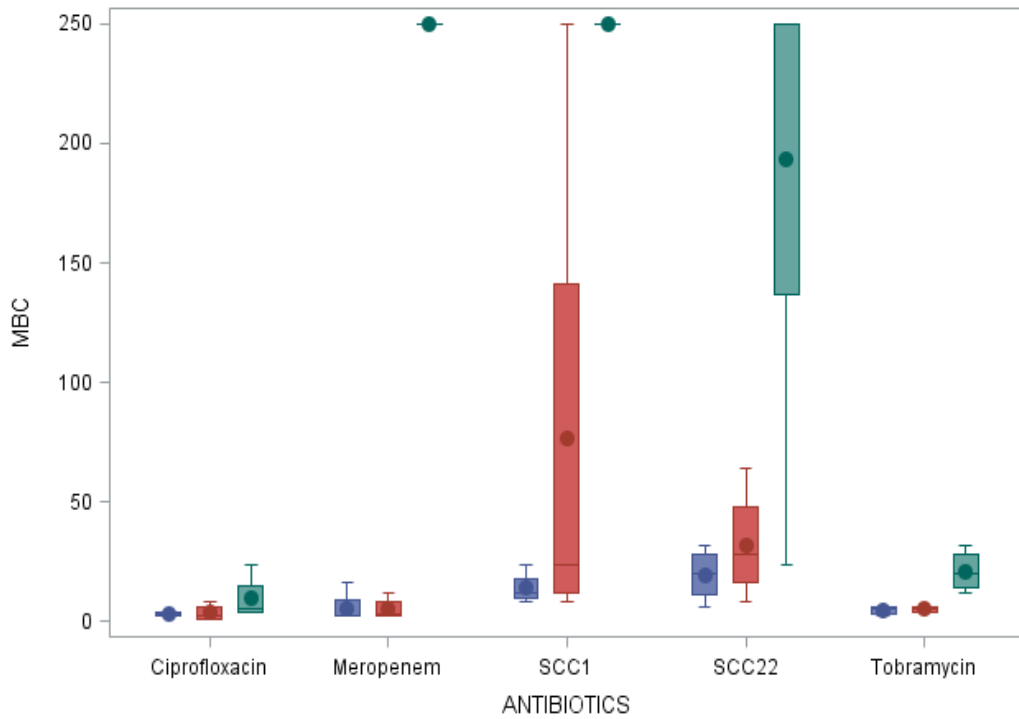


Figure 3.14: Box-and-whisker-plots of median (solid line within each box plot) and mean (shaded circles) MBC values ($\mu\text{g/mL}$) for all four *P. aeruginosa* strains (PAO1, PAO1/*gfp*, PDO300, and 7119) by growth medium (100% SCFM (blue), 90% SCFM + 0.1% mucin (final wt/vol) (red), or 90% SCFM + 1% mucin (final wt/vol) (green) and antibiotic.

<u>Antibiotic</u>	<u>Bacterial Strain</u>	<u>Growth Medium</u>		
		100% SCFM	90% SCFM + 0.1% mucin (final wt/vol)	90% SCFM + 1% mucin (final wt/vol)
Tobramycin	PAO1	2	4	8
	PAO1/ <i>gfp</i>	4	4	8
	PDO300	2	4	4
	7119	4	4	8
Ciprofloxacin	PAO1	1	1	1
	PAO1/ <i>gfp</i>	1	1	1
	PDO300	2	2	1
	7119	1	1	1
Meropenem	PAO1	2	1	1
	PAO1/ <i>gfp</i>	1	2	1
	PDO300	1	1	1
	7119	1	1	1
SCC-1	PAO1	12	12	24
	PAO1/ <i>gfp</i>	4	12	24
	PDO300	12	12	24
	7119	6	6	12
SCC-22	PAO1	12	8	16
	PAO1/ <i>gfp</i>	4	12	16
	PDO300	12	8	32
	7119	6	6	12

Table 3.1: MIC values ($\mu\text{g}/\text{mL}$) for each strain of *P. aeruginosa* (PAO1, PAO1/*gfp*, PDO300, and 7119) tested grown using three different growth media (100% SCFM with no mucin, 90% SCFM + 0.1% mucin (final wt/vol), or 90% SCFM + 1% mucin (final wt/vol)) and treated with Tobramycin, Ciprofloxacin, Meropenem, SCC-1, or SCC-22. MIC values were determined as the first set of replicates (and succeeding replicates) in which growth after 24 hours of treatment did not exceed the approximate 10^8 CFU/mL starting population density.

<u>Antibiotic</u>	<u>Bacterial Strain</u>	<u>Growth Medium</u>		
		100% SCFM	90% SCFM + 0.1% mucin (final wt/vol)	90% SCFM + 1% mucin (final wt/vol)
Tobramycin	PAO1	4	4	16
	PAO1/ <i>gfp</i>	6	6	24
	PDO300	2	4	12
	7119	6	6	32
Ciprofloxacin	PAO1	2	1	4
	PAO1/ <i>gfp</i>	4	1	4
	PDO300	4	4	6
	7119	2	8	24
Meropenem	PAO1	2	2	>250
	PAO1/ <i>gfp</i>	2	4	>250
	PDO300	2	2	>250
	7119	16	12	>250
SCC-1	PAO1	12	16	250
	PAO1/ <i>gfp</i>	24	>250	>250
	PDO300	12	32	250
	7119	8	8	>250
SCC-22	PAO1	16	64	250
	PAO1/ <i>gfp</i>	24	32	>250
	PDO300	32	24	>250
	7119	6	8	24

Table 3.2: MBC values ($\mu\text{g/mL}$) for each strains of *P. aeruginosa* (PAO1, PAO1/*gfp*, PDO300, and 7119) tested grown using three different growth media (100% SCFM with no mucin, 90% SCFM + 0.1% mucin (final wt/vol), or 90% SCFM + 1% mucin (final wt/vol)) and treated with Tobramycin, Ciprofloxacin, Meropenem, SCC-1, or SCC-22. MBC values were determined as the concentrations at which $\geq 99.9\%$ of the initial starting bacterial population density ($\sim 10^8$ CFU/mL) were killed off after 24 hours of treatment with respective antibiotics.

CHAPTER IV
BIOACTIVITY OF NOVEL SILVER CARBENE COMPLEXES AND SELECT
ANTIMICROBIALS AGAINST *PSEUDOMONAS AERUGINOSA* BIOFILMS
GROWN USING CF RELEVANT CONDITIONS

Introduction

One of the more recent paradigm shifts in microbiology is the notion that bacteria exist as biofilms; complex communities of surface attached and non-surface attached microorganisms encased in a self-produced exopolymeric substance (EPS) composed predominantly of water, ions, and various macromolecules such as polysaccharides, nucleic acids, and proteins (3, 42, 60, 76, 216, 222). Although biofilms are known to exist in many natural settings, it has become increasingly evident that this mode of existence is prevalent among patients that are highly susceptible to infection. One such case in which colonization of bacteria (specifically by the opportunistic pathogen *Pseudomonas aeruginosa*) is prevalent is in the case of cystic fibrosis (CF) (10, 77, 156, 157, 179, 245). It has been well established that *P. aeruginosa* favors a biofilm mode of existence within the CF lung environment (15, 106, 157, 208, 248). One of the hallmarks of this adopted mode of existence in the CF lung is that biofilms of *P.*

aeruginosa are highly resistant to common antimicrobial agents (3, 15, 38, 62, 63, 78, 102, 133, 168, 214, 215). This resistance of biofilms to antimicrobial therapy has been attributed to multiple factors including (but not limited to): nutrient gradients and reduced metabolic activity of cells within the biofilm, multi-drug resistance efflux pumps, altered gene expression in response to the biofilm phenotype, quorum sensing, stress induced physiological responses brought on by environmental changes, formation of 'persister' cell populations which consist of metabolically dormant cells that resemble a spore-like state that are resistant to the effects of antibiotics, and overall diffusivity of the antibiotic into the biofilm (42, 62, 81, 159, 214, 215). Of these myriad potential mechanisms for increased antibiotic resistance of biofilms to antimicrobial therapies, the most well studied case for *P. aeruginosa* biofilms is antibiotic effectiveness with respect to overall diffusivity through the biofilm, potential sequestration, and thus overall subsequent bioavailability of the antimicrobial itself.

Diffusivity and sequestration of antimicrobials within the EPS of biofilms has been cited as one of the main reasons why antimicrobial effectiveness is greatly reduced in biofilms (42, 62, 81, 159, 214, 215). However, variation across classes of antimicrobials also exists with respect to diffusivity through the EPS, with specific EPS chemical components acting as potential inhibitors (9). For example, recent evidence has shown that DNA found in the extracellular matrix of biofilms formed by *P. aeruginosa* can inhibit aminoglycoside effectiveness (9, 168), and in some cases act as a cation chelator, which creates cation limited

environments that cause bacteria to induce resistance gene expression to certain aminoglycosides (168). It is also known that the polyanionic, polysaccharide alginate (147, 148), which acts as a main architectural component of biofilms formed by some strains of *P. aeruginosa* from the CF lung (9, 15, 102, 157, 216, 248), has also been demonstrated to greatly inhibit the effects of the aminoglycoside antibiotics Tobramycin and Gentamicin (4, 5, 102, 130, 171). Further, even the β -lactam drug Imipenem (a member of the Carbapenem group) has actually been shown to induce gene expression of β -lactamases as well as expression of the genes responsible for alginate production in *P. aeruginosa* (11). In addition to DNA and alginate, the glycoprotein mucin, a significant component of sputum found in CF patients (22, 132, 158, 163, 190, 192, 234) has been demonstrated to not only enhance tolerance to Tobramycin, but actually promote the formation of *P. aeruginosa* biofilms (133). However, despite evidence for some antimicrobials being hindered by *P. aeruginosa* biofilms, there is also evidence that certain antimicrobials (namely the fluoroquinolone Ciprofloxacin) are able to penetrate the exopolysaccharides that would be found in the biofilm phenotype (130), despite some studies still suggesting delays of transport of fluorquinolones through *P. aeruginosa* biofilms (219, 235). Based on these data, and the fact that *P. aeruginosa* biofilms readily form in the lungs of patients with CF, it has become clear that more studies are still necessary exploring both novel antimicrobial therapies as well as a better understanding of

antimicrobial effectiveness on biofilms grown under nutritional conditions seen in the CF lung environment.

The continual escalation in antibiotic resistance has prompted researchers to explore alternative chemotherapeutic agents as a means to eradicate difficult to treat infections. More specifically, recent resurgence of silver based antimicrobials has garnered recent attention as an attractive chemotherapeutic option to treat challenging infections. One class of silver based antimicrobials that has proven highly effective is the N-heterocyclic silver carbene complexes (SCCs) (105, 120). SCCs afford extra binding stability to the metal center of the silver(I) cation thereby allowing the silver cation to be slowly released over time (120). Further, two SCC compounds (SCC-1 and SCC-22) have been well documented as effective broad spectrum, water soluble/stable antimicrobial compounds (31, 119, 139, 166, 177). However, despite showing significant promise as broad spectrum antimicrobials, few studies have examined the effectiveness of SCCs against the biofilm phenotype (166, 177). Further, in relation to the CF lung environment, despite some evidence that silver is very effective when used on *P. aeruginosa* biofilms (17, 166), there has only been one study examining the effects of a silver carbene complex used against *P. aeruginosa* biofilms grown under CF relevant conditions (166).

Based on the growing need to develop more effective antimicrobials to combat *P. aeruginosa* biofilms that form in the lungs of CF patients, the research described below sought to investigate how effective two silver carbene

complexes (SCC-1 and SCC-22) would be compared to other candidate antimicrobials from various drug classes (Tobramycin (aminoglycoside), Ciprofloxacin (fluoroquinolone), and Meropenem (β -lactam)) used against static biofilms of various strains of *P. aeruginosa* grown in CF relevant conditions. It was hypothesized that SCC complexes (SCC-1 and SCC-22) would be more effective than current clinically relevant antimicrobial compounds (Tobramycin, Ciprofloxacin, Meropenem) at eradicating *P. aeruginosa* biofilms grown under static conditions using 100% SCFM. In addition, it was hypothesized that the addition of mucin (1% wt/vol) to SCFM would impede the antimicrobial efficacy of all antimicrobial compounds tested. The following experiments sought to address the above mentioned hypotheses:

- Using a standard lab strain (PAO1), a PAO1 alginate overproducer (PDO300), and a mucoid CF clinical isolate (7119), establish static biofilm growth conditions using a defined synthetic cystic fibrosis medium (SCFM) (175) with and without the addition of mucin.
- Compare the killing efficacy of three clinically used antimicrobials to treat CF infections (Tobramycin, Ciprofloxacin, Meropenem) with two novel silver carbene complexes (SCC-1 and SCC-22) for static biofilms of three *P. aeruginosa* strains (PAO1, PDO300, and 7119) grown using SCFM.
- Examine the effects that mucin (1% wt/vol), when added to SCFM, has on all five antimicrobials under investigation.

Materials and Methods

Static P. aeruginosa Biofilm Growth Curves Using CF Relevant Conditions

Static biofilm growth curves for *P. aeruginosa* strains PAO1 (ATCC BAA-47), PDO300, and 7119 were established in TPP® Tissue Culture 24-well culture plates (MIDSCI™ Product #: TP92024, MIDSCI™, St. Louis, Missouri, USA) as follows. Overnight cultures of PAO1, PDO300, and 7119 were started by inoculating 5 mL of medium (100% SCFM or 90% SCFM + 1% mucin (final wt/vol)) with respective strains, which were then incubated with agitation (37°C/250 rpm) for approximately 12 hours. Cultures were diluted the next day 1:1000 into individual wells on 24-well culture plates by adding 2 µL of overnight culture into 2 mL of fresh growth medium. Plates for all strains/medium combinations were grown under static conditions at 37°C for 0, 3, 6, 12, and 24 hours until processing (see below). In addition to the above time points, static plates were also prepared as described, then incubated for 24 hours (37°C), rinsed three times with corresponding media, refilled with 2 mL fresh respective medium, and allowed to incubate for a further 24 hours prior to processing. Following indicated incubation times, 24-well culture plates were removed from the incubator, supernatant was removed and the surface attached biofilms were gently rinsed three times with 2 mL of corresponding media in order to remove excess planktonic cells. Next, 2 mL of sterile DI water was added to each biofilm well, and the wells were gently sonicated for 10 seconds to detach surface adhered cells. Following sonication, the resulting cell suspension was diluted

appropriately using sterile DI water and resulting dilutions were spread onto TSA plates using an Autoplate® 4000 automated spiral plater (Spiral Biotech, Inc., Bethesda, MD, USA). Plates were maintained at 37°C until visible colonies appeared (CFUs), following which plates were counted and CFU/mL were determined for each sample. All experiments were carried out in triplicate.

Treatment of P. aeruginosa Biofilms with Various Antimicrobial Compounds

Twenty four hour static biofilms were first established for PAO1, PDO300, and 7119 as described above. Briefly, overnight cultures were prepared in either 100% SCFM or 90% SCFM + 1% mucin (final wt/vol), and were incubated with agitation at 37°C and 250 rpm respectively for approximately 12 hours. The next day, overnight cultures were diluted 1:1000 using fresh corresponding medium in 24-well tissue culture plates, and plates were maintained in a 37°C incubator for 24 hours. Culture plates were removed from the incubator, and all wells were gently rinsed three times with 2 mL of fresh corresponding media. Stock solutions (10 mg/mL) of Tobramycin, Ciprofloxacin, Meropenem, SCC-1, and SCC-22 were prepared as outlined previously (see Chapter III). Stock solutions were diluted (using corresponding dissolvent) to 40x desired antimicrobial treatment concentrations. These 40x stocks were next pre-mixed in appropriate corresponding medium (i.e., that in which the static biofilms were grown) to final treatment concentrations of 0, 4, 8, 16, 32, 64, and 128 µg/mL. In addition, controls that included pre-mixed medium and antimicrobial dissolvent were also

generated. Two milliliters of appropriate antimicrobial/fresh medium concentration was added to corresponding wells, plates were placed back in the incubator (37°C) under static conditions, and challenged for a treatment length of approximately 24 hours. Next, culture plates were removed from the incubator, supernatant was decanted, and wells were gently rinsed three times with corresponding media to remove excess planktonic cells. Two milliliters of sterile DI water was then added to each well, and wells were gently sonicated for 10 seconds to dislodge surface adhered cells. Resulting suspensions were diluted accordingly in sterile DI water, and resulting dilutions were spiral plated onto TSA plates using an Autoplate® 4000 automated spiral plater (Spiral Biotech, Inc., Bethesda, MD, USA). TSA plates were maintained in a 37°C incubator until colonies appeared. Colony forming units (CFUs) were counted, and biofilm viability was measured as viable CFU/mL counts. All experiments were carried out in triplicate.

Results

Growth of Static Biofilms of Multiple P. aeruginosa Strains Using CF Relevant Growth Media

In order to establish growth conditions for static biofilms of *P. aeruginosa* strains PAO1, PDO300, and 7119, bacteria were grown in either 100% SCFM with no mucin or 90% SCFM + 1% mucin (final wt/vol) for various time points. *Pseudomonas aeruginosa* strains PAO1, PDO300, and 7119 all displayed similar static biofilm growth patterns for both 100% SCFM with no mucin and 90%

SCFM + 1% mucin (final wt/vol) (Figure 4.1A-C), indicating that mucin does not appear to have a substantial effect on static biofilm growth for all three strains investigated. Upon initial inoculation and immediate termination at zero hours, it was found that bacteria were still able to adhere to the 24 well culture dish, with more bacteria adhering when 100% SCFM was used as a growth medium compared to 90% SCFM + 1% mucin (final wt/vol) (Figure 4.1A-C). However, as static biofilms were allowed to grow for longer periods of time, the total number of surface adhered bacteria appeared to be similar among all three strains regardless of the two growth conditions (Figure 4.1A-C). It was observed that total abundance of static biofilm bacteria continues to rise exponentially for *P. aeruginosa* strains PAO1 and PDO300 in both growth conditions until approximately 24 hours, when growth appears to plateau (Figure 4.1A,B). Noticeably however, *P. aeruginosa* strain 7119 did not show a similar plateau after 24 hours of static growth conditions in either growth medium (Figure 4.1C).

Perhaps the most important finding of the static biofilm growth conditions for *P. aeruginosa* strains PAO1, PDO300, and 7119 in both 100% SCFM with no mucin and 90% SCFM + 1% mucin (final wt/vol) can be seen at the 24+ growth point (Figure 4.1A-C). This time point represented static biofilms that were grown for 24 hours, washed gently three times with fresh 100% SCFM with no mucin, were refilled with fresh corresponding media (either 100% SCFM with no mucin or 90% SCFM + 1% mucin (final wt/vol)), and then were incubated for a further 24 hours upon which the static growth was terminated. For *P. aeruginosa* strain

PAO1 and PDO300, total numbers of bacteria were slightly higher when growth in 90% SCFM + 1% mucin (final wt/vol) compared to 100% SCFM with no mucin (Figure 4.1A,B). *Pseudomonas aeruginosa* strain 7119 on the other hand displayed very similar number of surface adhered bacteria regardless of growth condition at the 24+ hour time point (Figure 4.1C). Further, despite subtle differences in abundance of bacteria in static biofilms relative to growth medium conditions at this specific time point (24+ hours), the overall relative abundance of surface adhered bacteria was approximately similar in static biofilms that were grown for only 24 hours (with strain 7119 being perhaps the only noticeable difference) (Figure 4.1A-C). Based on these results, it did not appear that washing the static biofilm grown for 24 hours to get rid of planktonic cells substantially altered the overall number of bacteria present in the surface adhered static biofilm. Therefore, based on these results it is reasonable to deduce that biofilms of *P. aeruginosa* strains PAO1, PDO300, and 7119 can be grown under static growth conditions using either 100% SCFM with no mucin or 90% SCFM + 1% mucin (final wt/vol) for 24 hours, and then subsequently rinsed with 100% SCFM without much alteration in surface adhered population numbers of *P. aeruginosa*. Further, these growth conditions for static biofilms of *P. aeruginosa* strains demonstrate an effective method to grow and subsequently treat static biofilms using different classes of antimicrobials in order to assess antimicrobial efficacy (see next section).

Effects of Silver Carbene Complexes and Other Antimicrobials Against Static Biofilms of P. aeruginosa Grown in CF Medium Without Mucin

Pseudomonas aeruginosa strains PAO1, PDO300, and 7119 were grown as static biofilms for 24 hours, and were treated for 24 hours with various concentrations of the antimicrobial compounds Tobramycin, Ciprofloxacin, Meropenem, and two novel silver carbene complexes (SCC-1 and SCC-22). Tobramycin and Ciprofloxacin had similar killing trends against *P. aeruginosa* strain PAO1, such that an approximate two-log reduction in surface adhered bacteria was observed beginning at 4 µg/mL (Figure 4.2A). However, increasing concentrations of both Tobramycin and Ciprofloxacin did not appear to have much impact on killing efficacy for *P. aeruginosa* strain PAO1 (Figure 4.2A). For *P. aeruginosa* strain PDO300, a nearly two-log reduction in bacteria was noted beginning approximately at 4 µg/mL for Tobramycin and approximately 8 µg/mL for Ciprofloxacin respectively (Figure 4.2B). Increasing concentration of Ciprofloxacin had very little impact on killing efficacy against *P. aeruginosa* strain PDO300 grown in 100% SCFM with no mucin, however Tobramycin was able to achieve approximately a three-log reduction in surface adhered bacteria at a concentration of 128 µg/mL (Figure 4.2B). *Pseudomonas aeruginosa* strain 7119 achieved approximately a two-log reduction in surface adhered bacteria, but not until a concentration of approximately 128 µg/mL (Figure 4.2C). For all three strains of *P. aeruginosa* grown as static biofilms in 100% SCFM with no mucin, Meropenem was observed to cause an initial decrease in biofilm mass, but was observed to reach a killing efficacy plateau at approximately 8 µg/mL (PAO1), 4

µg/mL (PDO300), 32 µg/mL (7119), with at most a one-log reduction in biofilm bacteria for all three strains investigated (Figure 4.2A-C). Both of the novel silver carbene complexes demonstrated the greatest efficacy at eradicating biofilm biomass for all three strains grown as static biofilms in 100% SCFM without added mucin (Figure 4.2A-C). While subtle decreases in viable bacteria were observed at lower concentrations of SCC-1 and SCC-22, both SCC-1 and SCC-22 were capable of completely eradicating static biofilms of *P. aeruginosa* strains PAO1, PDO300, and 7119 beginning at a concentration of 64 µg/mL (Figure 4.2A-C). In fact, one treatment for 24 hours using a concentration of 128 µg/mL of either SCC-1 or SCC-22 eliminated all viable biofilm bacteria for all three *P. aeruginosa* strains tested (Figure 4.2A-C). Thus, both SCC-1 and SCC-22 demonstrated greater killing efficacy against these *P. aeruginosa* static biofilms grown in 100% SCFM with no mucin compared to the other three clinically used antibiotics (Figure 4.2A-C).

Effects of Silver Carbene Complexes and Other Antimicrobials Against Static Biofilms of P. aeruginosa Grown in CF Medium With Mucin

The efficacy of various antimicrobial compounds (i.e., Tobramycin, Ciprofloxacin, Meropenem, SCC-1, and SCC-22) against static biofilms of *P. aeruginosa* strains PAO1, PDO300, and 7119 grown in 90% SCFM + 1% mucin (final wt/vol) was examined. All five antibiotics tested against *Pseudomonas aeruginosa* strains PAO1, PDO300, and 7119 displayed varying degrees of killing efficacy, with Ciprofloxacin being the most effective at consistently

reducing the bacterial population within static biofilms with increasing concentrations (Figure 4.3). A three-log reduction in PAO1 biofilm bacteria was achieved at a concentration of approximately 128 $\mu\text{g}/\text{mL}$ for Ciprofloxacin (Figure 4.3A). Both SCC-1 and SCC-22 were observed to be the least effective at reducing PAO1 static biofilms when grown in 90% SCFM + 1% mucin (final wt/vol), only at most achieving a one-log reduction in biofilm bacteria (Figure 4.3A). For *P. aeruginosa* strain PDO300, while Ciprofloxacin was again demonstrated to be the most consistent at gradually decreasing the static biofilm population density and ultimately achieving a maximum two-log reduction at between 64-128 $\mu\text{g}/\text{mL}$, Tobramycin, SCC-1, and SCC-22 were also able to capable of achieving a two-log reduction in biofilm bacteria at 128 $\mu\text{g}/\text{mL}$ (Figure 4.3B). Static biofilms of *Pseudomonas aeruginosa* strain 7119 grown in 90% SCFM + 1% mucin (final wt/vol) showed similar killing patterns for all five antibiotics tested compared to killing curves of static biofilms for PAO1 and PDO300, with Ciprofloxacin again displaying the greatest efficacy at reducing biofilm bacterial density (Figure 4.3A-C). Noticeably, both Ciprofloxacin and SCC-1 were able to achieve a similar three-log reduction in biofilm bacteria at a concentration of 128 $\mu\text{g}/\text{mL}$ (Figure 4.3C). Regardless of *P. aeruginosa* strain tested, Meropenem displayed a similar plateau effect in killing efficacy when used in 90% SCFM + 1% mucin that was also observed when the antibiotic was used against static biofilms grown in 100% SCFM with no mucin (Figures 4.2-4.3). In general, Tobramycin treatment of biofilms for all three strains of *P.*

aeruginosa resulted in no substantial reductions in biofilm bacteria, as its efficacy was also most prominent at a concentration of 128 µg/mL for all three strains (Figure 4.3), at most only causing a three-log reduction in bacteria for strains PDO300 and 7119 (Figure 4.3B,C).

Perhaps the most interesting result that was observed was when killing efficacy for the different antimicrobials were compared between static biofilms grown in 100% SCFM with no mucin and 90% SCFM + 1% mucin (final wt/vol) (Figures 4.2-4.3). By adding 1% mucin (final wt/vol) to the base SCFM medium, CFU/mL values were noticeably higher even at high antimicrobial concentrations (i.e., 64 and 128 µg/mL) compared to similar values when 100% SCFM with no mucin added was used to grow static biofilms (Figures 4.2-4.3). Further, while both SCC-1 and SCC-22 were able to completely eliminate static biofilms of *P. aeruginosa* strains PAO1, PDO300, and 7119 grown in 100% SCFM with no mucin added at a concentration of 128 µg/mL (Figure 4.2), neither compound was able to eradicate the biofilm at 128 µg/mL when grown in 90% SCFM + 1% mucin (final wt/vol) (Figure 4.3). In fact after 24 hours of treatment with the silver carbene complexes, only SCC-22 treatment resulted in a three-log reduction in biofilm bacterial density, and that was against *P. aeruginosa* strain 7119 (Figure 4.3C). Thus, the addition of mucin (at 1% final wt/vol) to SCFM appears to reduce the bioactivity of all antimicrobial compounds tested, but had the most noticeable effect on killing concentrations of both SCC-1 and SCC-22 (Figures 4.2-4.3).

Discussion/Conclusions

The nature of the CF lung environment poses a uniquely challenging arena for understanding the efficacy of antimicrobial treatment strategies. As has already been extensively documented, various strains of *P. aeruginosa* display resistance to a myriad of antibiotics (79, 103, 157, 181, 184, 185, 203, 230). This resistance is further enhanced when *P. aeruginosa* switches to a biofilm mode of existence within the lungs of CF patients such that the biofilms of *P. aeruginosa* actually display a greater resistance against antimicrobial treatment compared to planktonic counterparts (3, 15, 38, 62, 63, 78, 102, 133, 168, 214, 215). This was certainly noticed in the present investigation. Necessary killing concentrations were much higher for Tobramycin, Ciprofloxacin, and Meropenem against biofilms of various *P. aeruginosa* strains grown in 100% SCFM compared to similar planktonic growth conditions (see Chapter III). It is well known that diffusivity and sequestration of antimicrobial agents within the extracellular polymeric matrix of biofilms represents a possible explanation for this reduced efficacy of certain chemotherapeutic courses of treatment (42, 62, 81, 159, 214, 215). Further, it has been documented that DNA (a critical component of biofilm architecture) is able to inhibit aminoglycoside bioactivity (9, 168), and in some cases is capable of cation sequestration leading to induction of genes responsible for increased resistance to antibiotics (168). This could offer a possible explanation for the reduced bioactivity of Tobramycin against *P. aeruginosa* static biofilms grown in 100% SCFM with no mucin. Cation

sequestration caused by DNA in the biofilm may have induced aminoglycoside resistance genes, thereby reducing bioactivity of Tobramycin. Further, another component commonly found in biofilms is alginate, which has been previously demonstrated to also reduce the bioactivity of certain aminoglycoside antibiotics (4, 5, 102, 130, 171). It is very possible that upon *P. aeruginosa* forming static biofilms grown in 100% SCFM with no mucin, the production of alginate reduces the activity of Tobramycin again by acting as a potential sequester.

Although Meropenem (and Carbopenems in general) are used mostly against difficult infections in a last resort eradication effort (14, 79, 167), Meropenem did not show substantial reduction of static biofilm bacteria of *P. aeruginosa* grown in 100% SCFM without mucin. It has been demonstrated that certain β -lactam drugs can lead to β -lactamase gene induction (11). As Meropenem is a member of this class of drugs (79), it is very possible that the reduced bioactivity is again related to gene induction of antibiotic resistance genes in *P. aeruginosa*. Also, and a more likely explanation for reduced bioactivity of Meropenem, is the fact that Meropenem has been shown to have reduced stability occurring only one hour after being mixed in sterile DI water and maintained at 37° C (231). Therefore, regardless of concentration of Meropenem used against biofilms of *P. aeruginosa* grown at 37° C, the Meropenem may have already begun degradation within the first hour, thereby rendering even high concentrations less effective against the biofilm.

Interestingly, Ciprofloxacin (the fluoroquinolone representative investigated) also demonstrated reduced efficacy against static biofilms of *P. aeruginosa* grown in 100% SCFM with no mucin compared to its very effective nature against planktonic bacteria grown under similar conditions (see Chapter III). This reduced bioactivity is somewhat surprising as some studies have demonstrated that Ciprofloxacin is actually able to penetrate the exopolysaccharides commonly found in the biofilm (130). However, there is also some evidence suggesting that fluoroquinolones are also delayed in transport throughout *P. aeruginosa* biofilms (219, 235). Certainly the present data suggests that reduced bioactivity of Ciprofloxacin against *P. aeruginosa* biofilms grown under static conditions using 100% SCFM with no mucin is consistent with a delay in the antibiotic reaching all areas of the biofilm.

Despite Tobramycin, Meropenem, and Ciprofloxacin all showing limited bioactivity against static biofilms of *P. aeruginosa* strains grown in 100% SCFM with no mucin, both novel silver carbene complexes tested (SCC-1 and SCC-22) were highly effective at reducing the number of surface attached bacteria. Specifically, at concentrations of 64 µg/mL and 128 µg/mL, SCC-1 and SCC-22 displayed a much higher efficacy at eradicating *P. aeruginosa* biofilms grown in 100% SCFM with no mucin compared to Tobramycin, Ciprofloxacin, and Meropenem. Indeed, recent research has demonstrated that silver is an effective agent when used to treat *P. aeruginosa* biofilms (17, 166). The silver carbene complexes are afforded extra binding stability to the silver(I) cation, thereby

allowing for a more gradual release of the silver(I) cation over time (120). This slower release of the silver(I) cation may help explain why these compounds demonstrated such high efficacy against *P. aeruginosa* biofilms grown under static conditions in 100% SCFM with no mucin. By allowing for a slower release from the carbene carrier, the silver(I) cation is able to prevent the biofilm from continually growing or repairing. In addition, the incidence of silver resistance among bacterial isolates is relatively low, with very few resistance genes and mechanisms being described for silver (206). Although multiple modes of action for silver induced bacterial death have been proposed (73, 143, 193, 240), induction of resistance genes would be minimal due to the low number of reported silver resistant bacterial strains (206). Based on both SCC-1 and SCC-22 being able to completely eradicate *P. aeruginosa* biofilms grown in 100% SCFM with no mucin, and due to the low incidence of silver resistant strains of bacteria, both of these compounds demonstrate great promise as possible agents to be used in combating *P. aeruginosa* biofilms found in the CF lung environment.

One of the most noticeable findings with respect to antimicrobial efficacy against static biofilms of *P. aeruginosa* grown in CF relevant conditions, was the reduction in bioactivity for all five antimicrobials tested upon the addition of 1% mucin (final wt/vol) to the base SCFM medium. Certainly, the lower bioactivity for all five antimicrobials tested against *P. aeruginosa* static biofilms grown in 90% SCFM +1% mucin (final wt/vol) compared to planktonic counterparts could be

explained by the myriad of possibilities already described for the discrepancy in killing efficacy when biofilm growth using 100% SCFM was compared to planktonic counterparts (see above). However, it is the addition of mucin to SCFM in general (1% final wt/vol) that poses an even further complication to the already inherent resistance to antimicrobials displayed by the biofilm phenotype. It is well established that mucins (members of the glycosolated protein family) are found at high concentrations in the sputum of patients affected with CF (22, 132, 158, 163, 190, 192, 234). In general, the sputum of CF patients has been previously shown to cause noticeable affects on the bioactivity of various antimicrobial compounds (30, 110, 141, 142, 164). When comparing the bioactivity of Tobramycin, Ciprofloxacin, Meropenem, SCC-1, and SCC-22 against static biofilms of *P. aeruginosa* strains PAO1, PDO300, and 7119 grown in a medium intended to mimic the nutritional environment of the CF lung (175), it is readily observable that the addition of mucin (a key ingredient not included in the original formulation of SCFM (175)) at 1% (final wt/vol) causes a decrease in killing efficacy for all five antibiotics. It is well known that mucins not only promote *P. aeruginosa* biofilm formation, but are in fact also capable of increased tolerance to Tobramycin (133). This could explain the reduced bioactivity of Tobramycin when its activity is compared between *P. aeruginosa* biofilms grown under static conditions in 100% SCFM with no mucin versus 90% SCFM + 1% mucin (final wt/vol). Uniquely however, the killing efficacy for Ciprofloxacin and Meropenem did not differ between static biofilms grown in 100% SCFM with no

mucin added versus 90% SCFM + 1% mucin (final wt/vol). As was noticed previously (see Chapter III), the addition of mucin at 1% (final wt/vol) to SCFM caused the greatest reduction in bioactivity for both SCC-1 and SCC-22 when used against multiple strains of *P. aeruginosa* grown under planktonic conditions (see Chapter III). This is also certainly true for *P. aeruginosa* strains PAO1, PDO300, and 7119 even when grown as static biofilms. Again, it is very possible that the cysteine-rich side chains of mucin molecules (227) could be acting as a binding agent to the silver(I) cation after release from the carbene complex. If this is the case, and the silver(I) cation is binding to the sulfur-rich domains commonly found in mucin molecules, then it would be as though mucin is acting as an antagonist by binding silver(I) in its cysteine-rich residues. This in turn would reduce the free available silver(I) from binding to the sulfhydryl-rich domains in bacterial proteins, as this protein inactivation has been one proposed mechanism of how silver(I) acts to destroy bacteria (73, 143, 193). Due to the ability of both SCC-1 and SCC-22 to completely eradicate static biofilms of multiple strains of *P. aeruginosa* grown in 100% SCFM without mucin, overcoming the mucin barrier becomes a critical step in utilizing both of these compounds in treating microbial infections commonly found in the CF lung. One possible way of enhancing the antimicrobial efficacy of both SCC-1 and SCC-22 against *P. aeruginosa* biofilms grown under conditions that contain high mucin concentrations would be to also utilize nanoparticle encapsulation methods. Indeed, research has already shown that coating nanoparticles in varying

polyethylene glycol side chains can reduce mucoadhesivity and enhance penetration through human mucus (220, 221, 237). By encapsulating SCC-1 or SCC-22 into such nanoparticles, it may help to overcome initial binding to mucin molecules. Further, it may be possible to simply attach PEG side-chains onto certain silver carbene complexes (i.e., SCC-22) in an attempt to decrease mucoadhesivity directly. Due to the proven nature of SCC-1 and SCC-22 to kill off *P. aeruginosa* biofilms in CF growth conditions that do not contain mucin, it would be most adventitious to apply a combined therapy of both nanoparticle encapsulated silver carbene complexes and non-encapsulated silver carbene complexes.

In conclusion, the results from the experiments conducted indicate that indeed both SCC-1 and SCC-22 were more effective at eliminating static biofilms of *P. aeruginosa* grown in 100% SCFM with no mucin added compared to Tobramycin, Ciprofloxacin, and Meropenem. Further, it was demonstrated that the addition of 1% mucin (final wt/vol) to SCFM greatly reduced the bioactivity for all antimicrobial compounds under investigation. Based on these results, future work is warranted at utilizing both SCC-1 and SCC-22 as clinically useful antimicrobial compounds in the treatment of infections commonly associated with cystic fibrosis.

Figures/Tables

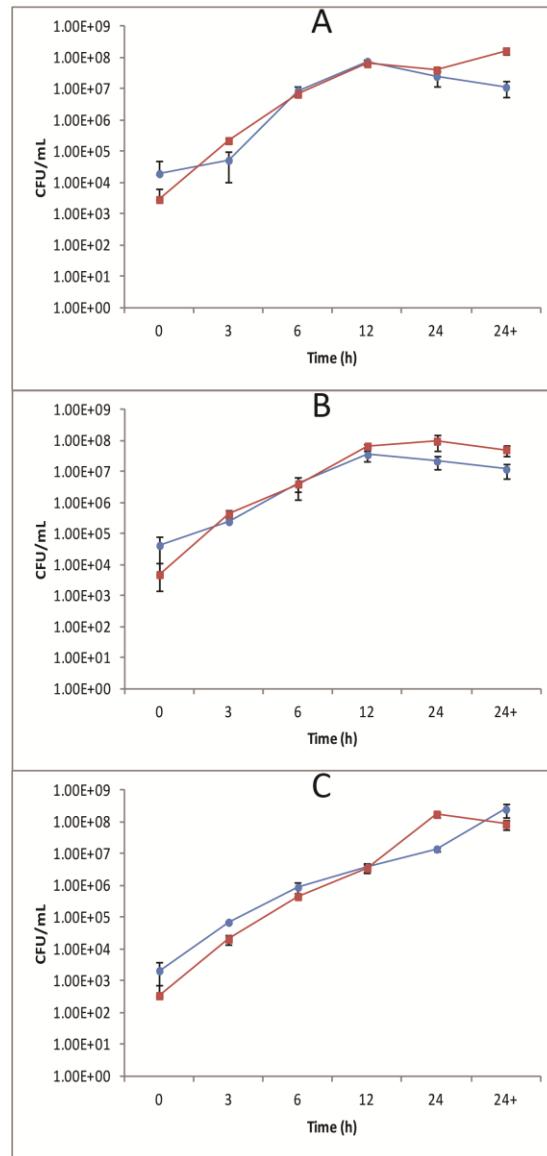


Figure 4.1: Growth curves of *P. aeruginosa* strains PAO1 (A), PDO300 (B), and 7119 (C) grown in 100% SCFM with no mucin (blue ●) and 90% SCFM supplemented with 1% mucin (final wt/vol) (red ■). Time points represent length of time biofilm was grown prior to termination of growth and subsequent plating. Time point 24+ indicates biofilm grown for 24 hours, rinsed with 100% SCFM, and subsequently allowed to grow for 24 hours more prior to termination of growth and plating. Error bars represent ± one standard deviation from the mean.

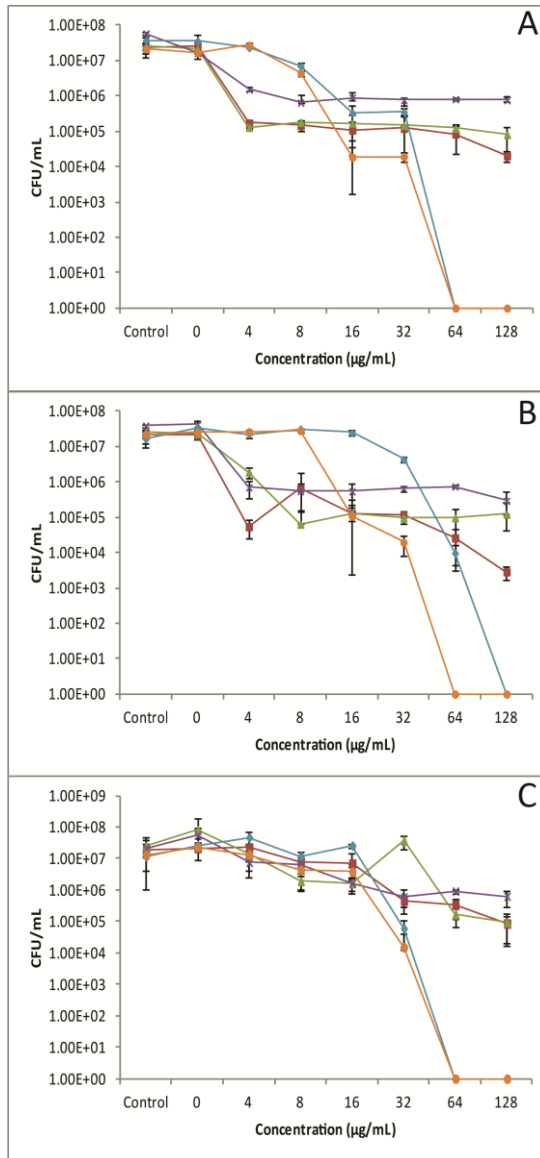


Figure 4.2: Killing curves of *P. aeruginosa* strains PAO1 (A), PDO300 (B), and 7119 (C) grown as static biofilms in 100% SCFM without mucin for 24 hours, and subsequently treated with Tobramycin (red ■), Ciprofloxacin (green ▲), Meropenem (purple X), SCC-1 (blue ◆), or SCC-22 (orange ●) at various concentrations for 24 hours. Controls included the addition of only the corresponding antimicrobial diluents. Error bars represent \pm one standard deviation from the mean.

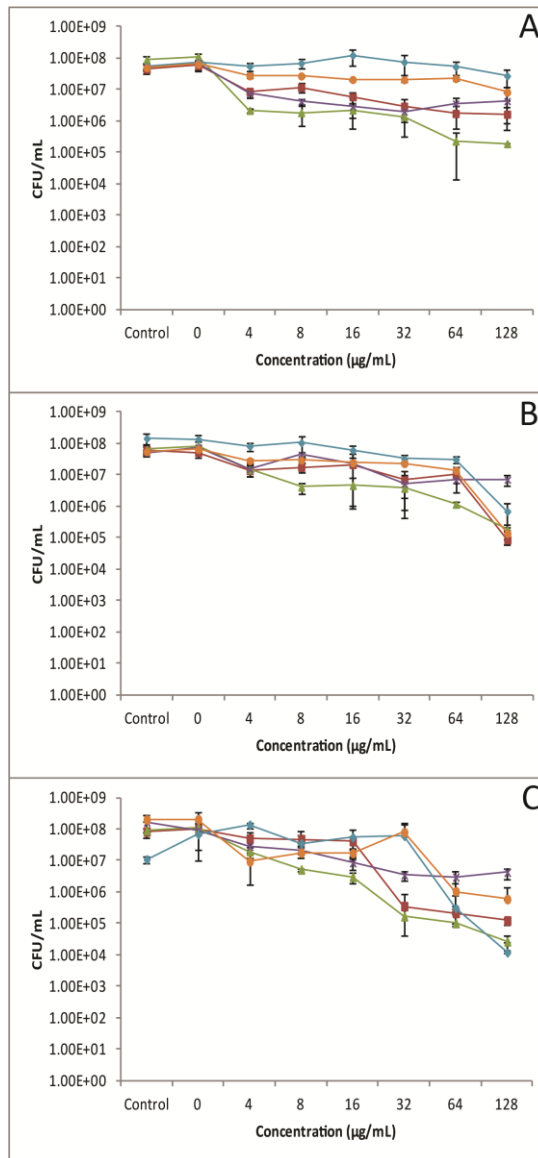


Figure 4.3: Killing curves of *P. aeruginosa* strains PAO1 (A), PDO300 (B), and 7119 (C) grown as static biofilms in 90% SCFM supplemented with 1% mucin (final wt/vol) for 24 hours, and subsequently treated with Tobramycin (red ■), Ciprofloxacin (green ▲), Meropenem (purple X), SCC-1 (blue ◆), or SCC-22 (orange ●) at various concentrations for 24 hours. Controls included the addition of only the corresponding antimicrobial diluents. Error bars represent ± one standard deviation from the mean.

CHAPTER V

SUMMARY

Integrative Microbial Treatment Strategies

The dynamic field of microbiology continues to evolve at an accelerated rate as new discoveries are made daily. The very complexity of microbial systems has prompted researchers to foster more integrative approaches when attempting to better understand such systems. One arena included within this line of thinking is in the development of more novel microbial treatment strategies. Whether these treatment strategies involve utilizing natural physiology of microorganisms in an attempt to treat widespread contamination issues, or if novel chemotherapeutic treatment strategies are developed to treat difficult to treat infections, it is abundantly clear that integrative approaches are critical to solve these complex problems.

The Case for Passive AMD Remediation Using Microbial Populations

As has already been extensively highlighted throughout, the widespread contamination by coal-derived acid mine drainage (AMD) of wetland ecosystems across the United States poses a very serious environmental concern (104, 202). Despite efforts to develop various active treatment options that attempt to clean

up AMD contamination (114, 252), both human intervention and high associated costs have prompted researchers to look at more passive treatment options. In particular, natural soil microbial populations coupled with the unique hydro(bio)geochemical nature of 'sheet flow' systems have shown great potential as a possible passive AMD treatment option (26, 27, 56, 91, 199-201). However, in order to employ such a passive model for AMD remediation, it is abundantly clear that a more basic understanding of the microbial systems of a 'sheet flow' site is necessary. To this end, multiple research projects were designed and carried out in order to better understand the microbial ecology of an AMD impacted site located in Mahoning County, Ohio (i.e., the Mushroom Farm). Research was conducted in order to identify the source of microorganisms responsible for Fe(II) oxidizing activities and to characterize associated Fe(II) oxidation rates. Research was also carried out to characterize native soil microorganism response to sustained AMD intrusion (and determine if such responses could be enhanced), as well as to determine if depth-dependent trends could be observed for microbial communities within mature iron mound sediment. It was found that Fe(II) oxidizing microorganisms inhabit both AMD discharge and 'pristine' soil not having previously been exposed to AMD at the Mushroom Farm. Further, microorganisms from both sources continue the metabolic oxidation and subsequent precipitation of dissolved Fe(II) even as pH continues to decrease. It was also noted that 'pristine' soil from the MF consists of metabolically diverse populations of microorganisms, while AMD and iron

iron mound sediment is primarily composed of acidophilic/acid tolerant microorganisms, many of which are capable of Fe(II) oxidation. It was found that when these metabolically diverse communities of microorganisms found in 'pristine' soil are exposed to sustained AMD, microbial populations begin to shift toward populations consisting of microorganisms capable of Fe(II) oxidation. Due to the fact that mature iron mound sediment from the MF consisted of already well established populations of microorganism capable of lithotrophic processes, the seeding of 'pristine' soil with such iron mound sediment acted to enhance the oxidative precipitation of dissolved Fe(II) from overlying AMD. This clearly demonstrates that as AMD has persisted at the Mushroom Farm, highly structured populations of Fe(II) oxidizing bacteria have developed. In fact, this was further verified by observing depth-dependent trends in microbial communities within the iron mound sediment found in the AMD flow path. Microbial communities in the upper strata of the iron mound sediment consisted of phylotypes containing organisms capable of photoautotrophy. Beginning at around 4 cm, iron mound sediment material consisted primarily of phylotypes that were most closely related to organisms capable of metabolic activities commonly found in anoxic environments. Noticeably throughout the 10 cm depth of the iron mound sediment, the most abundant phylotypes were attributed to groups of acidophilic bacteria capable of Fe(II) oxidation as well as Fe(III) reduction. Together, these data suggest that the 'sheet flow' characteristics found at the Mushroom Farm allows for the effective removal of dissolved Fe(II), and that the

microbial populations found at such sites greatly influence Fe(II) oxidation rates. Additionally, the very fact that microbial populations found in the native soil from such an AMD impacted site are capable of responding and adapting to AMD flow suggests a very promising future for passive AMD treatment strategies. Based on the data thus far generated from the AMD 'sheet flow' site known as the Mushroom Farm, it becomes clear that future directions should be aimed at taking such data and actually engineering a possible AMD treatment option. The basic research conducted now affords biologists and geologists the knowledge necessary to collaborate with other sciences in order to enact a successful passive treatment strategy aimed at remediating AMD contaminated sites.

The Case for Treating CF Related Infections

High incidence of morbidity and mortality among patients affected by cystic fibrosis has prompted researchers to employ an arsenal of techniques aimed at treating the underlying infections leading to such high rates. It is a well known fact that *Pseudomonas aeruginosa* is capable of colonizing the thick, viscous sputum of the CF lung, which in turn can lead to respiratory complications among CF patients (10, 77, 156, 157, 179, 245). In fact the environmental circumstances that pervade the CF lung environment afford an ideal niche upon which *P. aeruginosa* can establish residence and reach very high population densities (175, 176, 208). Furthermore, the ability of *P. aeruginosa* strains to form biofilm structures in the CF lung environment (15, 106,

157, 208, 248) poses an added complication in developing effective and efficient treatment options, specifically when acknowledging the notion that *P. aeruginosa* biofilms display a greater degree of tolerance to common antimicrobial agents compared to planktonic counterparts (3, 15, 38, 62, 63, 78, 102, 133, 168, 214, 215). Throw in the mix that CF sputum has been shown to reduce the bioactivity of various antimicrobial agents (30, 110, 141, 142, 164), and it becomes clear that more basic research and novel treatment approaches are necessary to determine a best course of action against CF relevant infections. To this end, research was conducted to examine the antimicrobial efficacy of two novel silver carbene complexes (SCC-1 and SCC-22) as well as three other clinically relevant antibiotics (Tobramycin, Ciprofloxacin, and Meropenem) using conditions that better approximate the CF lung environment. More specifically, experiments were carried out to investigate the effects that mucin has on the bioactivity of the above mentioned antimicrobials against planktonic and biofilm modes of existence for multiple strains of *P. aeruginosa* grown in a previously developed synthetic cystic fibrosis medium (SCFM) (175). It was found that while Tobramycin, Meropenem, and Ciprofloxacin were most effective at inhibiting/killing multiple strains of *P. aeruginosa* grown under planktonic conditions in 100% SCFM with no mucin, both SCC-1 and SCC-22 were also effective. However, it was observed that both SCC-1 and SCC-22 were the most effective at completely eradicating static biofilms of *P. aeruginosa* grown using 100% SCFM. Perhaps more important however, was the noticeable

effect that mucin had on decreasing the bioactivity for all antimicrobials tested. When mucin (1% final wt/vol) was added to SCFM, bioactivity for all five antimicrobials tested greatly decreased regardless of bacterial mode of growth (i.e., planktonic or biofilm). This shows that mucin, a key component of CF sputum (22, 132, 158, 163, 190, 192, 234) represents a substantial antagonist for multiple classes of antimicrobials, most noticeably for the two novel silver carbene complexes. While both SCC-1 and SCC-22 represent promising candidates for treating CF relevant infections, as noticed by their superior ability to eradicate static biofilms of *P. aeruginosa* grown in 100% SCFM with no mucin, it becomes clear that more research is needed. Specifically, future directions should focus on modifying/encapsulating the silver carbene complexes in order to overcome the problems posed by the mucus barrier in the CF lung environment.

The Future for Microbial Treatment Strategies

In conclusion, the data collected as a result of collaborating across the disciplines of biology, chemistry, geology, and medicine shines a positive light on the need for more integrative approaches to complex issues in biology. As it relates specifically to microbial treatment strategies, it becomes apparent that future advances in both directions (i.e., utilizing microbial systems as a ‘treating’ agent or developing more novel approaches to treat complex microbial infections) will require more unique collaborations employing such cross-

disciplinary approaches. As the field of microbiology continues to advance and evolve, it becomes clear that integrative scientists will undeniably shape the future and help bridge the gaps necessary in order to develop more effective microbial treatment strategies.

REFERENCES

1. **Agarwal, S., M. Gupta, and B. Choudhury.** 2013. Bioprocess development for nicotinic acid hydroxamate synthesis by acyltransferase activity of *Bacillus smithii* strain IITR6b2. *Journal of Industrial Microbiology & Biotechnology* **40**:937-946.
2. **Aguilera, A., V. Souza-Egipsy, F. Gómez, and R. Amils.** 2007. Development and structure of eukaryotic biofilms in an extreme acidic environment, Río Tinto (SW, Spain). *Microb. Ecol.* **53**:294-305.
3. **Alhede, M., K. N. Kragh, K. Qvortrup, M. Allesen-Holm, M. van Gennip, L. D. Christensen, P. O. Jensen, A. K. Nielsen, M. Parsek, D. Wozniak, S. Molin, T. Tolker-Nielsen, N. Hoiby, M. Givskov, and T. Bjarnsholt.** 2011. Phenotypes of non-attached *Pseudomonas aeruginosa* aggregates resemble surface attached biofilm. *PLoS One* **6**.
4. **Alipour, M., Z. E. Suntres, and A. Omri.** 2009. Importance of DNase and alginate lyase for enhancing free and liposome encapsulated aminoglycoside activity against *Pseudomonas aeruginosa*. *J. Antimicrob. Chemother.* **64**:317-325.
5. **Alkawash, M. A., J. S. Soothill, and N. L. Schiller.** 2006. Alginate lyase enhances antibiotic killing of mucoid *Pseudomonas aeruginosa* in biofilms. *APMIS* **114**:131-138.
6. **Alonso-Gutiérrez, J., A. Figueras, J. Albaigés, N. Jiménez, M. Viñas, A. M. Solanas, and B. Novoa.** 2009. Bacterial communities from shoreline environments (Costa da Morte, Northwestern Spain) affected by the Prestige oil spill. *Appl. Environ. Microbiol.* **75**:3407-3418.
7. **Altschul, S. F., T. L. Madden, A. A. Schäffer, J. Zhang, Z. Zhang, W. Miller, and D. J. Lipman.** 1997. Gapped BLAST and PSI-BLAST: a new generation of protein database search programs. *Nucleic Acids Res.* **25**:3389-3402.

8. **Amaral-Zettler, L. A., E. R. Zettler, S. M. Theroux, C. Palacios, A. Aguilera, and R. Amils.** 2011. Microbial community structure across the tree of life in the extreme Rio Tinto. *The ISME Journal* **5**:42-50.
9. **Aspe, M., L. Jensen, J. Melegrito, and M. Sun.** 2012. The role of alginate and extracellular DNA in biofilm-mediated *Pseudomonas aeruginosa* gentamicin resistance. *J. Exp. Microbiol. Immunol.* **16**:42-48.
10. **B Goldberg, J., and G. B Pier.** 2000. The role of the CFTR in susceptibility to *Pseudomonas aeruginosa* infections in cystic fibrosis. *Trends Microbiol.* **8**:514-520.
11. **Bagge, N., M. Schuster, M. Hentzer, O. Ciofu, M. Givskov, E. P. Greenberg, and N. Høiby.** 2004. *Pseudomonas aeruginosa* biofilms exposed to imipenem exhibit changes in global gene expression and β -lactamase and alginate production. *Antimicrob. Agents Chemother.* **48**:1175-1187.
12. **Baker, B. J., and J. F. Banfield.** 2003. Microbial communities in acid mine drainage. *FEMS Microbiol. Ecol.* **44**:139-152.
13. **Baker, B. J., L. R. Comolli, G. J. Dick, L. J. Hauser, D. Hyatt, B. D. Dill, M. L. Land, N. C. VerBerkmoes, R. L. Hettich, and J. F. Banfield.** 2010. Enigmatic, ultrasmall, uncultivated Archaea. *Proceedings of the National Academy of Sciences* **107**:8806-8811.
14. **Baughman, R. P.** 2009. The use of carbapenems in the treatment of serious infections. *Journal of Intensive Care Medicine* **24**:230-241.
15. **Bjarnsholt, T., P. Ø. Jensen, M. J. Fiandaca, J. Pedersen, C. R. Hansen, C. B. Andersen, T. Pressler, M. Givskov, and N. Høiby.** 2009. *Pseudomonas aeruginosa* biofilms in the respiratory tract of cystic fibrosis patients. *Pediatric Pulmonology* **44**:547-558.
16. **Bjarnsholt, T., P. Ø. Jensen, T. H. Jakobsen, R. Phipps, A. K. Nielsen, M. T. Rybtke, T. Tolker-Nielsen, M. Givskov, N. Høiby, and O. Ciofu.** 2010. Quorum sensing and virulence of *Pseudomonas aeruginosa* during lung infection of cystic fibrosis patients. *PLoS One* **5**:e10115.
17. **Bjarnsholt, T., K. Kirketerp-Møller, S. Kristiansen, R. Phipps, A. K. Nielsen, P. Ø. Jensen, N. Høiby, and M. Givskov.** 2007. Silver against *Pseudomonas aeruginosa* biofilms. *APMIS* **115**:921-928.

18. **Bjarnsholt, T., T. Tolker-Nielsen, N. Høiby, and M. Givskov.** 2010. Interference of *Pseudomonas aeruginosa* signalling and biofilm formation for infection control. *Expert Reviews in Molecular Medicine* **12**:e11.
19. **Blowes, D., C. Ptacek, J. Jambor, and C. Weisener.** 2003. The geochemistry of acid mine drainage. *Treatise on Geochemistry* **9**:149-204.
20. **Bohorquez, L. C., L. Delgado-Serrano, G. López, C. Osorio-Forero, V. Klepac-Ceraj, R. Kolter, H. Junca, S. Baena, and M. M. Zambrano.** 2012. In-depth characterization via complementing culture-independent approaches of the microbial community in an acidic hot spring of the Colombian Andes. *Microb. Ecol.* **63**:103-115.
21. **Bonnefoy, V., and D. S. Holmes.** 2012. Genomic insights into microbial iron oxidation and iron uptake strategies in extremely acidic environments. *Environ. Microbiol.* **14**:1597-1611.
22. **Boucher, R. C.** 2004. New concepts of the pathogenesis of cystic fibrosis lung disease. *Eur. Resp. J.* **23**:146-158.
23. **Bragg, P. D., and D. J. Rainnie.** 1974. Effect of silver ions on respiratory chain of *Escherichia coli*. *Can. J. Microbiol.* **20**:883-889.
24. **Brake, S., S. Hasiotis, and H. Dannelly.** 2004. Diatoms in acid mine drainage and their role in the formation of iron-rich stromatolites. *Geomicrobiol. J.* **21**:331-340.
25. **Brake, S. S., and S. T. Hasiotis.** 2010. Eukaryote-dominated biofilms and their significance in acidic environments. *Geomicrobiol. J.* **27**:534-558.
26. **Brantner, J. S., Z. J. Haake, J. E. Burwick, C. M. Menge, S. T. Hotchkiss, and J. M. Senko.** 2014. Depth-dependent geochemical and microbiological gradients in Fe (III) deposits resulting from coal mine-derived acid mine drainage. *Frontiers in Microbiology* **5**.
27. **Brantner, J. S., and J. M. Senko.** 2014. Response of soil-associated microbial communities to intrusion of coal mine-derived acid mine drainage. *Environ. Sci. Technol.* **48**:8556-8563.
28. **Brofft, J. E., J. V. McArthur, and L. J. Shimkets.** 2002. Recovery of novel bacterial diversity from a forested wetland impacted by reject coal. *Environ. Microbiol.* **4**:764-769.

29. **Brown, J. F., D. S. Jones, D. B. Mills, J. L. Macalady, and W. D. Burgos.** 2011. Application of a depositional facies model to an acid mine drainage site. *Appl. Environ. Microbiol.* **77**:545-554.
30. **Bryant, R. E., and D. Hammond.** 1974. Interaction of purulent material with antibiotics used to treat *Pseudomonas* infections. *Antimicrob. Agents Chemother.* **6**:702-707.
31. **Cannon, C. L., L. A. Hogue, R. K. Vajravelu, G. H. Capps, A. Ibricevic, K. M. Hindi, A. Kascatan-Nebioglu, M. J. Walter, S. L. Brody, and W. J. Youngs.** 2009. In vitro and murine efficacy and toxicity studies of nebulized SCC1, a methylated caffeine-silver(I) complex, for treatment of pulmonary infections. *Antimicrob. Agents Chemother.* **53**:3285-3293.
32. **Caporaso, J. G., K. Bittinger, F. D. Bushman, T. Z. DeSantis, G. L. Andersen, and R. Knight.** 2010. PyNAST: a flexible tool for aligning sequences to a template alignment. *Bioinformatics* **26**:266-267.
33. **Caporaso, J. G., J. Kuczynski, J. Stombaugh, K. Bittinger, F. D. Bushman, E. K. Costello, N. Fierer, A. G. Pena, J. K. Goodrich, J. I. Gordon, G. A. Huttley, S. T. Kelley, D. Knights, J. E. Koenig, R. E. Ley, C. A. Lozupone, D. McDonald, B. D. Muegge, M. Pirrung, J. Reeder, J. R. Sevinsky, P. J. Tumbaugh, W. A. Walters, J. Widmann, T. Yatsunenko, J. Zaneveld, and R. Knight.** 2010. QIIME allows analysis of high-throughput community sequencing data. *Nature Methods* **7**:335-336.
34. **Caporaso, J. G., C. L. Lauber, W. A. Walters, D. Berg-Lyons, C. A. Lozupone, P. J. Turnbaugh, N. Fierer, and R. Knight.** 2011. Global patterns of 16S rRNA diversity at a depth of millions of sequences per sample. *Proc. Natl. Acad. Sci. U. S. A.* **108**:4516-4522.
35. **Carnoy, C., R. Ramphal, A. Scharfman, J. M. Loguidice, N. Houdret, A. Klein, C. Galabert, G. Lamblin, and P. Roussel.** 1993. Altered carbohydrate composition of salivary mucins from patients with cystic fibrosis and the adhesion of *Pseudomonas aeruginosa*. *Am. J. Respir. Cell Mol. Biol.* **9**:323-334.
36. **Cavaletti, L., P. Monciardini, R. Bamonte, P. Schumann, M. Rohde, M. Sosio, and S. Donadio.** 2006. New lineage of filamentous, spore-forming, gram-positive bacteria from soil. *Appl. Environ. Microbiol.* **72**:4360-4369.
37. **Christensen, B., M. Laake, and T. Lien.** 1996. Treatment of acid mine water by sulfate-reducing bacteria: Results from a bench scale experiment. *Water Res.* **30**:1617-1624.

38. **Ciofu, O., T. Tolker-Nielsen, P. Ø. Jensen, H. Wang, and N. Høiby.** 2015. Antimicrobial resistance, respiratory tract infections and role of biofilms in lung infections in cystic fibrosis patients. *Advanced Drug Delivery Reviews* **85**: 7-23.
39. **Coates, J. D., K. A. Cole, R. Chakraborty, S. M. O'Connor, and L. A. Achenbach.** 2002. Diversity and ubiquity of bacteria capable of utilizing humic substances as electron donors for anaerobic respiration. *Appl. Environ. Microbiol.* **68**:2445-2452.
40. **Cole, J. R., Q. Wang, E. Cardenas, J. Fish, B. Chai, R. J. Farris, A. S. Kulam-Syed-Mohideen, D. M. McGarrell, T. Marsh, G. M. Garrity, and J. M. Tiedje.** 2009. The Ribosomal Database Project: improved alignments and new tools for rRNA analysis. *Nucleic Acids Res.* **37**:D141-D145.
41. **Colmer, A. R., and M. E. Hinkle.** 1947. The role of microorganisms in acid mine drainage: A preliminary report. *Science (New York, N.Y.)* **106**:253-256.
42. **Costerton, J. W., P. S. Stewart, and E. P. Greenberg.** 1999. Bacterial biofilms: A common cause of persistent infections. *Science* **284**:1318-1322.
43. **Coupland, K., and D. B. Johnson.** 2008. Evidence that the potential for dissimilatory ferric iron reduction is widespread among acidophilic heterotrophic bacteria. *FEMS Microbiol. Lett.* **279**:30-35.
44. **Cravotta, C. A.** 2008. Dissolved metals and associated constituents in abandoned coal-mine discharges, Pennsylvania, USA. Part 1: Constituent quantities and correlations. *Appl. Geochem.* **23**:166-202.
45. **Cravotta, C. A.** 2008. Dissolved metals and associated constituents in abandoned coal-mine discharges, Pennsylvania, USA. Part 2: Geochemical controls on constituent concentrations. *Appl. Geochem.* **23**:203-226.
46. **Cravotta, C. A.** 2003. Size and performance of anoxic limestone drains to neutralize acidic mine drainage. *J. Environ. Qual.* **32**:1277-1289.
47. **Cravotta, C. A., and M. K. Trahan.** 1999. Limestone drains to increase pH and remove dissolved metals from acidic mine drainage. *Appl. Geochem.* **14**:581-606.

48. **Cretoiu, M. S., G. W. Korthals, J. H. Visser, and J. D. van Elsas.** 2013. Chitin amendment increases soil suppressiveness toward plant pathogens and modulates the actinobacterial and oxalobacteraceal communities in an experimental agricultural field. *Appl. Environ. Microbiol.* **79**:5291-5301.
49. **Cutright, T. J., J. Senko, S. Sivaram, and M. York.** 2012. Evaluation of the phytoextraction potential at an acid mine drainage impacted site. *Soil. Sediment. Contam.* **21**:970-984.
50. **Dalvi, S., S. Azetsu, M. A. Patrauchan, D. F. Aktas, and B. Z. Fathepure.** 2012. Proteogenomic elucidation of the initial steps in the benzene degradation pathway of a novel halophile, *Arhodomonas* sp. strain Rozel, isolated from a hypersaline environment. *Appl. Environ. Microbiol.* **78**:7309-7316.
51. **Danahay, H., and A. D. Jackson.** 2005. Epithelial mucus-hypersecretion and respiratory disease. *Current Drug Targets - Inflammation and Allergy* **4**:651-664.
52. **Davies, D. G., M. R. Parsek, J. P. Pearson, B. H. Iglewski, J. Costerton, and E. Greenberg.** 1998. The involvement of cell-to-cell signals in the development of a bacterial biofilm. *Science* **280**:295-298.
53. **De la Torre, J. R., C. B. Walker, A. E. Ingalls, M. Könneke, and D. A. Stahl.** 2008. Cultivation of a thermophilic ammonia oxidizing archaeon synthesizing crenarchaeol. *Environ. Microbiol.* **10**:810-818.
54. **Delavat, F., M.-C. Lett, and D. Lièvreumont.** 2012. Novel and unexpected bacterial diversity in an arsenic-rich ecosystem revealed by culture-dependent approaches. *Biology Direct* **7**:28.
55. **Denholm, C., T. Danehy, S. Busler, K. Rowe, K. Bonfardine, and M. Dunn.** 2010. Presented at the 2010 National Meeting of the American Society of Mining and Reclamation, Pittsburgh, PA, Bridging Reclamation, Science, and the Community.
56. **DeSa, T. C., J. F. Brown, and W. D. Burgos.** 2010. Laboratory and field scale evaluation of low-pH Fe(II) oxidation at Hughes Borehole, Portage, Pennsylvania. *Mine Water Environ.* **29**:239-247.
57. **DeSantis, T. Z., P. Hugenholtz, N. Larsen, M. Rojas, E. L. Brodie, K. Keller, T. Huber, D. Dalevi, P. Hu, and G. L. Andersen.** 2006. Greengenes, a chimera-checked 16S rRNA gene database and workbench compatible with ARB. *Appl. Environ. Microbiol.* **72**:5069-5072.

58. **Diaby, N., B. Dold, H. R. Pfeifer, C. Holliger, D. B. Johnson, and K. B. Hallberg.** 2007. Microbial communities in a porphyry copper tailings impoundment and their impact on the geochemical dynamics of the mine waste. *Environ. Microbiol.* **9**:298-307.
59. **Dobritsa, A. P., M. Reddy, and M. Samadpour.** 2010. Reclassification of *Herbaspirillum putei* as a later heterotypic synonym of *Herbaspirillum huttiense*, with the description of *H. huttiense* subsp. *huttiense* subsp. nov. and *H. huttiense* subsp. *putei* subsp. nov., comb. nov., and description of *Herbaspirillum aquaticum* sp. nov. *Int. J. Syst. Evol. Microbiol.* **60**:1418-1426.
60. **Donlan, R. M.** 2002. Biofilms: microbial life on surfaces. *Emerg Infect Dis* **8**.
61. **Dowd, S. E., T. R. Callaway, R. D. Wolcott, Y. Sun, T. McKeegan, R. G. Hagevoort, and T. S. Edrington.** 2008. Evaluation of the bacterial diversity in the feces of cattle using 16S rDNA bacterial tag-encoded FLX amplicon pyrosequencing (bTEFAP). *BMC Microbiology* **8**.
62. **Drenkard, E.** 2003. Antimicrobial resistance of *Pseudomonas aeruginosa* biofilms. *Microbes and Infection* **5**:1213-1219.
63. **Drenkard, E., and F. M. Ausubel.** 2002. *Pseudomonas* biofilm formation and antibiotic resistance are linked to phenotypic variation. *Nature* **416**:740-743.
64. **Dridi, B., M.-L. Fardeau, B. Ollivier, D. Raoult, and M. Drancourt.** 2012. *Methanomassiliicoccus luminyensis* gen. nov., sp. nov., a methanogenic archaeon isolated from human faeces. *Int. J. Syst. Evol. Microbiol.* **62**:1902-1907.
65. **Dunbar, J., S. A. Eichorst, L. V. Gallegos-Graves, S. Silva, G. Xie, N. Hengartner, R. D. Evans, B. A. Hungate, R. B. Jackson, and J. P. Megonigal.** 2012. Common bacterial responses in six ecosystems exposed to 10 years of elevated atmospheric carbon dioxide. *Environ. Microbiol.* **14**:1145-1158.
66. **Edgar, R. C.** 2010. Search and clustering orders of magnitude faster than BLAST. *Bioinformatics* **26**:2460-2461.

67. **Edwards, K. J., P. L. Bond, T. M. Gihring, and J. F. Banfield.** 2000. An archaeal iron-oxidizing extreme acidophile important in acid mine drainage. *Science* **287**:1796-1799.
68. **Elshahed, M. S., N. H. Youssef, A. M. Spain, C. Sheik, F. Z. Najjar, L. O. Sukharnikov, B. A. Roe, J. P. Davis, P. D. Schloss, and V. L. Bailey.** 2008. Novelty and uniqueness patterns of rare members of the soil biosphere. *Appl. Environ. Microbiol.* **74**:5422-5428.
69. **Emerson, D., E. J. Fleming, and J. M. McBeth.** 2010. Iron-oxidizing bacteria: an environmental and genomic perspective. *Annu. Rev. Microbiol.* **64**:561-583.
70. **España, J. S., E. S. Pastor, and E. L. Pamo.** 2007. Iron terraces in acid mine drainage systems: a discussion about the organic and inorganic factors involved in their formation through observations from the Tintillo acidic river (Riotinto mine, Huelva, Spain). *Geosphere* **3**:133-151.
71. **Fahrbach, M., J. Kuever, M. Remesch, B. E. Huber, P. Kämpfer, W. Dott, and J. Hollender.** 2008. *Steroidobacter denitrificans* gen. nov., sp. nov., a steroidal hormone-degrading gammaproteobacterium. *Int. J. Syst. Evol. Microbiol.* **58**:2215-2223.
72. **Falteisek, L., and I. Čepička.** 2012. Microbiology of diverse acidic and non-acidic microhabitats within a sulfidic ore mine. *Extremophiles* **16**:911-922.
73. **Feng, Q. L., J. Wu, G. Q. Chen, F. Z. Cui, T. N. Kim, and J. O. Kim.** 2000. A mechanistic study of the antibacterial effect of silver ions on *Escherichia coli* and *Staphylococcus aureus*. *J. Biomed. Mater. Res.* **52**:662-668.
74. **FitzSimmons, S. C.** 1993. The changing epidemiology of cystic fibrosis. *The Journal of Pediatrics* **122**:1-9.
75. **Fleming, E. J., A. E. Langdon, M. Martinez-Garcia, R. Stepanauskas, N. J. Poulton, E. D. P. Masland, and D. Emerson.** 2011. What's new is old: resolving the identity of *Leptothrix ochracea* using single cell genomics, pyrosequencing and FISH. *PLoS One* **6**:e17769.
76. **Flemming, H. C., and J. Wingender.** 2010. The biofilm matrix. *Nat. Rev. Microbiol.* **8**:623-633.

77. **Folkesson, A., L. Jelsbak, L. Yang, H. K. Johansen, O. Ciofu, N. Hoiby, and S. Molin.** 2012. Adaptation of *Pseudomonas aeruginosa* to the cystic fibrosis airway: an evolutionary perspective. *Nat. Rev. Microbiol.* **10**:841-851.
78. **Folsom, J. P., L. Richards, B. Pitts, F. Roe, G. D. Ehrlich, A. Parker, A. Mazurie, and P. S. Stewart.** 2010. Physiology of *Pseudomonas aeruginosa* in biofilms as revealed by transcriptome analysis. *BMC Microbiology* **10**:294.
79. **Fowler, R. C., and N. D. Hanson.** 2014. Emergence of carbapenem resistance due to the novel insertion sequence ISPa8 in *Pseudomonas aeruginosa*. *PLoS One* **9**:e91299.
80. **Fujimura, R., Y. Sato, T. Nishizawa, K. Oshima, S.-W. Kim, M. Hattori, T. Kamijo, and H. Ohta.** 2012. Complete genome sequence of *Leptospirillum ferrooxidans* strain C2-3, isolated from a fresh volcanic ash deposit on the island of Miyake, Japan. *J. Bacteriol.* **194**:4122-4123.
81. **Fux, C. A., J. W. Costerton, P. S. Stewart, and P. Stoodley.** 2005. Survival strategies of infectious biofilms. *Trends Microbiol.* **13**:34-40.
82. **Galand, P. E., E. O. Casamayor, D. L. Kirchman, and C. Lovejoy.** 2009. Ecology of the rare microbial biosphere of the Arctic Ocean. *Proceedings of the National Academy of Sciences* **106**:22427-22432.
83. **Gan, Y., Q. Qiu, P. Liu, J. Rui, and Y. Lu.** 2012. Syntrophic oxidation of propionate in rice field soil at 15 and 30 C under methanogenic conditions. *Appl. Environ. Microbiol.* **78**:4923-4932.
84. **García-Moyano, A., E. Gonzalez-Toril, Á. Aguilera, and R. Amils.** 2012. Comparative microbial ecology study of the sediments and the water column of the Río Tinto, an extreme acidic environment. *FEMS Microbiol. Ecol.* **81**:303-314.
85. **Gibson, R. L., J. L. Burns, and B. W. Ramsey.** 2003. Pathophysiology and management of pulmonary infections in cystic fibrosis. *American Journal of Respiratory and Critical Care Medicine* **168**:918-951.
86. **Glenister, D., K. E. Salamon, K. Smith, D. Beighton, and C. Keevil.** 1988. Enhanced growth of complex communities of dental plaque bacteria in mucin-limited continuous culture. *Microbial Ecology in Health and Disease* **1**:31-38.

87. **Golyshina, O. V., T. A. Pivovarova, G. I. Karavaiko, T. F. Kondratéva, E. Moore, W.-R. Abraham, H. Lünsdorf, K. N. Timmis, M. M. Yakimov, and P. Golyshin.** 2000. *Ferroplasma acidiphilum* gen. nov., sp. nov., an acidophilic, autotrophic, ferrous-iron-oxidizing, cell-wall-lacking, mesophilic member of the Ferroplasmaceae fam. nov., comprising a distinct lineage of the Archaea. *Int. J. Syst. Evol. Microbiol.* **50**:997-1006.
88. **Gomez-Alvarez, V., G. M. King, and K. Nüsslein.** 2007. Comparative bacterial diversity in recent Hawaiian volcanic deposits of different ages. *FEMS Microbiol. Ecol.* **60**:60-73.
89. **Gontcharova, V., E. Youn, R. D. Wolcott, E. B. Hollister, T. J. Gentry, and S. E. Dowd.** 2010. Black box chimera check (B2C2): a Windows-based software for batch depletion of chimeras from bacterial 16S rRNA gene datasets. *The Open Microbiology Journal* **4**:47-52.
90. **González-Toril, E., E. Llobet-Brossa, E. Casamayor, R. Amann, and R. Amils.** 2003. Microbial ecology of an extreme acidic environment, the Tinto River. *Appl. Environ. Microbiol.* **69**:4853-4865.
91. **Gouin, M., E. Saracusa, C. Clemons, J. Senko, K. Kreider, and G. Young.** 2012. A mathematical model of a passive scheme for acid mine drainage remediation. *GEM-International Journal on Geomathematics*:1-27.
92. **Guo, X., H. Yin, J. Cong, Z. Dai, Y. Liang, and X. Liu.** 2013. RubisCO gene clusters found in a metagenome microarray from acid mine drainage. *Appl. Environ. Microbiol.* **79**:2019-2026.
93. **Hahn, M. W., P. Stadler, Q. L. Wu, and M. Pöckl.** 2004. The filtration–acclimatization method for isolation of an important fraction of the not readily cultivable bacteria. *J. Microbiol. Methods* **57**:379-390.
94. **Hallberg, K. B., K. Coupland, S. Kimura, and D. B. Johnson.** 2006. Macroscopic streamer growths in acidic, metal-rich mine waters in North Wales consist of novel and remarkably simple bacterial communities. *Appl. Environ. Microbiol.* **72**:2022-2030.
95. **Hallberg, K. B., and D. B. Johnson.** 2003. Novel acidophiles isolated from moderately acidic mine drainage waters. *Hydrometallurgy* **71**:139-148.

96. **Hao, C., L. Wang, Y. Gao, L. Zhang, and H. Dong.** 2010. Microbial diversity in acid mine drainage of Xiang Mountain sulfide mine, Anhui Province, China. *Extremophiles* **14**:465-474.
97. **Harmsen, M., L. Yang, S. J. Pamp, and T. Tolker-Nielsen.** 2010. An update on *Pseudomonas aeruginosa* biofilm formation, tolerance, and dispersal. *FEMS Immunology & Medical Microbiology* **59**:253-268.
98. **Hedrich, S., E. Heinzl, J. Seifert, and M. Schlömann.** 2009. Isolation of novel iron-oxidizing bacteria from an acid mine water treatment plant. *Advanced Materials Research* **71**:125-128.
99. **Hedrich, S., M. Schlömann, and D. B. Johnson.** 2011. The iron-oxidizing proteobacteria. *Microbiology* **157**:1551-1564.
100. **Heinzl, E., S. Hedrich, E. Janneck, F. Glombitza, J. Seifert, and M. Schlömann.** 2009. Bacterial diversity in a mine water treatment plant. *Appl. Environ. Microbiol.* **75**:858-861.
101. **Hengstmann, U., K.-J. Chin, P. H. Janssen, and W. Liesack.** 1999. Comparative phylogenetic assignment of environmental sequences of genes encoding 16S rRNA and numerically abundant culturable bacteria from an anoxic rice paddy soil. *Appl. Environ. Microbiol.* **65**:5050-5058.
102. **Hentzer, M., G. M. Teitzel, G. J. Balzer, A. Heydorn, S. Molin, M. Givskov, and M. R. Parsek.** 2001. Alginate overproduction affects *Pseudomonas aeruginosa* biofilm structure and function. *J. Bacteriol.* **183**:5395-5401.
103. **Henwood, C. J., D. M. Livermore, D. James, M. Warner, and P. S. Group.** 2001. Antimicrobial susceptibility of *Pseudomonas aeruginosa*: results of a UK survey and evaluation of the British Society for Antimicrobial Chemotherapy disc susceptibility test. *J. Antimicrob. Chemother.* **47**:789-799.
104. **Herlihy, A. T., P. R. Kaufmann, M. E. Mitch, and D. D. Brown.** 1990. Regional estimates of acid mine drainage impact on streams in the mid-atlantic and southeastern United States. *Water Air and Soil Pollution* **50**:91-107.
105. **Hindi, K. M., M. J. Panzner, C. A. Tessier, C. L. Cannon, and W. J. Youngs.** 2009. The medicinal applications of imidazolium carbene-metal complexes. *Chem. Rev.* **109**:3859-3884.

106. **Høiby, N., H. K. Johansen, C. Moser, O. Ciofu, P. Ø. Jensen, M. Kolpen, L. Mandsberg, M. Givskov, S. Molin, and T. Bjarnsholt.** 2011. *Pseudomonas aeruginosa* biofilms in the lungs of cystic fibrosis patients, p. 167-184, *Biofilm Infections*. Springer.
107. **Holt, K. B., and A. J. Bard.** 2005. Interaction of silver(I) ions with the respiratory chain of *Escherichia coli*: An electrochemical and scanning electrochemical microscopy study of the antimicrobial mechanism of micromolar Ag. *Biochemistry* **44**:13214-13223.
108. **Hoque, M. S., L. M. Broadhurst, and P. H. Thrall.** 2011. Genetic characterization of root-nodule bacteria associated with *Acacia salicina* and *A. stenophylla* (Mimosaceae) across south-eastern Australia. *Int. J. Syst. Evol. Microbiol.* **61**:299-309.
109. **Hoyles, L., H. Honda, N. A. Logan, G. Halket, R. M. La Ragione, and A. L. McCartney.** 2012. Recognition of greater diversity of *Bacillus* species and related bacteria in human faeces. *Res. Microbiol.* **163**:3-13.
110. **Hunt, B. E., A. Weber, A. Berger, B. Ramsey, and A. L. Smith.** 1995. Macromolecular mechanisms of sputum inhibition of tobramycin activity *Antimicrob. Agents Chemother.* **39**:34-39.
111. **Irie, Y., and M. Parsek.** 2008. Quorum sensing and microbial biofilms, p. 67-84, *Bacterial Biofilms*. Springer.
112. **Itoh, T., K. Yamanoi, T. Kudo, M. Ohkuma, and T. Takashina.** 2011. *Aciditerrimonas ferrireducens* gen. nov., sp. nov., an iron-reducing thermoacidophilic actinobacterium isolated from a solfataric field. *Int. J. Syst. Evol. Microbiol.* **61**:1281-1285.
113. **Johnson, D. B.** 1995. Selective solid media for isolating and enumerating acidophilic bacteria. *J. Microbiol. Methods* **23**:205-218.
114. **Johnson, D. B., and K. B. Hallberg.** 2005. Acid mine drainage remediation options: a review. *Sci. Total Environ.* **338**:3-14.
115. **Johnson, D. B., and K. B. Hallberg.** 2003. The microbiology of acidic mine waters. *Res. Microbiol.* **154**:466-473.
116. **Johnson, D. B., and K. B. Hallberg.** 2002. Pitfalls of passive mine water treatment. *Re/Views in Environmental Science and Bio/Technology* **1**:335-343.

117. **Johnson, D. B., K. B. Hallberg, and S. Hedrich.** 2014. Uncovering a microbial enigma: Isolation and characterization of the streamer-generating, iron-oxidizing, acidophilic bacterium "*Ferrovum myxofaciens*". *Appl. Environ. Microbiol.* **80**:672-680.
118. **Johnson, D. B., J. H. M. Macvicar, and S. Rolfe.** 1987. A new solid medium for the isolation and enumeration of *Thiobacillus ferrooxidans* and acidophilic heterotrophic bacteria. *J. Microbiol. Methods* **7**:9-18.
119. **Kascatan-Nebioglu, A., A. Melaiye, K. Hindi, S. Durmus, M. J. Panzner, L. A. Hogue, R. J. Mallett, C. E. Hovis, M. Coughenour, S. D. Crosby, A. Milsted, D. L. Ely, C. A. Tessier, C. L. Cannon, and W. J. Youngs.** 2006. Synthesis from caffeine of a mixed N-heterocyclic carbene-silver acetate complex active against resistant respiratory pathogens. *J. Med. Chem.* **49**:6811-6818.
120. **Kascatan-Nebioglu, A., M. J. Panzner, C. A. Tessier, C. L. Cannon, and W. J. Youngs.** 2007. N-Heterocyclic carbene-silver complexes: A new class of antibiotics. *Coord. Chem. Rev.* **251**:884-895.
121. **Kay, C. M., O. F. Rowe, L. Rocchetti, K. Coupland, K. B. Hallberg, and D. B. Johnson.** 2013. Evolution of microbial "streamer" growths in an acidic, metal-contaminated stream draining an abandoned underground copper mine. *Life* **3**:189-210.
122. **Kerem, B.-s., J. M. Rommens, J. A. Buchanan, D. Markiewicz, T. K. Cox, A. Chakravarti, M. Buchwald, and L.-C. Tsui.** 1989. Identification of the cystic fibrosis gene: genetic analysis. *Science* **245**:1073-1080.
123. **Kirby, C. S., H. M. Thomas, G. Southam, and R. Donald.** 1999. Relative contributions of abiotic and biological factors in Fe(II) oxidation in mine drainage. *Appl. Geochem.* **14**:511-530.
124. **Kirchner, S., J. L. Fothergill, E. A. Wright, C. E. James, E. Mowat, and C. Winstanley.** 2012. Use of artificial sputum medium to test antibiotic efficacy against *Pseudomonas aeruginosa* in conditions more relevant to the cystic fibrosis lung. *Journal of visualized experiments : JoVE*:e3857.
125. **Klasen, H.** 2000. Historical review of the use of silver in the treatment of burns. I. Early uses. *Burns* **26**:117-130.
126. **Klasen, H.** 2000. A historical review of the use of silver in the treatment of burns. II. Renewed interest for silver. *Burns* **26**:131-138.

127. **Klebensberger, J., O. Rui, E. Fritz, B. Schink, and B. Philipp.** 2006. Cell aggregation of *Pseudomonas aeruginosa* strain PAO1 as an energy-dependent stress response during growth with sodium dodecyl sulfate. *Archives of Microbiology* **185**:417-427.
128. **Kopecky, J., M. Kyselkova, M. Omelka, L. Cermak, J. Novotna, G. Grundmann, Y. Moënné-Loccoz, and M. Sagova-Mareckova.** 2011. Environmental mycobacteria closely related to the pathogenic species evidenced in an acidic forest wetland. *Soil Biology and Biochemistry* **43**:697-700.
129. **Kumar, N., E. O. Omoregie, J. Rose, A. Masion, J. R. Lloyd, L. Diels, and L. Bastiaens.** 2014. Inhibition of sulfate reducing bacteria in aquifer sediment by iron nanoparticles. *Water Res.* **51**:64-72.
130. **Kumon, H., K. i. Tomochika, T. Matunaga, M. Ogawa, and H. Ohmori.** 1994. A sandwich cup method for the penetration assay of antimicrobial agents through *Pseudomonas* exopolysaccharides. *Microbiol. Immunol.* **38**:615-619.
131. **Kuti, J. L., C. H. Nightingale, R. F. Knauff, and D. P. Nicolau.** 2004. Pharmacokinetic properties and stability of continuous-infusion meropenem in adults with cystic fibrosis. *Clinical Therapeutics* **26**:493-501.
132. **Lamblin, G., S. Degroote, J.-M. Perini, P. Delmotte, A. Scharfman, M. Davril, J.-M. Lo-Guidice, N. Houdret, V. Dumur, and A. Klein.** 2001. Human airway mucin glycosylation: a combinatorial of carbohydrate determinants which vary in cystic fibrosis. *Glycoconjugate Journal* **18**:661-684.
133. **Landry, R. M., D. D. An, J. T. Hupp, P. K. Singh, and M. R. Parsek.** 2006. Mucin-*Pseudomonas aeruginosa* interactions promote biofilm formation and antibiotic resistance. *Mol. Microbiol.* **59**:142-151.
134. **Lansdown, A. B. G.** 2002. Silver I: Its antibacterial properties and mechanism of action. *Journal of Wound Care* **11**:125-130.
135. **Larouche, J. R., W. B. Bowden, R. Giordano, M. B. Flinn, and B. C. Crump.** 2012. Microbial biogeography of arctic streams: exploring influences of lithology and habitat. *Frontiers in Microbiology* **3**.

136. **Larson, L. N., M. Fitzgerald, K. Singha, M. N. Gooseff, J. L. Macalady, and W. Burgos.** 2013. Hydrogeochemical niches associated with hyporheic exchange beneath an acid mine drainage-contaminated stream. *Journal of Hydrology* **501**:163-174.
137. **Lauber, C. L., K. S. Ramirez, Z. Aanderud, J. Lennon, and N. Fierer.** 2013. Temporal variability in soil microbial communities across land-use types. *The ISME Journal* **7**:1641-1650.
138. **Lazdunski, A. M., I. Ventre, and S. Bleves.** 2007. Cell–cell communication: Quorum sensing and regulatory circuits in *Pseudomonas aeruginosa*, p. 279-310, *Pseudomonas*. Springer.
139. **Leid, J. G., A. J. Ditto, A. Knapp, P. N. Shah, B. D. Wright, R. Blust, L. Christensen, C. B. Clemons, J. P. Wilber, G. W. Young, A. G. Kang, M. J. Panzner, C. L. Cannon, Y. H. Yun, W. J. Youngs, N. M. Seckinger, and E. K. Cope.** 2012. In vitro antimicrobial studies of silver carbene complexes: activity of free and nanoparticle carbene formulations against clinical isolates of pathogenic bacteria. *J. Antimicrob. Chemother.* **67**:138-148.
140. **Lepleux, C., S. Uroz, C. Collignon, J.-L. Churin, M.-P. Turpault, and P. Frey-Klett.** 2013. A short-term mineral amendment impacts the mineral weathering bacterial communities in an acidic forest soil. *Res. Microbiol.* **164**:729-739.
141. **Levy, J.** 1986. Antibiotic activity in sputum. *The Journal of Pediatrics* **108**:841-846.
142. **Levy, J., A. L. Smith, M. A. Kenny, B. Ramsey, and F. D. Schoenknecht.** 1983. Bioactivity of gentamicin in purulent sputum from patients with cystic fibrosis or bronchiectasis: Comparison with activity in serum. *J. Infect. Dis.* **148**:1069-1076.
143. **Liau, S. Y., D. C. Read, W. J. Pugh, J. R. Furr, and A. D. Russell.** 1997. Interaction of silver nitrate with readily identifiable groups: relationship to the antibacterial action of silver ions. *Lett. Appl. Microbiol.* **25**:279-283.
144. **Liljeqvist, M., J. Valdes, D. S. Holmes, and M. Dopson.** 2011. Draft genome of the psychrotolerant acidophile *Acidithiobacillus ferrivorans* SS3. *J. Bacteriol.* **193**:4304-4305.

145. **Lima, L. J., V. van der Velpen, J. Wolkers-Rooijackers, H. J. Kamphuis, M. H. Zwietering, and M. R. Nout.** 2012. Microbiota dynamics and diversity at different stages of industrial processing of cocoa beans into cocoa powder. *Appl. Environ. Microbiol.* **78**:2904-2913.
146. **Lin, X., S. Green, M. Tfaily, O. Prakash, K. Konstantinidis, J. Corbett, J. Chanton, W. Cooper, and J. Kostka.** 2012. Microbial community structure and activity linked to contrasting biogeochemical gradients in bog and fen environments of the Glacial Lake Agassiz Peatland. *Appl. Environ. Microbiol.* **78**:7023-7031.
147. **Linker, A., and R. S. Jones.** 1966. A new polysaccharide resembling alginic acid isolated from pseudomonads. *Journal of Biological Chemistry* **241**:3845-3851.
148. **Linker, A., and R. S. Jones.** 1964. A polysaccharide resembling alginic acid from a *Pseudomonas* micro-organism. *Nature* **204**: 187-188.
149. **Lovley, D. R., and E. J. P. Phillips.** 1986. Organic matter mineralization with reduction of ferric iron in anaerobic sediments. *Appl. Environ. Microbiol.* **51**:683-689.
150. **Lovley, D. R., and E. J. P. Phillips.** 1987. Rapid assay for microbially reducible ferric iron in aquatic sediments. *Appl. Environ. Microbiol.* **53**:1536-1540.
151. **Lozupone, C., and R. Knight.** 2005. UniFrac: a new phylogenetic method for comparing microbial communities. *Appl. Environ. Microbiol.* **71**:8228-8235.
152. **Lozupone, C. A., M. Hamady, S. T. Kelley, and R. Knight.** 2007. Quantitative and qualitative beta diversity measures lead to different insights into factors that structure microbial communities. *Appl. Environ. Microbiol.* **73**:1576-1585.
153. **Lu, S., K. Chourey, M. Reiche, S. Nietzsche, M. B. Shah, T. R. Neu, R. L. Hettich, and K. Küsel.** 2013. Insights into the structure and metabolic function of microbes that shape pelagic iron-rich aggregates ("iron snow"). *Appl. Environ. Microbiol.* **79**:4272-4281.
154. **Lu, S., S. Gischkat, M. Reiche, D. M. Akob, K. B. Hallberg, and K. Küsel.** 2010. Ecophysiology of Fe-cycling bacteria in acidic sediments. *Appl. Environ. Microbiol.* **76**:8174-8183.

155. **Lucheta, A., X. Otero, F. Macías, and M. Lambais.** 2013. Bacterial and archaeal communities in the acid pit lake sediments of a chalcopyrite mine. *Extremophiles* **17**:941-951.
156. **Lyczak, J. B., C. L. Cannon, and G. B. Pier.** 2000. Establishment of *Pseudomonas aeruginosa* infection: lessons from a versatile opportunist. *Microbes and Infection* **2**:1051-1060.
157. **Lyczak, J. B., C. L. Cannon, and G. B. Pier.** 2002. Lung infections associated with cystic fibrosis. *Clin. Microbiol. Rev.* **15**:194-222.
158. **MacLeod, D. L., J. Velayudhan, T. F. Kenney, J. H. Therrien, J. L. Sutherland, L. M. Barker, and W. R. Baker.** 2012. Fosfomycin enhances the active transport of tobramycin in *Pseudomonas aeruginosa*. *Antimicrob. Agents Chemother.* **56**:1529-1538.
159. **Mah, T.-F. C., and G. A. O'Toole.** 2001. Mechanisms of biofilm resistance to antimicrobial agents. *Trends Microbiol.* **9**:34-39.
160. **Mahenthiralingam, E., A. Baldwin, and P. Vandamme.** 2002. *Burkholderia cepacia* complex infection in patients with cystic fibrosis. *J. Med. Microbiol.* **51**:533-538.
161. **Marasco, R., E. Rolli, M. Fusi, A. Cherif, A. Abou-Hadid, U. El-Bahairy, S. Borin, C. Sorlini, and D. Daffonchio.** 2013. Plant growth promotion potential is equally represented in diverse grapevine root-associated bacterial communities from different biopedoclimatic environments. *BioMed Research International* **2013**.
162. **Mathee, K., O. Ciofu, C. Sternberg, P. W. Lindum, J. I. Campbell, P. Jensen, A. H. Johnsen, M. Givskov, D. E. Ohman, and M. Søren.** 1999. Mucoid conversion of *Pseudomonas aeruginosa* by hydrogen peroxide: a mechanism for virulence activation in the cystic fibrosis lung. *Microbiology* **145**:1349-1357.
163. **Matsui, H., V. E. Wagner, D. B. Hill, U. E. Schwab, T. D. Rogers, B. Button, R. M. Taylor, R. Superfine, M. Rubinstein, B. H. Iglewski, and R. C. Boucher.** 2006. A physical linkage between cystic fibrosis airway surface dehydration and *Pseudomonas aeruginosa* biofilms. *Proc. Natl. Acad. Sci. U. S. A.* **103**:18131-18136.
164. **Mendelman, P. M., A. L. Smith, J. Levy, A. Weber, B. Ramsey, and R. L. Davis.** 1985. Aminoglycoside penetration, inactivation, and efficacy in cystic fibrosis sputum. *Am. Rev. Respir. Dis.* **132**:761-765.

165. **Milanowski, R., S. Kosmala, B. Zakryś, and J. Kwiatowski.** 2006. Phylogeny of photosynthetic euglenophytes based on combined chloroplast and cytoplasmic SSU rDNA sequence analysis. *Journal of Phycology* **42**:721-730.
166. **Miller, J. K., J. S. Brantner, H. T. Badawy, P. O. Wagers, C. Clemons, K. L. Kreider, P. Wilber, A. Milsted, Y. H. Yun, W. J. Youngs, and G. Young.** 2013. Mathematical modeling of *Pseudomonas aeruginosa* biofilm growth and treatment in the cystic fibrosis lung. *Mathematical Medicine and Biology*.
167. **Mohr, J. F.** 2008. Update on the efficacy and tolerability of meropenem in the treatment of serious bacterial infections. *Clinical Infectious Diseases* **47**:S41-S51.
168. **Mulcahy, H., L. Charron-Mazenod, and S. Lewenza.** 2008. Extracellular DNA chelates cations and induces antibiotic resistance in *Pseudomonas aeruginosa* biofilms. *PLoS Pathog.* **4**:e1000213.
169. **Muramatsu, H., R. Murakami, Z. H. Ibrahim, K. Murakami, N. Shahab, and K. Nagai.** 2011. Phylogenetic diversity of acidophilic actinomycetes from Malaysia. *The Journal of Antibiotics* **64**:621-624.
170. **Nepomnyashchaya, Y. N., G. B. Slobodkina, R. V. Baslerov, N. A. Chernyh, E. A. Bonch-Osmolovskaya, A. I. Netrusov, and A. I. Slobodkin.** 2012. *Moorella humiferrea* sp. nov., a thermophilic, anaerobic bacterium capable of growth via electron shuttling between humic acid and Fe (III). *Int. J. Syst. Evol. Microbiol.* **62**:613-617.
171. **Nichols, W. W., S. Dorrington, M. Slack, and H. Walmsley.** 1988. Inhibition of tobramycin diffusion by binding to alginate. *Antimicrob. Agents Chemother.* **32**:518-523.
172. **Nicomrat, D., W. A. Dick, and O. H. Tuovinen.** 2006. Assessment of the microbial community in a constructed wetland that receives acid coal mine drainage. *Microb. Ecol.* **51**:83-89.
173. **Oliver, A., R. Cantón, P. Campo, F. Baquero, and J. Blázquez.** 2000. High frequency of hypermutable *Pseudomonas aeruginosa* in cystic fibrosis lung infection. *Science* **288**:1251-1253.
174. **Oliver, A., and A. Mena.** 2010. Bacterial hypermutation in cystic fibrosis, not only for antibiotic resistance. *Clinical Microbiology and Infection* **16**:798-808.

175. **Palmer, K. L., L. A. Aye, and M. Whiteley.** 2007. Nutritional cues control *Pseudomonas aeruginosa* multicellular behavior in cystic fibrosis sputum. *J. Bacteriol.* **189**:8079-8087.
176. **Palmer, K. L., L. M. Mashburn, P. K. Singh, and M. Whiteley.** 2005. Cystic fibrosis sputum supports growth and cues key aspects of *Pseudomonas aeruginosa* physiology. *J. Bacteriol.* **187**:5267-5277.
177. **Panzner, M. J., A. Deeraksa, A. Smith, B. D. Wright, K. M. Hindi, A. Kascatan-Nebioglu, A. G. Torres, B. M. Judy, C. E. Hovis, J. K. Hilliard, R. J. Mallett, E. Cope, D. M. Estes, C. L. Cannon, J. G. Leid, and W. J. Youngs.** 2009. Synthesis and in vitro efficacy studies of silver carbene complexes on biosafety level 3 bacteria. *Eur. J. Inorg. Chem.*:1739-1745.
178. **Partanen, P., J. Hultman, L. Paulin, P. Auvinen, and M. Romantschuk.** 2010. Bacterial diversity at different stages of the composting process. *BMC Microbiology* **10**:94.
179. **Pier, G. B.** 2002. CFTR mutations and host susceptibility to *Pseudomonas aeruginosa* lung infection. *Current Opinion in Microbiology* **5**:81-86.
180. **Pillet, L., C. de Vargas, and J. Pawlowski.** 2011. Molecular identification of sequestered diatom chloroplasts and kleptoplastidy in foraminifera. *Protist* **162**:394-404.
181. **Poole, K.** 2005. Aminoglycoside resistance in *Pseudomonas aeruginosa*. *Antimicrob. Agents Chemother.* **49**:479-487.
182. **Price, M. N., P. S. Dehal, and A. P. Arkin.** 2010. FastTree 2—approximately maximum-likelihood trees for large alignments. *PLoS One* **5**:e9490.
183. **Qiu, Y.-L., Y. Sekiguchi, H. Imachi, Y. Kamagata, I.-C. Tseng, S.-S. Cheng, A. Ohashi, and H. Harada.** 2004. Identification and isolation of anaerobic, syntrophic phthalate isomer-degrading microbes from methanogenic sludges treating wastewater from terephthalate manufacturing. *Appl. Environ. Microbiol.* **70**:1617-1626.
184. **Rhomberg, P. R., and R. N. Jones.** 2007. Contemporary activity of meropenem and comparator broad-spectrum agents: MYSTIC program report from the United States component (2005). *Diagnostic Microbiology and Infectious Disease* **57**:207-215.

185. **Rhomberg, P. R., and R. N. Jones.** 2009. Summary trends for the Meropenem Yearly Susceptibility Test Information Collection program: a 10-year experience in the United States (1999–2008). *Diagnostic Microbiology and Infectious Disease* **65**:414-426.
186. **Riordan, J. R., J. M. Rommens, B.-s. Kerem, N. Alon, R. Rozmahel, Z. Grzelczak, J. Zielenski, S. Lok, N. Plavsic, J.-L. Chou, M.L. Drumm, M.C. Iannuzzi, F.S. Collins, and L-C. Tsui.** 1989. Identification of the cystic fibrosis gene: cloning and characterization of complementary DNA. *Science* **245**:1066-1073.
187. **Roden, E. E., J. M. McBeth, M. Blöthe, E. M. Percak-Dennett, E. J. Fleming, R. R. Holyoke, G. W. Luther III, D. Emerson, and J. Schieber.** 2012. The microbial ferrous wheel in a neutral pH groundwater seep. *Frontiers in Microbiology* **3**.
188. **Roden, E. E., and M. M. Urrutia.** 1999. Ferrous iron removal promotes microbial reduction of crystalline iron(III) oxides. *Environ. Sci. Technol.* **33**:1847-1853.
189. **Rommens, J. M., M. C. Iannuzzi, B.-s. Kerem, M. L. Drumm, G. Melmer, M. Dean, R. Rozmahel, J. L. Cole, D. Kennedy, N. Hidaka, M. Zsiga, M. Buchwald, J.R. Riordan, L.-C. Tsui, and F.S. Collins.** 1989. Identification of the cystic fibrosis gene: chromosome walking and jumping. *Science* **245**:1059-1065.
190. **Rose, M. C., and J. A. Voynow.** 2006. Respiratory tract mucin genes and mucin glycoproteins in health and disease. *Physiological reviews* **86**:245-278.
191. **Rowe, O. F., J. Sánchez-España, K. B. Hallberg, and D. B. Johnson.** 2007. Microbial communities and geochemical dynamics in an extremely acidic, metal-rich stream at an abandoned sulfide mine (Huelva, Spain) underpinned by two functional primary production systems. *Environ. Microbiol.* **9**:1761-1771.
192. **Rubin, B. K.** 2009. Mucus, phlegm, and sputum in cystic fibrosis. *Respir. Care* **54**:726-732.
193. **Russell, A. D., and W. B. Hugo.** 1994. Antimicrobial activity and action of silver. *Progress in Medicinal Chemistry* **31**:351-370.

194. **Ryzinska-Paier, G., R. Sommer, J. M. Haider, S. Knetsch, C. Frick, A. K. Kirschner, and A. H. Farnleitner.** 2011. Acid phosphatase test proves superior to standard phenotypic identification procedure for *Clostridium perfringens* strains isolated from water. *J. Microbiol. Methods* **87**:189-194.
195. **Sahl, J. W., R. Schmidt, E. D. Swanner, K. W. Mandernack, A. S. Templeton, T. L. Kieft, R. L. Smith, W. E. Sanford, R. L. Callaghan, and J. B. Mitton.** 2008. Subsurface microbial diversity in deep-granitic-fracture water in Colorado. *Appl. Environ. Microbiol.* **74**:143-152.
196. **Sánchez-Andrea, I., N. Rodríguez, R. Amils, and J. L. Sanz.** 2011. Microbial diversity in anaerobic sediments at Rio Tinto, a naturally acidic environment with a high heavy metal content. *Appl. Environ. Microbiol.* **77**:6085-6093.
197. **Santofimia, E., E. González-Toril, E. López-Pamo, M. Gomariz, R. Amils, and Á. Aguilera.** 2013. Microbial diversity and its relationship to physicochemical characteristics of the water in two extreme acidic pit lakes from the Iberian pyrite belt (SW Spain). *PLoS One* **8**:e66746.
198. **Satoh, A., M. Watanabe, A. Ueki, and K. Ueki.** 2002. Physiological properties and phylogenetic affiliations of anaerobic bacteria isolated from roots of rice plants cultivated on a paddy field. *Anaerobe* **8**:233-246.
199. **Senko, J. M., D. Bertel, T. J. Quick, and W. D. Burgos.** 2011. The influence of phototrophic biomass on Fe and S redox cycling in an acid mine drainage impacted system. *Mine Water Environ.* **30**:38-46.
200. **Senko, J. M., P. Wanjugi, M. Lucas, M. A. Bruns, and W. D. Burgos.** 2008. Characterization of Fe(II) oxidizing bacterial activities and communities at two acidic Appalachian coalmine drainage-impacted sites. *The ISME Journal* **2**:1134-1145.
201. **Senko, J. M., G. X. Zhang, J. T. McDonough, M. A. Bruns, and W. D. Burgos.** 2009. Metal reduction at low pH by a *Desulfosporosinus* species: Implications for the biological treatment of acidic mine drainage. *Geomicrobiol. J.* **26**:71-82.
202. **Service, U. S. F., and U. S. B. o. Mines.** 1993. Acid drainage from mines on the national forests: A management challenge. Forest Service.

203. **Shawar, R. M., D. L. MacLeod, R. L. Garber, J. L. Burns, J. R. Stapp, C. R. Clausen, and S. Tanaka.** 1999. Activities of tobramycin and six other antibiotics against *Pseudomonas aeruginosa* isolates from patients with cystic fibrosis. *Antimicrob. Agents Chemother.* **43**:2877-2880.
204. **Sheik, C. S., W. H. Beasley, M. S. Elshahed, X. Zhou, Y. Luo, and L. R. Krumholz.** 2011. Effect of warming and drought on grassland microbial communities. *The ISME Journal* **5**:1692-1700.
205. **Sievert, S. M., T. Heidorn, and J. Kuever.** 2000. *Halothiobacillus kellyi* sp. nov., a mesophilic, obligately chemolithoautotrophic, sulfur-oxidizing bacterium isolated from a shallow-water hydrothermal vent in the Aegean Sea, and emended description of the genus *Halothiobacillus*. *Int. J. Syst. Evol. Microbiol.* **50**:1229-1237.
206. **Silver, S.** 2003. Bacterial silver resistance: molecular biology and uses and misuses of silver compounds. *FEMS Microbiol. Rev.* **27**:341-353.
207. **Singer, P. C., and W. Stumm.** 1970. Acidic mine drainage: The rate determining step. *Science* **167**:1121-1123.
208. **Singh, P. K., A. L. Schaefer, M. R. Parsek, T. O. Moninger, M. J. Welsh, and E. P. Greenberg.** 2000. Quorum-sensing signals indicate that cystic fibrosis lungs are infected with bacterial biofilms. *Nature* **407**:762-764.
209. **Smith, A. L., S. B. Fiel, N. Mayer-Hamblett, B. Ramsey, and J. L. Burns.** 2003. Susceptibility testing of *Pseudomonas aeruginosa* isolates and clinical response to parenteral antibiotic administration: lack of association in cystic fibrosis. *Chest* **123**:1495-1502.
210. **Sogin, M. L., H. G. Morrison, J. A. Huber, D. M. Welch, S. M. Huse, P. R. Neal, J. M. Arrieta, and G. J. Herndl.** 2006. Microbial diversity in the deep sea and the underexplored "rare biosphere". *Proceedings of the National Academy of Sciences* **103**:12115-12120.
211. **Sorokin, D. Y., T. P. Tourova, A. M. Lysenko, and G. Muyzer.** 2006. Diversity of culturable halophilic sulfur-oxidizing bacteria in hypersaline habitats. *Microbiology* **152**:3013-3023.
212. **Sriramulu, D. D.** 2010. Amino Acids enhance adaptive behaviour of *Pseudomonas aeruginosa* in the cystic fibrosis lung environment. *Microbiology Insights* **3**:17-26.

213. **Sriramulu, D. D., H. Lünsdorf, J. S. Lam, and U. Römling.** 2005. Microcolony formation: a novel biofilm model of *Pseudomonas aeruginosa* for the cystic fibrosis lung. *J. Med. Microbiol.* **54**:667-676.
214. **Stewart, P. S.** 2002. Mechanisms of antibiotic resistance in bacterial biofilms. *International Journal of Medical Microbiology* **292**:107-113.
215. **Stewart, P. S., and J. William Costerton.** 2001. Antibiotic resistance of bacteria in biofilms. *The Lancet* **358**:135-138.
216. **Stoodley, P., K. Sauer, D. Davies, and J. W. Costerton.** 2002. Biofilms as complex differentiated communities. *Annual Reviews in Microbiology* **56**:187-209.
217. **Stookey, L. L.** 1970. Ferrozine: A new spectrophotometric reagent for iron. *Anal. Chem.* **42**:779-781.
218. **Stumm, W., and J. Morgan.** 1996. *Aquatic chemistry: Chemical equilibrium and rates in natural waters*, 3 ed. Wiley-Interscience, Hoboken, New Jersey.
219. **Suci, P., M. Mittelman, F. Yu, and G. Geesey.** 1994. Investigation of ciprofloxacin penetration into *Pseudomonas aeruginosa* biofilms. *Antimicrob. Agents Chemother.* **38**:2125-2133.
220. **Suh, J., K. L. Choy, S. K. Lai, J. S. Suk, B. C. Tang, S. Prabhu, and J. Hanes.** 2007. PEGylation of nanoparticles improves their cytoplasmic transport. *Int. J. Nanomed.* **2**:735-741.
221. **Suk, J. S., S. K. Lai, Y. Y. Wang, L. M. Ensign, P. L. Zeitlin, M. P. Boyle, and J. Hanes.** 2009. The penetration of fresh undiluted sputum expectorated by cystic fibrosis patients by non-adhesive polymer nanoparticles. *Biomaterials* **30**:2591-2597.
222. **Sutherland, I. W.** 2001. The biofilm matrix—an immobilized but dynamic microbial environment. *Trends Microbiol.* **9**:222-227.
223. **Swan, B. K., M. Martinez-Garcia, C. M. Preston, A. Sczyrba, T. Woyke, D. Lamy, T. Reinthaler, N. J. Poulton, E. D. P. Masland, and M. L. Gomez.** 2011. Potential for chemolithoautotrophy among ubiquitous bacteria lineages in the dark ocean. *Science* **333**:1296-1300.

224. **Tanner, R. S.** 2007. Cultivation of bacteria and fungi, p. 69-78. *In* C. J. Hurst, R. L. Crawford, J. L. Garland, D. A. Lipson, A. L. Mills, and L. D. Stetzenbach (ed.), *Manual of Environmental Microbiology*. American Society for Microbiology, Washington, DC.
225. **Tarutis, W. J., and R. F. Unz.** 1995. Iron and manganese release in coal mine drainage wetland microcosms. *Water Sci. Technol.* **32**:187-192.
226. **Tarutis, W. J., R. F. Unz, and R. P. Brooks.** 1992. Behavior of sedimentary Fe and Mn in a natural wetland receiving acidic mine drainage, Pennsylvania, USA *Appl. Geochem.* **7**:77-85.
227. **Thornton, D. J., K. Rousseau, and M. A. McGuckin.** 2008. Structure and function of the polymeric mucins in airways mucus. *Annu. Rev. Physiol.* **70**:459-486.
228. **Tischler, J. S., R. J. Jwair, N. Gelhaar, A. Drechsel, A.-M. Skirl, C. Wiacek, E. Janneck, and M. Schlömann.** 2013. New cultivation medium for “*Ferrovum*” and *Gallionella*-related strains. *J. Microbiol. Methods* **95**:138-144.
229. **Tyson, G. W., I. Lo, B. J. Baker, E. E. Allen, P. Hugenholtz, and J. F. Banfield.** 2005. Genome-directed isolation of the key nitrogen fixer *Leptospirillum ferrodiazotrophum* sp. nov. from an acidophilic microbial community. *Appl. Environ. Microbiol.* **71**:6319-6324.
230. **Unal, S., and J. A. Garcia-Rodriguez.** 2005. Activity of meropenem and comparators against *Pseudomonas aeruginosa* and *Acinetobacter* spp. isolated in the MYSTIC Program, 2002–2004. *Diagnostic Microbiology and Infectious Disease* **53**:265-271.
231. **Viaene, E., H. Chanteux, H. Servais, M.-P. Mingeot-Leclercq, and P. M. Tulkens.** 2002. Comparative stability studies of antipseudomonal β -lactams for potential administration through portable elastomeric pumps (home therapy for cystic fibrosis patients) and motor-operated syringes (intensive care units). *Antimicrob. Agents Chemother.* **46**:2327-2332.
232. **Vile, M. A., and R. K. Wieder.** 1993. Alkalinity generation by Fe(III) reduction versus sulfate reduction in wetlands constructed for acid mine drainage treatment. *Water Air Soil Pollut.* **69**:425-441.

233. **Volant, A., A. Desoeuvre, C. Casiot, B. Lauga, S. Delpoux, G. Morin, J. Personné, M. Héry, F. Elbaz-Poulichet, and P. Bertin.** 2012. Archaeal diversity: temporal variation in the arsenic-rich creek sediments of Carnoulès Mine, France. *Extremophiles* **16**:645-657.
234. **Voynow, J. A., and B. K. Rubin.** 2009. Mucins, mucus, and sputum. *Chest* **135**:505-512.
235. **Vrany, J. D., P. S. Stewart, and P. A. Suci.** 1997. Comparison of recalcitrance to ciprofloxacin and levofloxacin exhibited by *Pseudomonas aeruginosa* biofilms displaying rapid-transport characteristics. *Antimicrob. Agents Chemother.* **41**:1352-1358.
236. **Wang, Q., G. M. Garrity, J. M. Tiedje, and J. R. Cole.** 2007. Naive Bayesian classifier for rapid assignment of rRNA sequences into the new bacterial taxonomy. *Appl. Environ. Microbiol.* **73**:5261-5267.
237. **Wang, Y. Y., S. K. Lai, J. S. Suk, A. Pace, R. Cone, and J. Hanes.** 2008. Addressing the PEG mucoadhesivity paradox to engineer nanoparticles that "slip" through the human mucus barrier. *Angew. Chem.-Int. Edit.* **47**:9726-9729.
238. **Waters, C. M., and B. L. Bassler.** 2005. Quorum sensing: cell-to-cell communication in bacteria. *Annu. Rev. Cell Dev. Biol.* **21**:319-346.
239. **Weiss, J. V., J. A. Rentz, T. Plaia, S. C. Neubauer, M. Merrill-Floyd, T. Lilburn, C. Bradburne, J. P. Megonigal, and D. Emerson.** 2007. Characterization of neutrophilic Fe (II)-oxidizing bacteria isolated from the rhizosphere of wetland plants and description of *Ferritrophicum radicolica* gen. nov. sp. nov., and *Sideroxydans paludicola* sp. nov. *Geomicrobiol. J.* **24**:559-570.
240. **Wells, T. N. C., P. Scully, G. Paravicini, A. E. I. Proudfoot, and M. A. Payton.** 1995. Mechanism of irreversible inactivation of phosphomannose isomerases by silver ions and flomoxone. *Biochemistry* **34**:7896-7903.
241. **Wolin, E. A., M. J. Wolin, and R. S. Wolfe.** 1963. Formation of methane by bacterial extracts. *The Journal of Biological Chemistry* **238**:2882-2886.
242. **Wu, X., Z. L. Wong, P. Sten, S. Engblom, P. Österholm, and M. Dopson.** 2013. Microbial community potentially responsible for acid and metal release from an Ostrobothnian acid sulfate soil. *FEMS Microbiol. Ecol.* **84**:555-563.

243. **Yabe, S., Y. Aiba, Y. Sakai, M. Hazaka, and A. Yokota.** 2011. *Thermogemmatispora onikobensis* gen. nov., sp. nov. and *Thermogemmatispora foliorum* sp. nov., isolated from fallen leaves on geothermal soils, and description of Thermogemmatisporaceae fam. nov. and Thermogemmatisporales ord. nov. within the class Ktedonobacteria. *Int. J. Syst. Evol. Microbiol.* **61**:903-910.
244. **Yang, L., K. B. Barken, M. E. Skindersoe, A. B. Christensen, M. Givskov, and T. Tolker-Nielsen.** 2007. Effects of iron on DNA release and biofilm development by *Pseudomonas aeruginosa*. *Microbiology* **153**:1318-1328.
245. **Yang, L., L. Jelsbak, and S. Molin.** 2011. Microbial ecology and adaptation in cystic fibrosis airways. *Environ. Microbiol.* **13**:1682-1689.
246. **Yergeau, E., K. K. Newsham, D. A. Pearce, and G. A. Kowalchuk.** 2007. Patterns of bacterial diversity across a range of Antarctic terrestrial habitats. *Environ. Microbiol.* **9**:2670-2682.
247. **Yin, H., L. Cao, G. Qiu, D. Wang, L. Kellogg, J. Zhou, X. Liu, Z. Dai, J. Ding, and X. Liu.** 2008. Molecular diversity of 16S rRNA and gyrB genes in copper mines. *Archives of Microbiology* **189**:101-110.
248. **Yu, H., and N. E. Head.** 2002. Persistent infections and immunity in cystic fibrosis. *Front Biosci* **7**:D442-457.
249. **Zemanick, E. T., S. D. Sagel, and J. K. Harris.** 2011. The airway microbiome in cystic fibrosis and implications for treatment. *Curr. Opin. Pediatr.* **23**:319-324.
250. **Zhang, J., T. Yue, and Y. Yuan.** 2013. *Alicyclobacillus* contamination in the production line of kiwi products in China. *PLoS One* **8**:e67704.
251. **Ziegler, S., B. Waidner, T. Itoh, P. Schumann, S. Spring, and J. Gescher.** 2013. *Metallibacterium scheffleri* gen. nov., sp. nov., an alkalizing gammaproteobacterium isolated from an acidic biofilm. *Int. J. Syst. Evol. Microbiol.* **63**:1499-1504.
252. **Ziemkiewicz, P. F., J. G. Skousen, D. L. Brant, P. L. Sterner, and R. J. Lovett.** 1997. Acid mine drainage treatment with armored limestone in open limestone channels. *J. Environ. Qual.* **26**:1017-1024.

253. **Zinger, L., B. Shahnava, F. Baptist, R. A. Geremia, and P. Choler.** 2009. Microbial diversity in alpine tundra soils correlates with snow cover dynamics. *The ISME Journal* **3**:850-859.

APPENDIX

 **Copyright Clearance Center**  **RightsLink**     **Live Chat**

 **ACS Publications** Most Trusted. Most Cited. Most Read. **Title:** Response of Soil-Associated Microbial Communities to Intrusion of Coal Mine-Derived Acid Mine Drainage **Author:** Justin S. Brantner, John M. Senko **Publication:** Environmental Science & Technology **Publisher:** American Chemical Society **Date:** Aug 1, 2014
Copyright © 2014, American Chemical Society

Logged in as:
Justin Brantner
 **LOGOUT**

PERMISSION/LICENSE IS GRANTED FOR YOUR ORDER AT NO CHARGE

This type of permission/license, instead of the standard Terms & Conditions, is sent to you because no fee is being charged for your order. Please note the following:

- Permission is granted for your request in both print and electronic formats, and translations.
- If figures and/or tables were requested, they may be adapted or used in part.
- Please print this page for your records and send a copy of it to your publisher/graduate school.
- Appropriate credit for the requested material should be given as follows: "Reprinted (adapted) with permission from (COMPLETE REFERENCE CITATION). Copyright (YEAR) American Chemical Society." Insert appropriate information in place of the capitalized words.
- One-time permission is granted only for the use specified in your request. No additional uses are granted (such as derivative works or other editions). For any other uses, please submit a new request.

 **BACK**

 **CLOSE WINDOW**

Copyright © 2014 Copyright Clearance Center, Inc. All Rights Reserved. [Privacy statement](#).
Comments? We would like to hear from you. E-mail us at customer@copyright.com

A1: Written consent for reuse of data/figures appearing in **Brantner, J.S. & Senko, J.M.** 2014. Response of soil-associated microbial communities to intrusion of coal mine-derived acid mine drainage. Environmental Science and Technology **48**:8556-8563. [Copyright © 2014, American Chemical Society] (27)

[Print](#)

[Close](#)

RE: Follow Up to Dissertation Reuse Request

From: **Copyright** (Copyright@ACS.org)
Sent: Thu 12/18/14 2:41 PM
To: Justin Brantner (justin3@zips.uakron.edu)

Dear Justin Brantner,

Regarding your message below and the permission that you received from RightsLink, that is all you need. You should give a copy of that RightsLink permission to your Graduate School if they require proof that you were granted permission. Please use the credit line wording included on the RightsLink permission in the figure captions.

C. Arleen Courtney
Copyright Associate
Copyright, Permissions, & Licensing
Office of Secretary & General Counsel
American Chemical Society
1155 Sixteenth Street, NW
Washington, DC 20036
Email a_courtney@acs.org / Dept. Email copyright@acs.org
Tel. 202-872-4368 / Fax. 202-776-8112

From: Justin Brantner [mailto:justin3@zips.uakron.edu]
Sent: Thursday, December 18, 2014 1:08 PM
To: Copyright
Subject: Follow Up to Dissertation Reuse Request

<https://blu176.mail.live.com/ol/mail.mvc/PrintMessages?mkt=en-us>

6/11/2015

A2: E-mail consent for reuse of data/figures appearing in **Brantner, J.S. & Senko, J.M.** 2014. Response of soil-associated microbial communities to intrusion of coal mine-derived acid mine drainage. Environmental Science and Technology **48**:8556-8563. [Copyright © 2014, American Chemical Society] (27)

[Print](#)[Close](#)

Re: Usage of Figures and Data in Dissertation

From: Frontiers in Microbiology Editorial Office
(microbiology.editorial.office@frontiersin.org)
Sent: Fri 12/19/14 8:38 AM
To: justin3@zips.uakron.edu

Dear Justin,

Thank you for your email. If you wish to reproduce and data or figures in your dissertation you may do so as long as this is in accordance with the copyright conditions:

Copyright © 2014 Brantner, Haake, Burwick, Menge, Hotchkiss and Senko. This is an open-access article distributed under the terms of the Creative Commons Attribution License (CC BY). The use, distribution or reproduction in other forums is permitted, provided the original author(s) or licensor are credited and that the original publication in this journal is cited, in accordance with accepted academic practice. No use, distribution or reproduction is permitted which does not comply with these terms.

This means that they can be reproduced as long as the original source and authors are fully cited.

Please let me know if I can be of further assistance.

Kind regards,

Alice Rolandini Jensen

Frontiers | Microbiology Editorial Office
Journal Manager: [Sara Bosshart](#)
www.frontiersin.org | twitter.com/FrontiersIn
EPFL - Innovation Square, building 1
Lausanne, Switzerland | T +41(0)21 510 17 23

For technical issues, please contact our IT Helpdesk <support@frontiersin.org>

----- Forwarded message -----
From: **Justin Brantner** <justin3@zips.uakron.edu>
Date: Thu, Dec 18, 2014 at 3:24 PM
Subject: Usage of Figures and Data in Dissertation
To: info@frontiersin.org

Hello,

<https://blu176.mail.live.com/ol/mail.mvc/PrintMessages?mkt=en-us>

6/11/2015

A3: Written approval for the reuse of certain data/figures appearing in **Brantner, J.S., Haake, Z.J., Burwick, J.E., Menge, C.M., Hotchkiss, S.T. & Senko, J.M.** 2014. Depth-dependent geochemical and microbiological gradients in Fe(III) deposits resulting from coal mine-derived acid mine drainage. *Frontiers in Microbiology* **5**. [Copyright © 2014 Brantner, Haake, Burwick, Menge, Hotchkiss and Senko] (26)